

Ice core based climate reconstruction from the Mongolian Altai

Inauguraldissertation
der Philosophisch-naturwissenschaftlichen Fakultät
der Universität Bern

vorgelegt von
Pierre-Alain Herren
von Mühleberg

Leiterin der Arbeit:
Prof. Dr. Margit Schwikowski
Departement für Chemie und Biochemie

Ice core based climate reconstruction from the Mongolian Altai

Inauguraldissertation
der Philosophisch-naturwissenschaftlichen Fakultät
der Universität Bern

vorgelegt von
Pierre-Alain Herren
von Mühleberg

Leiterin der Arbeit:
Prof. Dr. Margit Schwikowski
Departement für Chemie und Biochemie

Von der Philosophisch-naturwissenschaftlichen Fakultät angenommen.

Bern, 19. September 2013

Der Dekan:

Prof. Dr. S. Decurtins

Un type qui se trompe en disant quelque chose de faux dit peut-être quelque chose de vrai
Philippe Geluck

Summary

Climate change has become a serious challenge to society in past decades. Changes in atmospheric conditions combined with sea level rise are expected to affect changes in economic wealth, modify the distribution of the earth's most fertile land, and induce major migration of populations. Future climate scenarios still suffer large uncertainties. This is due to disagreement in climate models results, uncertainties in 21st century greenhouse gas emissions and discrepancy in paleoclimate reconstructions used to calibrate climate models. Nevertheless, model runs and observation clearly suggest that 20th century warming is human induced and can be attributed to the additional forcing of anthropogenic emissions. However, climate change has strong regional expression. More and more paleoclimate reconstructions aim to capture regional signals in order to place these recent climate changes in a long-term context. Regional estimates of the Medieval Warm Period (MWP) are still insufficient mostly due to limited data prior the Little Ice Age (LIA) and poor regional coverage. In this study the region of interest is continental Asia, more specifically the Altai mountain range located between the Siberian forest and the deserts of Central Asia. In recent decades this part of the globe experienced enhanced warming. Together with the Arctic it belongs to most affected regions of current climate change. The internal climate variability of this part of Central Asia still lacks understanding. For example changes in the Siberian High intensity, located above the Altai during wintertime have been associated to Eurasian climate. Current Central Asian climate reconstructions are strongly biased towards tree-ring chronologies.

The initial goals of this study was to extend paleoclimate records derived from the Belukha ice core located on the north slope of the Altai, and to test the identified correlation between solar forcing and temperature in the Altai region for a warm climate interval such as the MWP. Here we present the results of a newly collected ice core from the Tsambagarav massif located on the southern slope of the Altai. A strong northwest to southeast precipitation gradient in the Altai suggest longer climate archives in the Mongolian Altai. The new record was assumed to provide additional regional paleoclimate records for improved understanding of the regional climate. The dating of the Tsambagarav ice core allowed studying Holocene glacier fluctuations and reconstruction of accumulation rates. Biogenic species measured in the ice core reflect temperature changes of the Siberian forests. The Tsambagarav paleoclimate records combined with climate reconstructions of the Belukha ice core, drilled during summer 2001 and located 350 km northwest of the Tsambagarav massif, enabled to investigate the spatial representativeness of the proxies.

The Tsambagarav ice core was dated with a variety of methods, including identification of reference horizons, annual layer counting, nuclear dating with ²¹⁰Pb, ³H, and a novel ¹⁴C technique. This gives confidence in the obtained chronology. The upper 36 m weq embody 200 years of climate information, suitable for climate reconstruction with annual resolution. Strong annual layer thinning characterizes the lower 20 m weq. To obtain a continuous age-depth profile, an empirical equation was implemented, linking

the upper and lower part of the ice core. The accumulation reconstruction indicates changes in the precipitation pattern over the last 6000 years. The most recent 200 years are influenced by relative humid conditions, preceded by an arid period beginning around 5000 years BP. During the build-up phase of the glacier around 6000 years BP, the derived accumulation suggests an increase in precipitation. This is in agreement with other reconstructions, pointing to a consistent precipitation evolution for the Altai region.

As dating of the basal ice revealed a build-up of the glacier at roughly 6000 years BP, this suggests complete glacier disappearance during the Holocene Climate Optimum (HCO) as observed in various other places of the globe. The waxing of the glacier provides benchmarks for the end of the HCO and the onset of the Neoglaciation at around 6000 years BP. The total glacier disappearance indicates higher temperatures at that time compared to present, especially since the period preceding the Neoglaciation experienced humid climatic conditions. High accumulation during the build-up of the glacier combined with decreasing temperatures is a plausible hypothesis for the onset of the glaciers in the Tsambagarav mountain range. For complete melting of the glacier in the Tsambagarav massif a minimal ELA-shift of 430 m is required. Extrapolated to the surrounding glaciated areas it can be assumed that most Mongolian Altai glaciers disappeared as well. Accordingly, most glaciers in the Mongolian Altai are not remnants from the Last Glacial Maximum, but instead they were formed during the second part of the Holocene. This provides new insight into the glaciation/deglaciation process of the Mongolian Altai.

Based on the dating of the Tsambagarav ice core, mid-Holocene climate records are available from the Altai region. The water stable isotope record is controlled by temperature and atmospheric moisture source signals. Therefore we excluded the $\delta^{18}\text{O}$ records as temperature proxy. However, concentrations of biogenic species measured in the ice core were used to reconstruct a 3200 year long temperature record. Similar to an ice core study from tropical South America, we argue that sources of those biogenic species are emissions from soil and vegetation in the Siberian plains and are controlled by temperature variations. This novel temperature record of the Siberian forests together with two independent records located north and south on the Asian continent suggests elevated temperature at the start of the current era. This period can be assigned to the Roman Warm Period (RWP). The occurrence within individual records considered for comparison differ in time and in magnitude yet all show the same pattern. We argue that Siberia experienced a pronounced RWP. The agreement with other Asian records indicates a pronounced continental occurrence. The rapid transition to colder climate is consistent with the Migration period. Due to resolution issues and boundary effects comparison to present warming is difficult. On a long-term perspective (100 years) current temperatures in Siberia are at least as warm as any time during the past 3200 years.

Paleoclimate reconstructions derived from two ice cores located in the Altai mountain range (Belukha and Tsambagarav) provide the unique opportunity to test their spatial representativeness. Regarding melt rates, long-term trends are similar for the north and south side of the Altai. Increased melting in recent decades affected the glacier's mass

balance independent of their geographical location in the mountain range. Differences on smaller timescale can partly be attributed to dating uncertainties, concentration of the accumulation period during summer months in the Mongolian Altai and local geometric influences. The Mongolian melt record reflects anthropogenically modified radiation changes attributed to 'dimming' and 'brightening' of the atmosphere. SO_4^{2-} and NO_3^- concentrations in both ice cores follow anthropogenic Eastern European emission estimates of SO_2 and NO_x . This further supports the hypothesis of a radiation controlled surface melting in the Altai. Biogenic emissions and forest fires reconstruction in both ice cores have identical trends, suggesting large-scale phenomena. The agreement of most proxies, particularly on decadal resolution, between two 350 km distant sites demonstrates the strength of ice-core based climate proxies. This motivates investigation of new sites to aid the regional climate reconstruction.

The initial goal to extend the paleoclimate reconstructions derived from the Belukha ice core succeeded, since the Tsambagarav ice core contains 6000 years of climate information. The strong thinning of the annual layer combined with reduced accumulation rates affected the resolution of the reconstructions. A 3200 year temperature reconstruction was based on 20-year time-steps. Nevertheless, the two precisely dated ice cores improved our understanding of past climate conditions in the Altai and can be used for further regional climate reconstructions.

Contents

Summary	i
Abbreviations	viii
1 Introduction	1
1.1 Outline of the thesis	1
1.2 Paleoclimate perspective on climate change	2
1.3 Polar and alpine ice cores as paleoclimate archive	7
1.4 Motivation of this study	10
References	10
2 Regional setting	19
2.1 Drilling expedition	19
2.1.1 Deep drilling campaign in 2009	20
2.1.2 Reconnaissance expedition 2011	21
2.2 Geography of the Altai Mountains	23
2.3 Climate of the Altai	27
2.4 Paleoclimatic studies from the Altai	29
2.4.1 Ice core	30
2.4.2 Lake sediments	32
2.4.3 Tree-rings	36
References	38
3 Methods	47
3.1 Sample processing	48
3.2 Liquid scintillation counting (^3H)	49
3.3 α -spectroscopy (^{210}Pb)	50
3.4 Accelerator mass spectrometry (^{14}C)	51
3.5 Major ions	52
3.6 $\delta^{18}\text{O}$	53
3.7 $^{10}\text{Beryllium}$	55
References	56
4 Onset of Neoglaciation in Mongolia	59
Abstract	60
4.1 Introduction	60
4.2 Regional setting	62

Contents

4.3	Experimental Methods	64
4.3.1	Ice core drilling	64
4.3.2	Glaciological survey	65
4.3.3	Analytical methods	66
4.4	Dating of the ice core archive for the period AD 1815-2009	67
4.4.1	Identification of reference horizons	68
4.4.2	Annual layer counting	69
4.4.3	Radioactive dating with ^{210}Pb	70
4.4.4	Glacier flow model	71
4.5	Millennial ice from the Mongolian Altai	72
4.5.1	Complex age-depth relation derived from ^{14}C data	72
4.5.2	Neoglacial ice at bedrock	73
4.6	Accumulation reconstruction	74
4.6.1	Accumulation rates for the period AD 1815 to 2009	74
4.6.2	Accumulation trends for the past 6 kyr	75
4.7	Conclusions	77
	Acknowledgements	78
	References	78
5	Late-Holocene temperature reconstruction for Siberia	87
	Abstract	88
5.1	Importance of regionally resolved paleoclimate records for northern Asia	88
5.2	Biogenic emissions as temperature proxy	90
5.3	Calibration and assessment of a new temperature proxy	91
5.4	Late-Holocene temperature reconstruction for the Siberian plains	95
5.5	Pronounced warm climate during the Roman Warm Period	97
5.6	Reconstructed 20 th century temperature increase	99
	References	100
6	Comparison of two Altai ice cores	105
	Abstract	106
6.1	Introduction	106
6.2	Methods	108
6.2.1	Dating	108
6.2.2	Chemical analysis	109
6.2.3	Ice core melt percent	109
6.3	Results and Discussion	111
6.3.1	200-year melt percent record of the Mongolian Altai	111
6.3.2	Unprecedented melting in high altitude Altai	111
6.3.3	Incident solar radiation archived in the melt record	113
6.3.4	Geochemical record comparison	114
6.4	Conclusions	120
	Acknowledgements	120
	References	120

7	10-Beryllium	127
	References	130
8	Outlook	133
9	Appendix	137
	9.1 Supplementary information I	137
	9.2 Totality of conducted ¹⁴ C measurements	139
	9.3 Snowpit samples during fieldwork 2009 and 2011	140
	9.4 Raw geochemistry & stable isotope records	142
	Curriculum vitae	157

Abbreviations

ALC	Annual Layer Counting
AMP	Annual Melt Percent
AMS	Accelerator Mass Spectrometer
BK01	Belukha ice core 2001
BK03	Belukha ice core 2003
CE	Current Era
DACP	Dark Ages Cold Period
EAWM	East Asian Winter Monsoon
EC	Elemental Carbon
ELA	Equilibrium Line Altitude
FELICS	Fast Electromechanical Lightweight Ice Coring System
GEBA	Global Energy Balance Archive
GHG	GreenHouse Gas
GPR	Ground Penetrating Radar
HCO	Holocene Climate Optimum
IC	Ion Chromatography
IPCC	Intergovernmental Panel on Climate Change
IRMS	Isotope Ratio Mass Spectrometer
ITCZ	InterTropical Convergence Zone
IWEP	Institute for Water and Environmental Problems, Barnaul, Russia
LGM	Last Glacial Maximum
LIA	Little Ice Age
MWP	Medieval Warm Period
NAO	North Atlantic Oscillation
NCR	Neutron Counting Rates
OC	Organic Carbon
PAGES	Past Global chanGES
PCA	Principle Component Analysis
PDO	Pacific Decadal Oscillation
PDSI	Palmer Drought Severity Index
PSI	Paul Scherrer Institut
POC	Particulate Organic Carbon
RWP	Roman Warm Period
SH	Siberian High
SSN	Sun Spot Numbers
TSI	Total Solar Irradiance
TU	Tritium Unit

1 Introduction

Global warming has been largely discussed during past decades. At first the essential question was if current warming is human induced or related to natural variability. To answer this question, scientists searched for the longest available instrumental records in order to have a long-term perspective. It was rapidly recognized that instrumental measurements covered too short time periods. The longest quasi-global temperature record starts 1850. Thus other methods would be required to investigate the climate history and its interaction with human activities on centennial or millennial timescales. A variety of climate archives were identified and new methods developed to introduce further proxies. With ongoing research anthropogenic induced global warming has been generally accepted. The remaining open questions are: What share of current warming can be attributed to anthropogenic activities? What is the role of internal climate variability? How important are external forcing factors such as the sun? Additionally, climate change has a strong regional expression, which requires regionally resolved paleoclimate records.

1.1 Outline of the thesis

The aim of this thesis is to reconstruct past climate conditions from an ice core drilled during summer 2009 in the Mongolian Altai. The work is subdivided in 8 parts. *Chapter 1* introduces the concept of climate change and the general role of paleoclimatology. The importance of regional climate archives is presented together with the current state of ice core science. The chapter ends with the goal and motivation of this thesis. In *Chapter 2* two field campaigns conducted in 2009 and 2011 are presented. Second the Altai and Western Mongolia is introduced with a separate part discussing the climate and the weather in the Altai. Finally, available paleoclimate records of the region are summarized. In *Chapter 3* the different methods and instruments applied in this thesis are introduced, from the sample preparation to the dating methods and the climate proxies. *Chapter 4* describes the dating of the Tsambagarav ice core together with Holocene glacier fluctuations and reconstructed accumulation rates. *Chapter 5* presents a long-term tem-

1 Introduction

perature reconstruction based on biogenic species measured in the ice core. This record suggests that the Roman Warm Period was regionally and temporally pronounced in Siberia. The observation of recent warming in Siberia, which is not seen in other climate archives, makes it a valuable contribution in understanding regional climate. *Chapter 6* compares two ice cores 350 km distant. Differences and similarities of various measured species (geochemical and stable isotopes) are presented. *Chapter 7* is a progress report about ^{10}Be measurement in the ice core. *Chapter 8* finally gives an outlook in future perspectives.

1.2 Paleoclimate perspective on climate change

The importance to understand earth climate was recognized from an early stage and preceded the work of IPCC assessment reports (IPCC, 2007). However, their introduction accelerated the processes of understanding the earth climate and resulted in broader public awareness. The increased atmospheric CO_2 level has been used to demonstrate the drastic changes the earth has undergone since the industrial period. Fig. 1.1 shows direct atmospheric CO_2 measurements¹ initiated in 1960 by Keeling (1961) together with atmospheric mixing ratio of CO_2 of the past 800 kyr measured in Antarctic ice cores (Lüthi et al., 2008).

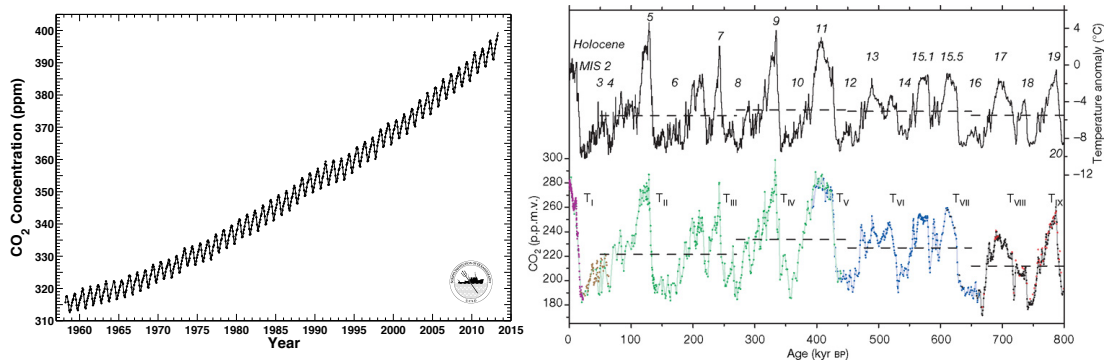


Figure 1.1: (*left*) Atmospheric CO_2 concentrations measured at Mauna Loa ('Keeling curve'). (*right*) Compilation of CO_2 records and EPICA Dome C temperature anomaly over the past 800 kyr (from Lüthi et al. 2008).

Comparing the two curves separately does not depict the ongoing changes in atmospheric composition. However, combining those curves for the last 10 kyr illustrates clearly the

¹<http://keelingcurve.ucsd.edu>

1.2 Paleoclimate perspective on climate change

drastic increase in CO₂ and other greenhouse gases (GHG) since the beginning of the industrial era around AD 1800 (Fig. 1.2). Without the long-term perspective the actual

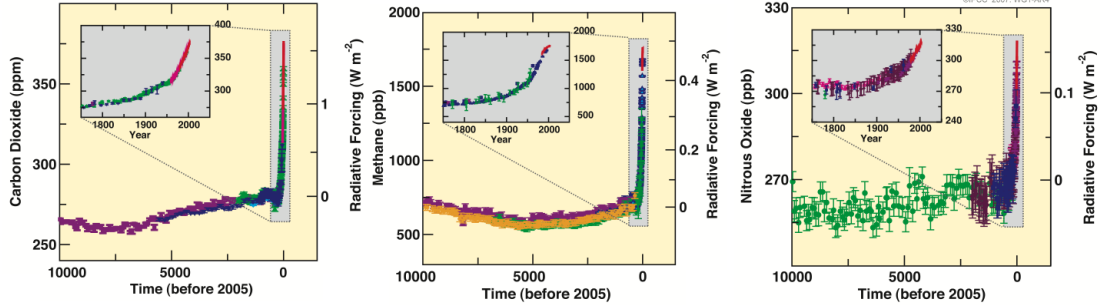


Figure 1.2: Atmospheric concentrations of CO₂ (*left*), CH₄ (*middle*) and N₂O (*right*) over the last 10 kyr (large panels) and since AD 1750 (inset panels). Measurements are shown from ice cores (symbols with different colors for different studies) and atmospheric samples (red lines). The corresponding radiative forcings are shown on the right hand axes of the large panels. Graph modified from IPCC (2007).

CO₂ increase would not appear as severe. This demonstrates the importance of paleoclimate archives to understand the earth climate and the changes it is undergoing. The increase of GHG concentrations and their effect on the radiation balance of the globe is shown in Fig. 1.2.

Two examples of direct observations of recent climate change are illustrated in Fig. 1.3. The increase in temperature accelerated during recent decades (DelSole et al., 2011; Rahmstorf et al., 2012; Wallace et al., 2012). Elevated temperatures are the main cause of the sea level rise, due to thermal expansion of the water and melting of glaciers and ice sheets (Rahmstorf, 2007; Grinsted et al., 2010; Radić and Hock, 2011). Shrinking Northern hemisphere snow cover further supplements the picture of a changing climate with the associated changes in the radiative feedback (Brown, 2000).

Paleoclimate records from different archives can be combined to compile global or hemispheric reconstructions. Fig 1.4 shows 5 Northern Hemisphere temperature reconstructions for the last millennium (Jones et al., 1998; Mann et al., 1999; Briffa, 2000; Briffa et al., 2001; Moberg et al., 2005). The records have large differences yet follow a similar trend. Amplitude, duration and geographical extent remain largely uncertain. However, three distinct phases are generally accepted for the past millennium. (i) Net warming since AD 1850 (0.6°C) shown by observation and proxy data (Jones et al., 2013). (ii) The Little Ice Age (LIA, AD 1400-1700) when the Northern Hemisphere experienced cold conditions (e.g., Fischer et al., 1998). (iii) The Medieval Warm Period (MWP, AD

1 Introduction

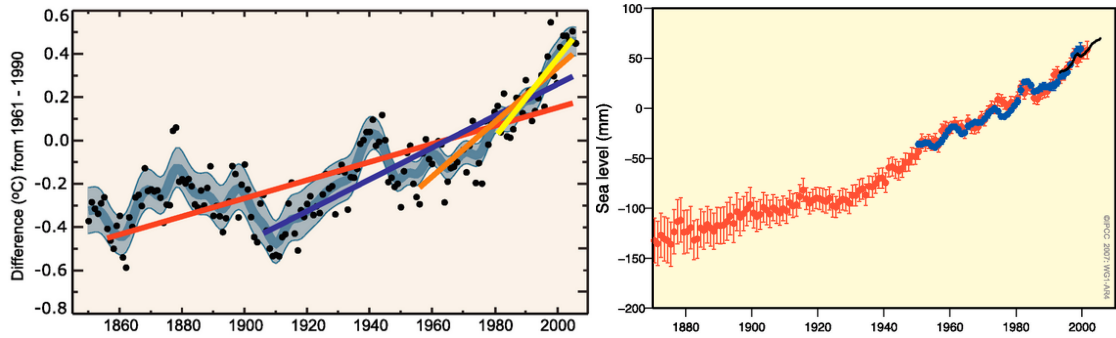


Figure 1.3: (*left*) Annual global mean temperatures (black dots) with 90% error range (pale blue band). Linear trends are shown for the last 25 (yellow), 50 (orange), 100 (purple) and 150 years (red). (*right*) Annual averages of the global mean sea level based on reconstructed sea level fields since 1870 (red), tide gauge measurements since 1950 (blue) and satellite altimetry since 1992 (black). Compiled from IPCC (2007).

950 to 1250) for which most records show elevated temperature (Lamb, 1965). Absence of precisely dated proxies, varying chronological precision, nonsteady proxy-temperature relation and short calibration periods induce large reconstruction uncertainties especially further back in time. Studying warm or cold intervals, such as the LIA or MWP are necessary for understanding the mechanism driving the climate besides long-term trends. This is especially true for present conditions. The question whether the MWP presented warmer conditions than present has often been addressed. A recent study stipulates that the MWP was characterized by warm conditions matching or exceeding the level of the past decade in some regions, but falls well below global recent levels (Mann et al., 2009). More work is required to confine the duration, magnitude and spatial extent of these characteristic climate phases.

A good example to illustrate the difficulty of capturing the regional expression of these events, is the discussion about the occurrence of the LIA in the Southern Hemisphere (e.g., Thompson et al., 1986). Meanwhile various approaches such as lichenometry, limnology or multiproxy reconstructions suggest a cold period in the Southern Hemisphere during the last millennium (Jomelli et al., 2011; Neukom et al., 2011; Orsi et al., 2012). Onset and duration are still debated. Fig. 1.5 shows the regional resolved temperature evolution of the past 150 years. All the continents experienced warming in the 20th century, which is very likely due to the observed increase in anthropogenic greenhouse gas concentrations (Jones et al., 2013).

To separate human induced changes from natural climate variability on a continental

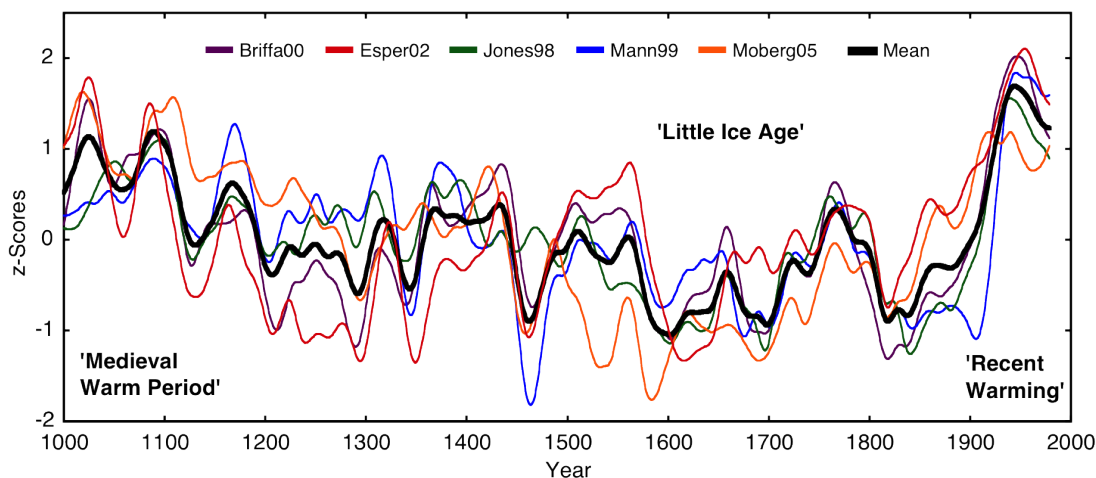


Figure 1.4: Large-scale temperature reconstructions scaled to the same mean and variance over the common period 1000-1979 AD, and their arithmetic mean. The normalization highlights the similarity between the records, but broadly ignores the differing calibration statistics with instrumental data, and their particular 'shapes' and distribution of variance, e.g. during the instrumental and pre-instrumental periods. Graph modified from Esper et al. (2005).

scale, a combination of model runs and observations was considered. A first model run was forced by measured atmospheric conditions, including anthropogenic influences (yellow in Fig. 1.5), and a second neglected anthropogenic changes thus simulating an undisturbed climate (blue in Fig. 1.5). The first model calculation reproduces precisely the observation, whereas the second model run does not capture recent warming. The difference between the two model outputs can be used to attribute anthropogenic emissions as major driver of the current climate change. The continents have large differences in model run quality (uncertainty), start and magnitude of the warming. Since past climate has a strong regional expression, there is no indication that future climate will not as well. Regionally resolved observations are too short to capture the extent of the continental differences, especially for remote areas. This can be seen as further motivation to create proxy records for local climate variation. The goal is to find and process global and local climate proxies to provide past climate estimates capturing the spatial and temporal differences with small uncertainties.

Studying climate evolution beyond the instrumental period is essential to improve climate predictability, especially for separating natural climate variability from human induced changes. Chronologies of climate parameters, such as temperature or precipitation, derived from natural archives provide the opportunity to investigate duration and magnitude of natural climate variations (Crowley, 2000). A central concept of mod-

1 Introduction

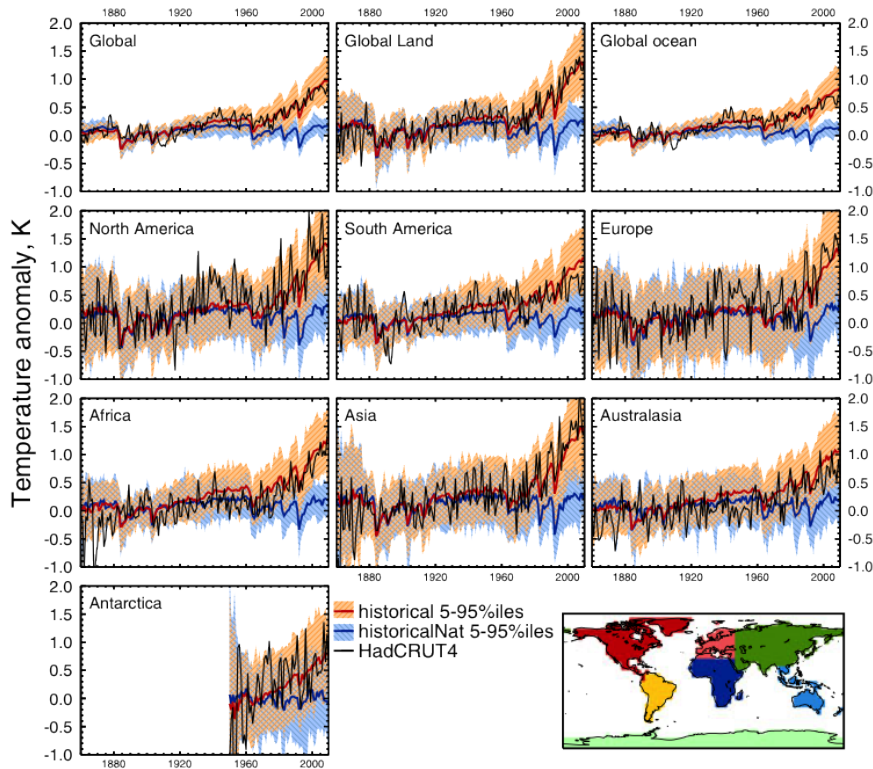


Figure 1.5: Global, land, ocean, and continental annual mean temperatures for CMIP3 and CMIP5 historical (red) and historicalNat (blue) MME and HadCRUT4 (black). Weighted model means shown as thick dark lines and 5-95% ranges shown as shaded areas. Continental regions as defined in insert. Temperatures shown with respect to 1880-1919 period apart for Antarctica, which is shown with respect to the mean of the period 1951-1980. Graph modified from Jones et al. (2013).

ern climatology is to express climate states in spatio-temporal patterns, such as the El Niño-Southern Oscillation (e.g., Trenberth and Hoar, 1997), the Pacific Decadal Oscillation (e.g., Mantua et al., 1997), the North Atlantic Oscillation (e.g., Hurrell, 1995) or the Arctic Oscillation (e.g., Wallace and Gutzler, 1981). There is no indication that past climate was not as well governed by such climatic patterns. Proper characterization and interpretation of past climate variability therefore requires a dense network of paleoclimate proxy records. Well established archives to reconstruct past climate conditions are: Tree rings, pollen, corals, lake and marine sediments, glacier ice, speleothems and historical documents (Jones et al., 2009).

Most climate paleoclimate reconstructions suffer from marked losses of centennial and multidecadal variations (von Storch et al., 2004). Comparison of large-scale temperature reconstructions over the past millennium reveals agreement on major climatic episodes,

1.3 Polar and alpine ice cores as paleoclimate archive

but substantial divergence in reconstructed (absolute) temperature amplitude (Esper et al., 2005). The perfect paleoclimatic record does not exist. Long-term reconstructions are in general affected by dating uncertainties. Tree-ring chronologies are assumed to underestimate cooling effect of volcanic eruptions (Mann et al., 2012) and are subject to spectral bias (Franke et al., 2013). Ice core based reconstructions mainly store climate signals related to precipitation. Thinning of the annual layers affect the resolution and are challenging for precise dating (Thompson et al., 1998). The origin of the data and the method used to process the records have a substantial influence on the final climate reconstruction (Mann et al., 2007; Ammann and Wahl, 2007; Burger et al., 2006). For this reason climate models are limited in precise projection, since the data used to calibrate are affected by uncertainties. To improve the skills of models for better climate projection more accurate paleoclimate records are essential. Amplitudes, precise chronologies, temporal and spatial resolution of past climate conditions are required (Hegerl et al., 2006). With precise models it will be possible to further disentangle human induced changes from internal climate variability in the earth system.

1.3 Polar and alpine ice cores as paleoclimate archive

The simplest way to investigate the impact of current atmospheric CO₂ mixing ratio is to study past intervals with similar concentrations. Paleoclimate reconstructions (Dowsett et al., 2009) suggest that during the warm interglacials of the Pliocene epoch (~ 5.3 to 2.6 Myr ago), global annual mean sea surface temperatures were 2 to 3°C higher than the pre-industrial era (Lunt et al., 2012). Estimates of former atmospheric CO₂ concentrations range between 280 and 450 ppmv (Seki et al., 2010; Pagani et al., 2010). However, these estimates are based on proxies such as foraminifera or model calculations, which are indirectly linked to atmospheric compositions. The direct reconstruction of the atmosphere is only possible through measuring the composition of air bubbles enclosed in ice cores (e.g., Neftel et al., 1982; Chappellaz et al., 1990; Lorius et al., 1990; Petit et al., 1999). Unfortunately Pliocene ice is not available for such measurements. For the moment projects exist to find 1.5 Myr old ice in Antarctica (Fischer et al., 2013).

The recent North Greenland Eemian Ice Drilling (NEEM) project aimed to retrieve Eemian interglacial (130 to 115 kyr ago) ice (Dahl-Jensen et al., 2013). It is expected that the last interglacial experienced a climate warmer than present. North Greenland surface temperatures after the onset of the Eemian (126 kyr ago) peaked at $8 \pm 4^\circ\text{C}$ above the mean of the past millennium (Dahl-Jensen et al., 2013). During this period

1 Introduction

the Greenland ice sheet was 130 ± 300 m lower than present. The exceptional heat of July 2012 with extensive surface melt over the whole Greenlandic ice sheet may have been typical Eemian summer conditions. With additional warming such surface melt events might become more common (Dahl-Jensen et al., 2013). This is a good example how using past warm conditions as example for future climate conditions to confine climate predictability. In general ice core records from Antarctica and Greenland provide global climate reconstructions. Due to fast inter-hemispheric mixing of most GHG, ice cores from the two major ice sheet covering long periods are the most appropriate to reconstruct atmospheric composition. The majority of alpine ice cores do not cover a period exceeding the Holocene. Exceptions are Colle Gniffeti in the Alps (Jenk et al., 2009), Sajama and Illimani in the Bolivian Andeans (Thompson et al., 1998; Sigl et al., 2009) and Dunde in the Tibetan Plateau (Thompson et al., 1989). However, strong thinning of the annual layers prevent using the lowest part of the ice core for climate reconstructions. While Greenland and Antarctica are sparsely or not at all populated, alpine ice cores provide data directly from densely populated areas. Fig. 1.6 shows available temperature sensitive paleoclimate archives with data back to AD 1000. There is large potential for improvement in spatial coverage of past climate records. Current millennial regional reconstructions for Asia are strongly biased towards tree-ring proxies (PAGES2k-Consortium 2013, Fig. 1.7). Other archives must be included for a wholistic reconstruction of past climate states. However, requirements for suitable ice core site, such as flat bed topography, cold ice and undisturbed flow lines limit the potential drilling sites.

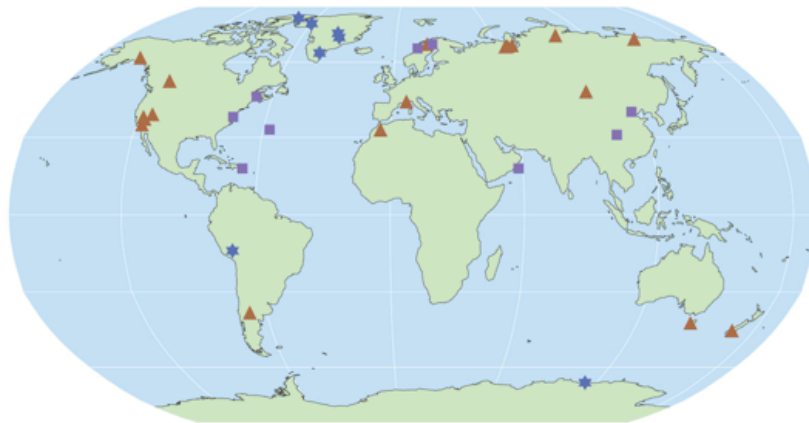


Figure 1.6: Locations of temperature-sensitive proxy records with data back to AD 1000, *tree rings*: brown triangles; *ice core/ice boreholes*: blue stars; *other records including low-resolution records*: purple squares. Graph modified from IPCC 2007.

1.3 Polar and alpine ice cores as paleoclimate archive

For the mid-latitudes and the Polar Regions an often-used indicator of unprecedented warming is the vanishing of the glaciers. The retreat of glaciers can be related to rising temperature from local to global scale (Oerlemans, 2005; Zemp et al., 2006; Fischer, 2010). Because of potential contribution to future sea-level rise and their impact on water resources, the volume and melt rate of glaciers under changing climate conditions has been discussed in details (e.g., Yao et al., 2004; Chevallier et al., 2011; Radić and Hock, 2011; Giesen and Oerlemans, 2013). Rapid disintegration of glaciers such as the Columbia glacier in Alaska, is often used as examples of global warming. The physics of such tidewater glacier are in general complex and require a thoughtful analysis. The retreat is generally not solely temperature driven but related to complicated interactions between the ocean water temperature and glaciological flow laws (Paterson and Waddington, 1984; Colgan et al., 2012). However, current glacier retreat uncovers ancient embedded organic particles (Miller et al., 2012), wood fragments (Ivy-Ochs et al., 2009), or archeological remnants (Baroni and Orombelli, 1996; Grosjean et al., 2007; Nesje et al., 2012). These artifacts exposed at the front of the glacier tongues can be dated and allow for reconstructing glacier fluctuation chronologies. Results suggest present glacier extensions in the Alpine region being similar to Mid-Holocene conditions 5 kyr ago. While during the Mid-Holocene warm conditions were caused by strong solar insolation (Wanner et al., 2008), present glacier retreat is rather attributed to human induced warming. Chapter 4 (Herren et al. 2013) of this work illustrates the unique possibility of alpine ice cores to contribute in determining minimal glacier extent. Through dating of glacier ice frozen to the bedrock the timing of glacier formation can be determined. The approach allowed suggesting total glacier disappearance in the Mongolian Altai Mountains during the Mid-Holocene. This result puts present glacier extent into perspective. Numerous open questions remain regarding the climate-glacier interaction. A well known example is the debate about the age of the Kilimanjaro ice (Kaser et al., 2004; Thompson and Mosley-Thompson, 2011). Well-dated ice cores can provide precise dates of minimum glacier extent.

Alpine ice cores have been used to derive either directly climate parameters like temperature or precipitation (e.g., Kellerhals et al., 2010; Herren et al., 2013), past atmospheric composition (e.g., Schwikowski et al., 1999; Kaspari et al., 2009) or to investigate climate states such as the Monsoon or the El-Niño-Oscillation (Kaspari et al., 2007; Thompson et al., 2013).

1.4 Motivation of this study

The initial goal to retrieve and analyze a second ice core in the Altai was to extend the climate record from the Belukha ice core further back in time. Especially the interaction between solar forcing and temperature identified for the period AD 1250 to 1850 should be further investigated (Eichler et al., 2009). The question if a warm period such as the MWP was as well driven by the variability in solar forcing was of the utmost importance for improving our understanding in past Siberian climate fluctuations. The strong north-west to southeast precipitation gradient in the Altai suggests longer climate archives in the Mongolian Altai. A 3,200 year temperature record for Siberia is presented based on biogenic species measured in the ice core. The approach is similar to Kellerhals et al. (2010). Biogenic emissions in the Siberian forests seem to be controlled by temperature variations.

Additional motivation is to provide regional paleoclimate records for improved understanding of the regional climate. Having two ice core archives from such a remote place like the Altai provides the unique opportunity to reconstruct regional climate. Similarities or differences between the Siberian and Mongolian Altai can be used to identify spatial extent of climate states with its according variability. The aim is to provide past regional climate information, especially since current Central Asian climate reconstructions are strongly biased towards tree-ring proxies (PAGES2k-Consortium, 2013).

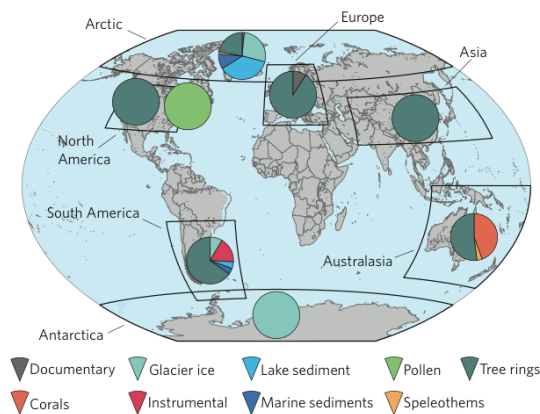


Figure 1.7: Boxes show the continental-scale regions used in this study. The pie charts represent the fraction of proxy data types used for each regional reconstruction. Graph taken from PAGES2k-Consortium (2013).

References

- Ammann, C. M., Wahl, E. R., 2007. The importance of the geophysical context in statistical evaluations of climate reconstruction procedures. *Climatic Change* 85 (1-2), 71–88.
- Baroni, C., Orombelli, G., 1996. The Alpine "Iceman" and Holocene climatic change. *Quaternary Research* 46 (1), 78–83.
- Briffa, K. R., 2000. Annual climate variability in the Holocene: Interpreting the message of ancient trees. *Quaternary Science Reviews* 19 (1–5), 87–105.
- Briffa, K. R., Osborn, T. J., Schweingruber, F. H., Harris, I. C., Jones, P. D., Shiyatov, S. G., Vaganov, E. A., 2001. Low-frequency temperature variations from a northern tree ring density network. *Journal of Geophysical Research* 106 (D3), 2929–2941.
- Brown, R. D., 2000. Northern Hemisphere snow cover variability and change, 1915–97. *Journal of Climate* 13 (13), 2339–2355.
- Burger, G., Fast, I., Cubasch, U., 2006. Climate reconstruction by regression - 32 variations on a theme. *Tellus Series A-Dynamic Meteorology and Oceanography* 58 (2), 227–235.
- Chappellaz, J., Barnola, J. M., Raynaud, D., Korotkevich, Y. S., Lorius, C., 1990. Ice-core record of atmospheric methane over the past 160,000 years. *Nature* 345 (6271), 127–131.
- Chevallier, P., Pouyaud, B., Suarez, W., Condom, T., 2011. Climate change threats to environment in the tropical Andes: glaciers and water resources. *Regional Environmental Change* 11 (1), 179–187.
- Colgan, W., Pfeffer, W. T., Rajaram, H., Abdalati, W., Balog, J., 2012. Monte Carlo ice flow modeling projects a new stable configuration for Columbia Glacier, Alaska, c. 2020. *The Cryosphere* 6 (6), 1395–1409.
- Crowley, T. J., 2000. Causes of climate change over the past 1000 years. *Science* 289 (5477), 270–277.
- Dahl-Jensen, D., Albert, M. R., Aldahan, A., Azuma, N., Balslev-Clausen, D., Baumgartner, M., Berggren, A. M., Bigler, M., Binder, T., Blunier, T., Bourgeois, J. C., Brook, E. J., Buchardt, S. L., Buizert, C., Capron, E., Chappellaz, J., Chung, J., Clausen,

1 Introduction

- H. B., Cvijanovic, I., Davies, S. M., Ditlevsen, P., Eicher, O., Fischer, H., Fisher, D. A., Fleet, L. G., Gfeller, G., Gkinis, V., Gogineni, S., Goto-Azuma, K., Grinsted, A., Gudlaugsdottir, H., Guillevic, M., Hansen, S. B., Hansson, M., Hirabayashi, M., Hong, S., Hur, S. D., Huybrechts, P., Hvidberg, C. S., Iizuka, Y., Jenk, T., Johnsen, S. J., Jones, T. R., Jouzel, J., Karlsson, N. B., Kawamura, K., Keegan, K., Kettner, E., Kipfstuhl, S., Kjær, H. A., Koutnik, M., Kuramoto, T., Köhler, P., Laepple, T., Landais, A., Langen, P. L., Larsen, L. B., Leuenberger, D., Leuenberger, M., Leuschen, C., Li, J., Lipenkov, V., Martinerie, P., Maselli, O. J., Masson-Delmotte, V., McConnell, J. R., Miller, H., Mini, O., Miyamoto, A., Montagnat-Rentier, M., Mulvaney, R., Muscheler, R., Orsi, A. J., Paden, J., Panton, C., Pattyn, F., Petit, J., Pol, K., Popp, T., Possnert, G., Prié, F., Prokopiou, M., Quiquet, A., Rasmussen, S. O., Raynaud, D., Ren, J., Reutenauer, C., Ritz, C., Röckmann, T., Rosen, J. L., Rubino, M., Rybak, O., Samyn, D., Sapart, C. J., Schilt, A., Schmidt, A. M. Z., Schwander, J., Schüpbach, S., Seierstad, I., Severinghaus, J. P., Sheldon, S., Simonsen, S. B., Sjolte, J., Solgaard, A. M., Sowers, T., Sperlich, P., Steen-Larsen, H. C., Steffen, K., Steffensen, J. P., Steinhage, D., Stocker, T. F., Stowasser, C., Sturevik, A. S., Sturges, W. T., Sveinbjörnsdottir, A., Svensson, A., Tison, J. L., Uetake, J., Vallelonga, P., van de Wal, R. S. W., van der Wel, G., Vaughn, B. H., Vinther, B., Waddington, E., Wegner, A., Weikusat, I., White, J. W. C., Wilhelms, F., Winstrup, M., Witrant, E., Wolff, E. W., Xiao, C., Zheng, J., 2013. Eemian interglacial reconstructed from a Greenland folded ice core. *Nature* 493 (7433), 489–494.
- DelSole, T., Tippett, M. K., Shukla, J., 2011. A significant component of unforced multidecadal variability in the recent acceleration of global warming. *Journal of Climate* 24 (3), 909–926.
- Dowsett, H. J., Robinson, M. M., Foley, K. M., 2009. Pliocene three-dimensional global ocean temperature reconstruction. *Climate of the Past* 5 (4), 769–783.
- Eichler, A., Olivier, S., Henderson, K., Laube, A., Beer, J., Papina, T., Gäggeler, H., Schwikowski, M., 2009. Temperature response in the Altai region lags solar forcing. *Geophysical Research Letters* 36 (1), L01808.
- Esper, J., Wilson, R. J. S., Frank, D. C., Moberg, A., Wanner, H., Luterbacher, J., 2005. Climate: Past ranges and future changes. *Quaternary Science Reviews* 24 (20–21), 2164–2166.
- Fischer, A., 2010. Glaciers and climate change: Interpretation of 50 years of direct mass balance of Hintereisferner. *Global and Planetary Change* 71 (1–2), 13–26.

1.4 Motivation of this study

- Fischer, H., Severinghaus, J., Brook, E., Wolff, E., Albert, M., Alemany, O., Arthern, R., Bentley, C., Blankenship, D., Chappellaz, J., Creyts, T., Dahl-Jensen, D., Dinn, M., Frezzotti, M., Fujita, S., Gallee, H., Hindmarsh, R., Hudspeth, D., Jugie, G., Kawamura, K., Lipenkov, V., Miller, H., Mulvaney, R., Pattyn, F., Ritz, C., Schwander, J., Steinhage, D., van Ommen, T., Wilhelms, F., 2013. Where to find 1.5 million yr old ice for the IPICS 'oldest ice' ice core. *Climate of the Past Discussions* 9 (3), 2771–2815.
- Fischer, H., Werner, M., Wagenbach, D., Schwager, M., Thorsteinsson, T., Wilhelms, F., Kipfstuhl, J., Sommer, S., 1998. Little ice age clearly recorded in northern Greenland ice cores. *Geophysical Research Letters* 25 (10), 1749–1752.
- Franke, J., Frank, D., Raible, C., Esper, J., Brönnimann, S., 2013. Spectral biases in tree-ring climate proxies. *Nature Climate Change* 3 (4), 360–364.
- Giesen, R., Oerlemans, J., 2013. Climate-model induced differences in the 21st century global and regional glacier contributions to sea-level rise. *Climate Dynamics*, 1–18.
- Grinsted, A., Moore, J. C., Jevrejeva, S., 2010. Reconstructing sea level from paleo and projected temperatures 200 to 2100 ad. *Climate Dynamics* 34 (4), 461–472.
- Grosjean, M., Suter, P. J., Trachsel, M., Wanner, H., 2007. Ice-borne prehistoric finds in the Swiss Alps reflect Holocene glacier fluctuations. *Journal of Quaternary Science* 22 (3), 203–207.
- Hegerl, G. C., Crowley, T. J., Hyde, W. T., Frame, D. J., 2006. Climate sensitivity constrained by temperature reconstructions over the past seven centuries. *Nature* 440 (7087), 1029–1032.
- Herren, P.-A., Eichler, A., Machguth, H., Papina, T., Tobler, L., Zapf, A., Schwikowski, M., 2013. The onset of Neoglaciation 6000 years ago in western Mongolia revealed by an ice core from the Tsambagarav mountain range. *Quaternary Science Reviews* 69 (C), 59–68.
- Hurrell, J. W., 1995. Decadal trends in the North-Atlantic Oscillation - Regional temperatures and precipitation. *Science* 269 (5224), 676–679.
- IPCC, 2007. *Climate Change 2007 - The Physical Science Basis: Working Group I Contribution to the Fourth Assessment Report of the IPCC*. Cambridge University Press, Cambridge, UK and New York, NY, USA.

1 Introduction

- Ivy-Ochs, S., Kerschner, H., Maisch, M., Christl, M., Kubik, P. W., Schlüchter, C., 2009. Latest Pleistocene and Holocene glacier variations in the European Alps. *Quaternary Science Reviews* 28 (21–22), 2137–2149.
- Jenk, T. M., Szidat, S., Bolius, D., Sigl, M., Gäggeler, H., Wacker, L., Ruff, M., Barbante, C., Boutron, C. F., Schwikowski, M., 2009. A novel radiocarbon dating technique applied to an ice core from the Alps indicating late Pleistocene ages. *Journal of Geophysical Research* 114 (D14), D14305.
- Jomelli, V., Khodri, M., Favier, V., Brunstein, D., Ledru, M.-P., Wagnon, P., Blard, P.-H., Sicart, J.-E., Braucher, R., Grancher, D., Bourlès, D. L., Braconnot, P., Vuille, M., 2011. Irregular tropical glacier retreat over the Holocene epoch driven by progressive warming. *Nature* 474 (7350), 196–199.
- Jones, G. S., Stott, P. A., Christidis, N., 2013. Attribution of observed historical near-surface temperature variations to anthropogenic and natural causes using CMIP5 simulations. *Journal of Geophysical Research* 118 (10), 4001–4024.
- Jones, P. D., Briffa, K. R., Barnett, T. P., Tett, S., 1998. High-resolution palaeoclimatic records for the last millennium: interpretation, integration and comparison with General Circulation Model control-run temperatures. *The Holocene* 8 (4), 455–471.
- Jones, P. D., Briffa, K. R., Osborn, T. J., Lough, J. M., 2009. High-resolution palaeoclimatology of the last millennium: a review of current status and future prospects. *The Holocene* 19 (1), 3–49.
- Kaser, G., Hardy, D. R., Mölg, T., Bradley, R. S., Hyera, T. M., 2004. Modern glacier retreat on Kilimanjaro as evidence of climate change: observations and facts. *International Journal of Climatology* 24 (3), 329–339.
- Kaspari, S., Mayewski, P., Handley, M., 2009. Recent increases in atmospheric concentrations of Bi, U, Cs, S and Ca from a 350-year Mount Everest ice core record. *Journal of Geophysical Research* 114 (D4), D04302.
- Kaspari, S., Mayewski, P., Kang, S., Sneed, S., Hou, S., Hooke, R., Kreutz, K., Introne, D., Handley, M., Maasch, K., Qin, D., Ren, J., 2007. Reduction in northward incursions of the South Asian 1400 AD inferred from a Mt. Everest ice core. *Geophysical Research Letters* 34 (16), L16701.
- Keeling, C. D., 1961. The concentration and isotopic abundances of carbon dioxide in rural and marine air. *Geochimica et Cosmochimica Acta* 24 (3–4), 277–298.

- Kellerhals, T., Brütsch, S., Sigl, M., Knüsel, S., Gäggeler, H., Schwikowski, M., 2010. Ammonium concentration in ice cores: A new proxy for regional temperature reconstruction? *Journal of Geophysical Research* 115 (D16), D16123.
- Lamb, H. H., 1965. The early medieval warm epoch and its sequel. *Palaeogeography, Palaeoclimatology, Palaeoecology* 1, 13–37.
- Lorius, C., Jouzel, J., Raynaud, D., Hansen, J., Letreut, H., 1990. The ice-core record - Climate sensitivity and future greenhouse warming. *Nature* 347 (6289), 139–145.
- Lunt, D. J., Haywood, A. M., Schmidt, G. A., Salzmann, U., Valdes, P. J., Dowsett, H. J., Loptson, C. A., 2012. On the causes of mid-Pliocene warmth and polar amplification. *Earth and Planetary Science Letters* 321, 128–138.
- Lüthi, D., Le Floch, M., Bereiter, B., Blunier, T., Barnola, J.-M., Siegenthaler, U., Raynaud, D., Jouzel, J., Fischer, H., Kawamura, K., Stocker, T. F., 2008. High-resolution carbon dioxide concentration record 650,000–800,000 years before present. *Nature* 453 (7193), 379–382.
- Mann, M. E., Bradley, R. S., Hughes, M. K., 1999. Northern Hemisphere temperatures during the past millennium: Inferences, uncertainties, and limitations. *Geophysical Research Letters* 26 (6), 759–762.
- Mann, M. E., Fuentes, J. D., Rutherford, S., 2012. Underestimation of volcanic cooling in tree-ring-based reconstructions of hemispheric temperatures. *Nature Geoscience* 5 (3), 202–205.
- Mann, M. E., Rutherford, S., Wahl, E., Ammann, C., 2007. Robustness of proxy-based climate field reconstruction methods. *Journal of Geophysical Research* 112 (D12), D12109.
- Mann, M. E., Zhang, Z., Rutherford, S., Bradley, R. S., Hughes, M. K., Shindell, D., Ammann, C., Faluvegi, G., Ni, F., 2009. Global signatures and dynamical origins of the Little Ice Age and Medieval Climate Anomaly. *Science* 326 (5957), 1256–1260.
- Mantua, N. J., Hare, S. R., Zhang, Y., Wallace, J. M., Francis, R. C., 1997. A Pacific interdecadal climate oscillation with impacts on salmon production. *Bulletin American Meteorology Society* 78 (6), 1069–1079.
- Miller, G. H., Geirsdóttir, Á., Zhong, Y., Larsen, D. J., Otto-Bliesner, B. L., Holland, M. M., Bailey, D. A., Refsnider, K. A., Lehman, S. J., Southon, J. R., Anderson,

1 Introduction

- C., Björnsson, H., Thordarson, T., 2012. Abrupt onset of the Little Ice Age triggered by volcanism and sustained by sea-ice/ocean feedbacks. *Geophysical Research Letters* 39 (2), L02708.
- Moberg, A., Sonechkin, D. M., Holmgren, K., Datsenko, N. M., Karlen, W., 2005. Highly variable Northern Hemisphere temperatures reconstructed from low- and high-resolution proxy data. *Nature* 433 (7026), 613–617.
- Neftel, A., Oeschger, H., Schwander, J., Stauffer, B., Zumbunn, R., 1982. Ice core sample measurements give atmospheric CO₂ content during the past 40,000 yr. *Nature* 295 (5846), 220–223.
- Nesje, A., Pilo, L. H., Finstad, E., Solli, B., Wangen, V., Odegard, R. S., Isaksen, K., Storen, E. N., Bakke, D. I., Andreassen, L. M., 2012. The climatic significance of artefacts related to prehistoric reindeer hunting exposed at melting ice patches in southern Norway. *The Holocene* 22 (4), 485–496.
- Neukom, R., Luterbacher, J., Villalba, R., Küttel, M., Frank, D., Jones, P. D., Grosjean, M., Wanner, H., Aravena, J. C., Black, D. E., Christie, D. A., D'Arrigo, R., Lara, A., Morales, M., Soliz-Gamboa, C., Srur, A., Urrutia, R., von Gunten, L., 2011. Multiproxy summer and winter surface air temperature field reconstructions for southern South America covering the past centuries. *Climate Dynamics* 37 (1-2), 35–51.
- Oerlemans, J., 2005. Extracting a climate signal from 169 glacier records. *Science* 308 (5722), 675–677.
- Orsi, A. J., Cornuelle, B. D., Severinghaus, J. P., 2012. Little Ice Age cold interval in West Antarctica: Evidence from borehole temperature at the West Antarctic Ice Sheet (WAIS) Divide. *Geophysical Research Letters* 39 (9), L09710.
- Pagani, M., Liu, Z., LaRiviere, J., Ravelo, A. C., 2010. High Earth-system climate sensitivity determined from Pliocene carbon dioxide concentrations. *Nature Geoscience* 3 (1), 27–30.
- PAGES2k-Consortium, 2013. Continental-scale temperature variability during the past two millennia. *Nature Geoscience* 6 (5), 339–346.
- Paterson, W. S. B., Waddington, E. D., 1984. Past precipitation rates derived from ice core measurements: Methods and data analysis. *Reviews of Geophysics* 22 (2), 123.

- Petit, J., Jouzel, J., Raynaud, D., Barkov, N. I., Barnola, J. M., Basile, I., Bender, M., Chappellaz, J., Davis, M., Delaygue, G., Delmotte, M., Kotlyakov, V. M., Legrand, M., Lipenkov, V. Y., Lorius, C., Pepin, L., Ritz, C., Saltzman, E., Stievenard, M., 1999. Climate and atmospheric history of the past 420,000 years from the Vostok ice core, Antarctica. *Nature* 399 (6735), 429–436.
- Radić, V., Hock, R., 2011. Regionally differentiated contribution of mountain glaciers and ice caps to future sea-level rise. *Nature Geoscience* 4 (2), 91–94.
- Rahmstorf, S., 2007. A semi-empirical approach to projecting future sea-level rise. *Science* 315 (5810), 368–370.
- Rahmstorf, S., Foster, G., Cazenave, A., 2012. Comparing climate projections to observations up to 2011. *Environmental Research Letters* 7 (4), 044035.
- Schwikowski, M., Döscher, A., Gäggeler, H. W., Schotterer, U., 1999. Anthropogenic versus natural sources of atmospheric sulphate from an Alpine ice core. *Tellus* 51 (5), 1–14.
- Seki, O., Foster, G. L., Schmidt, D. N., Mackensen, A., Kawamura, K., Pancost, R. D., 2010. Alkenone and boron-based Pliocene pCO₂ records. *Earth and Planetary Science Letters* 292 (1-2), 201–211.
- Sigl, M., Jenk, T., Kellerhals, T., Szidat, S., 2009. Towards radiocarbon dating of ice cores. *Journal of Glaciology* 55 (194), 985–996.
- Thompson, L. G., Davis, M. E., Mosley-Thompson, E., Sowers, T. A., Henderson, K., Zagorodnov, V., Lin, P.-N., Mikhalevko, V. N., Campen, R. K., Bolzan, J. F., Cole-Dai, J., Francou, B., 1998. A 25,000-year tropical climate history from Bolivian ice cores. *Science* 282 (5395), 1858–1864.
- Thompson, L. G., Mosley-Thompson, E., 2011. A paleoclimatic perspective on the 21st century glacier loss on Kilimanjaro, Tanzania. *Annals of Glaciology* 52 (59), 60–68.
- Thompson, L. G., Mosley-Thompson, E., Davis, M. E., Bolzan, J. F., Dai, J., Klein, L., Yao, T., Wu, X., Xie, Z., Gundestrup, N., 1989. Holocene–late Pleistocene climatic ice core records from Qinghai-tibetan plateau. *Science* 246 (4929), 474–477.
- Thompson, L. G., Mosley-Thompson, E., Davis, M. E., Zagorodnov, V. S., Howat, I. M., Mikhalevko, V. N., Lin, P.-N., 2013. Annually resolved ice core records of Tropical climate variability over the past ~1800 years. *Science* 340 (6135), 945–950.

1 Introduction

- Thompson, L. G., MosleyThompson, E., Dansgaard, W., Grootes, P. M., 1986. The Little Ice-Age as recorded in the stratigraphy of the Tropical Quelccaya ice cap. *Science* 234 (4774), 361–364.
- Trenberth, K. E., Hoar, T. J., 1997. El Niño and climate change. *Geophysical Research Letters* 24 (23), 3057–3060.
- von Storch, H., Zorita, E., Jones, J. M., Dimitriev, Y., Gonzalez-Rouco, F., Tett, S., 2004. Reconstructing past climate from noisy data. *Science* 306 (5696), 679–682.
- Wallace, J. M., Fu, Q., Smoliak, B. V., Lin, P., Johanson, C. M., 2012. From the Cover: Simulated versus observed patterns of warming over the extratropical Northern Hemisphere continents during the cold season. *Proceedings of the National Academy of Sciences* 109 (36), 14337–14342.
- Wallace, J. M., Gutzler, D. S., 1981. Teleconnections in the geopotential height fields during the Northern Hemisphere winter. *Monthly Weather Review* 109 (4), 784–812.
- Wanner, H., Beer, J., Bütikofer, J., Crowley, T. J., Cubasch, U., Flückiger, J., Goosse, H., Grosjean, M., Joos, F., Kaplan, J. O., Küttel, M., Müller, S. A., Prentice, I. C., Solomina, O., Stocker, T. F., Tarasov, P., Wagner, M., Widmann, M., 2008. Mid- to Late Holocene climate change: an overview. *Quaternary Science Reviews* 27 (19-20), 1791–1828.
- Yao, T., Wang, Y., Liu, S., Pu, J., Shen, Y., Lu, A., 2004. Recent glacial retreat in High Asia in China and its impact on water resource in Northwest China. *Science in China Series D: Earth Sciences* 47 (12), 1065–1075.
- Zemp, M., Haeberli, W., Hoelzle, M., Paul, F., 2006. Alpine glaciers to disappear within decades? *Geophysical Research Letters* 33 (13), L13504.

2 Regional setting

The aim of this chapter is to put the results of this study in a geographical and scientific context and to address open questions of the current understanding of the regional climate. Topics treated in this chapter are directly or indirectly related to ice core science. The Altai stretches over four countries (China, Kazakhstan, Mongolia and Russia, Fig. 2.1), which render a comprehensive and overall investigation difficult, because crossing the borders involves major administrative efforts, especially while travelling with equipment required for fieldwork. During the existence of the U.S.S.R. most of the studies have been published in Russian, limiting the access to their results. Thus, some incompleteness or biased explanation may occur.

This chapter is separated in four parts. First, two field campaigns conducted within this project are presented. Second, the geography, including some simplified geology, the present glacier extent, and the hydrology is introduced. The third part discusses the climate and the weather system affecting the Altai. The fourth part summarizes available paleoclimate records of the Altai and the surrounding mountain ranges.

2.1 Drilling expedition

A reconnaissance expedition to drill a shallow ice core was planned for summer 2008. The goal was to clarify open questions prior to carrying out a deep drilling campaign in such a remote area. The open questions were:

- Can a glacier suitable for ice core reconstruction be found?
- Is the geometry of the glacier suitable for ice core drilling?
- What is the ice thickness?
- Are the geochemical species and stable isotopes preserved in the ice?
- Does the logistics allow transport of the ice frozen from the glacier to the PSI?

2 Regional setting



Figure 2.1: Location of the different mountain ranges, countries and rivers of Central Asia mentioned in the text (map composed with <http://www.geomapapp.org>).

Due to logistical problems the reconnaissance study had to be cancelled. Nevertheless, the plan for a deep-drilling campaign was maintained for the summer 2009. Thus potential drill sites had to be pre-selected and rated with maps and satellite-images (Fig. 2.2 & 2.3). It was planned to take the final decision in the field. Tsambagarav massif was pre-selected due to a study conducted in 1991, showing preserved water stable isotope records at Tsast Uul (Schotterer et al., 1997), the highest point of the massif. Flat-top mountains, high elevation of glaciers and suitable geometry (Tsutomu and Davaa, 2007) makes this region interesting for ice core drilling.

2.1.1 Deep drilling campaign in 2009

The deep drilling campaign was conducted between the 20th of June and the 14th of July 2009. The expedition members were flown from Barnaul to the Tsambagarav massif with a stopover in Aktash. During the overflight of the massif, the glaciation of the Tsast Uul

2.1 Drilling expedition

ice cap (highest point of the massif) appeared less suitable for drilling. It is strongly asymmetric with a steep ice face directly north of the summit. Additionally, poor visibility hampered the access to the summit with the helicopter. Preliminary radio echo sounding on Khukh Nuru Uul, the second highest ice cap in the Tsambagarav massive, provided a glacier depth of 70 m. On the basis of those parameters it was decided to drill at Khukh Nuru Uul (48°39.34 N, 90°50.83 E, 4130 m asl). From the 3th to 10th July 2009, a 72 m surface-to-bedrock ice core and a 52 m parallel core were drilled with the Fast Electromechanical Lightweight Ice Coring System (FELICS, Ginot et al. 2002). The parallel core did not reach bedrock because of time constraints. Additionally, a snow pit and two snowfall-events were sampled (Table 9.2). Simultaneous to the drilling ice thickness measurements were performed with radio echo soundings (Malå Ground Penetrating Radar (GPR) system with 100 and 200 MHz unshielded antennas), combined with a GPS survey. In total 2030 m of radar profiles were measured with roughly half of the profiles located on the summit of Khukh Nuru Uul to construct a detailed map of the bed topography around the drill site (Fig. 4.2). Details of the glaciological survey are described in Section 4.3.2. After drilling, a thermistor chain was lowered in the borehole for 24 hours to measure ice temperature at different depths (Fig. 4.3). The ice was then transported frozen to PSI via Barnaul. In the remainder of this thesis the term *Tsambagarav ice core* is used when referring to the ice core from Khukh Nuru Uul glacier.

2.1.2 Reconnaissance expedition 2011

The dating of the 2009 Tsambagarav ice core revealed strong thinning and consequently prevented very high-resolution reconstruction in the deepest part. For higher resolved records, the idea of a second ice core from a thicker Mongolian Altai glacier arised. Additionally, cross validation of the first record and investigation of further climate driven processes, e.g. reconstruction of desertification history, would allow for new and unique scientific perspectives in this remote area.

A joint Russian-Swiss expedition was planned for June 2011. The fieldwork had two distinct goals: First, investigating the suitability of the Sutai Uul Mountain (46°37 N, 93°36 E, 4210 m asl, 2.3) for deep drilling, and second re-measure the 2009 borehole temperature and determine accumulation in 2010 on Tsambagarav glacier. The Sutai Uul located north-west of the Gobi desert with presumably lower accumulation rates than Tsambagarav glacier was considered as an ideal site for ice core based climate reconstruction. The aim was to assess the thickness and the topography of the ice

2 Regional setting

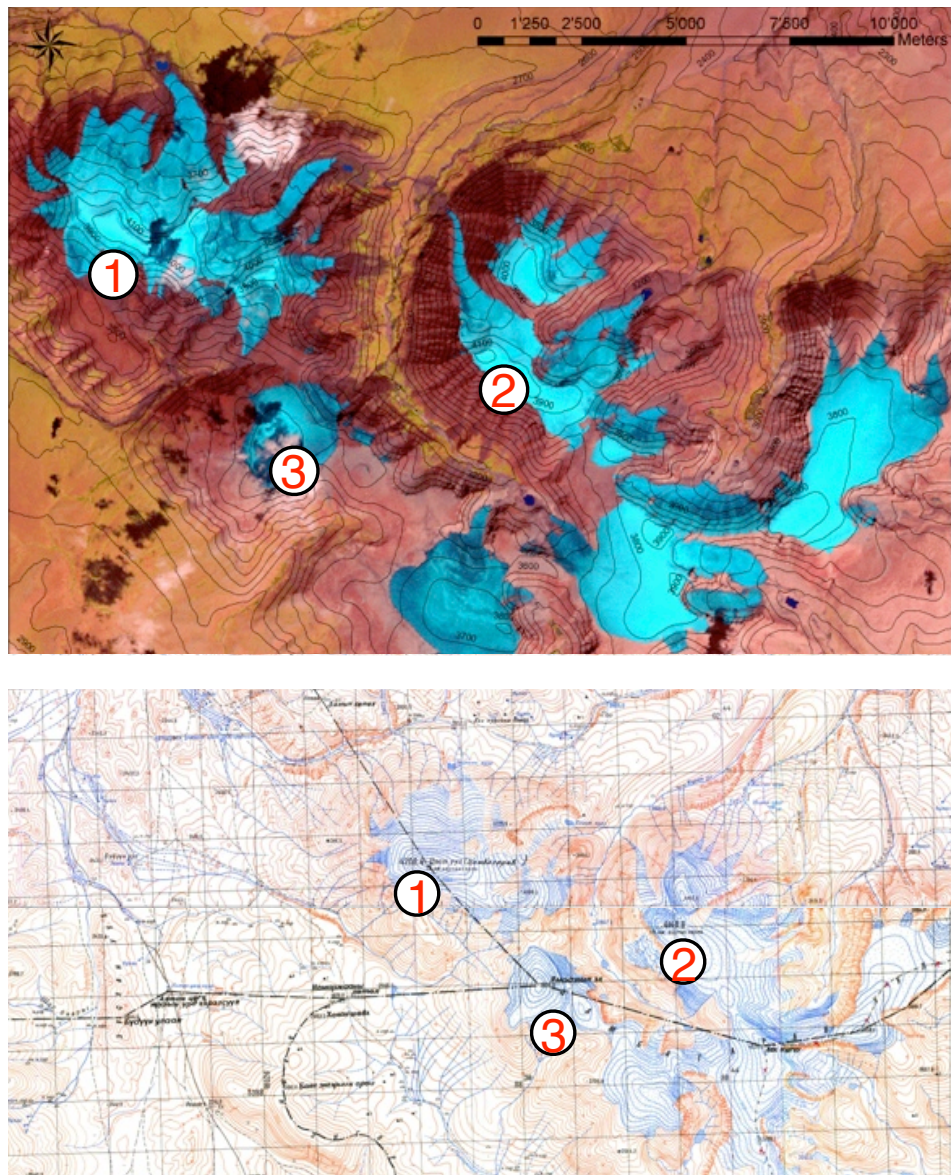


Figure 2.2: Landsat images with SRTM DHM elevations (solid lines 100 m intervals, *top*) and U.S.S.R. maps (*bottom*) of the Tsambagarav massif. ①-③: pre-selected sites for potential deep drilling. ① Tsast Uul summit, ② Khukh Nuru Uul, ③ unnamed summit.

cap with GPR. Snow pit data should provide estimates of annual accumulation and abundance of surface melting on the glacier. Because the GPR devices arrived with a delay of six weeks they could not be deployed during the expedition and the glaciology survey had to be cancelled. Nevertheless, a snow pit was dug on the summit of Sutai

2.2 Geography of the Altai Mountains

Uul and the samples were analyzed (Table 9.3). The topography of the summit was confirmed to be excellent for drilling. The summit of Sutai Uul is a concentric ice cap. Estimation of ice thickness ranges between 80 to 120 m. The assumption of lower annual accumulation rates is supported by higher concentrations of major ions in the snow pit compared to the last 10 years at Tsambagarav. The depth (60 cm) of the snow pit neither allows for counting annual layers nor confirms a preserved climate signal. Referring to Chapter 4 the Sutai Uul most probably melted completely during the HCO, thus the climate record would not be longer but rather higher resolved compared to the Tsambagarav ice core (Herren et al., 2013). Massive ice lenses were found in the snow pit, preventing sampling of the deeper snow. The melt features are stronger than on the more northerly located Tsambagarav, and probably alter the chronological storage of the climate signal. Finally, logistics are challenging in this area: GPR and GPS arrived with a large delay and roads in western Mongolia are not suitable for the transport of ice cores. Helicopter support from Russia would be a prerequisite for a potential drilling expedition. However, Sutai Uul is located further away from the Russian border making it difficult and expensive to organize helicopter flights. The delayed delivery of the GPR affected the schedule of the expedition. Thus the re-measurement of the borehole temperature and determination of 2010 accumulation at Tsambagarav had to be cancelled as well.

2.2 Geography of the Altai Mountains

The Altai Mountain system is located in the northern part of Central Asia, a geographical vast region, which covers a variety of mountain systems such as the Himalayas, Tibetan Plateau, Altai, Tien Shan, Pamir and Karakoram (Fig. 2.1). The mountain ranges experience diverse climatic conditions ranging from intense monsoon rainfall in the Himalayas, extreme dryness in the Karakoram, to pronounced continental conditions with seasonal differences of 40°C in the Altai (Rupper et al., 2009; Bolch et al., 2012). Despite the distance and the different weather conditions all these ranges contain glaciated areas even though in different extent. These glaciers respond differently to climatic changes such as variation in radiation, and changes in precipitation as well as temperature. Accordingly ice core based paleoclimatic investigations will aim for different objectives given by the study site selected. While the Himalayas and the Tibetan Plateau can be used to investigate changes in the northward intrusion and intensity of the monsoon (Kaspari et al., 2007; Thompson, 2000), studies in the Tien Shan Mountains reconstruct past synoptic conditions and air pollution based on different geochemical species (Kreutz and Sholkovitz, 2000). Of all these mountain ranges the Altai is least known and experienced

2 Regional setting

limited scientific attention.

The different mountain ranges building the Altai stretch over approximately 1200 km (Fig. 2.3). The range is in general classified in three parts, the western Russian Altai, the southern Chinese Altai and the eastern Mongolian Altai (Lehmkuhl et al., 2011). To the north are the large Siberian forest planes, to the south the Gobi and Dzungarian desert. The northeast foothills of the Russian Altai are linked to the Sayan Mountains, whereas the southeast part extends into the Gobi Altai. To the east the so-called Valley of the Great Lakes leads over to the Khangay Mountains (Fig. 2.3).



Figure 2.3: Location of the different sites mentioned in the text. ① Tsambagarav, ② Belukha, ③ Sutai Uul, ④ Lake Hoton Nuur, ⑤ Lake Akkol & Lake Grusha, ⑥ Lake Uzunkol & Lake Kendegeulukol, ⑦ Lake Telmen, ⑧ Uvs Nuur, ⑨ Lake Teletskoye, ⑩ Tarvagatay, ⑪ Sol Dav. Map modified from Klinge (2001).

V-shaped valleys dominate the relief in the Russian and the northern Chinese Altai. The highest elevations of the Altai are located in this part, with the summits of Belukha and Tavan Bogd, having altitudes of 4506 and 4374 m asl, respectively. Moving east towards Mongolia, the landscape changes into vast plains interrupted by isolated mountain systems separated by glacial cirques and U-shaped troughs. The altitude of the plains

2.2 Geography of the Altai Mountains

ranges approximately from 1400 to 2500 m asl, while the mountain tops reach up to 4000 m asl. Their foothills are in general wide with gently inclined ridges. Due to the rather dry climate with relatively warm summers the climatic snow line is located at high elevations of 3500 to 3900 m asl. In general glaciation in the Altai is confined to the highest elevations and includes Plateau glaciers, cirque glaciers, isolated ice patches and several smaller valley glaciers. The current status of the glaciers in the Altai has been discussed in various publications (e.g., Klinge et al., 2003; Klinge, 2001). For the Russian Altai the glaciated area is greater than 900 km² (Bussemer, 2001), approximately 300 km² in the Chinese Altai (Shi, 1992) and between 500 and 850 km² in the Mongolian Altai (Klinge, 2001; Arendt et al., 2012). The current ELA varies strongly depending on precipitation and location of the glaciers. Table 2.1 summarizes different ELA estimations in the Altai.

Table 2.1: Estimation of ELA for the Russian (1), Mongolian (2-5) and Chinese Altai (7) together with Khangay Mountains (6) from Lehmkuhl et al. (2011).

Mountain massif	Peak Elevation [m asl]	Ice margin [m asl]	ELA [m asl]
1. Chuja Mountains	3936	2350-2700	3150-3300
2. Ikh-Türgen	4029	3100	3500
3. Türgen Khairkhan	3966	2900-3200	3500
4. Tsambagarav Uul	4208	3300-3600	3700
5. Munk Khairkhan	4204	3300-3500	>3700
6. Otgon Tenger (Khangay)	3905	3400-3600	3750
7. Tavan Bogd (Chinese Altai)	4374	2416	3300

Glacier fluctuation studies in this region are mainly limited to the Pleistocene and describe the Last Glacial Maximum (LGM) (Lehmkuhl, 1998; Lehmkuhl et al., 2011). For the Mongolian Altai the understanding of Holocene glacier variations and their future evolution in a changing climate is still incomplete (Lehmkuhl, 2012; Komatsu et al., 2000). Agatova et al. (2012) presents to our knowledge the only study describing Holocene glacier fluctuation in the Russian Altai and refutes the hypothesis of continuous glacier shrinkage since the LGM. The work is based on lichenometry, geomorphological methods and radiocarbon dates of formerly buried wood pieces. Reconstructed timberline in currently glaciated area indicates substantial glacier retreat or even complete deglaciation during the Holocene Climate Optimum (HCO), a warm interval \sim 8 kyr ago. A study described later in this work (Herren et al. (2013), see Chapter 4) stipulates total glacier disappearance in the majority of the Mongolian Altai during the HCO succeeded by an advance 6 kyr ago.

Studies describing the present glaciological situation are rare and generally concentrate

2 Regional setting

on single glaciers rather than a mountain system. The extreme continental climate of Siberia results in low winter precipitation (Section 2.3). Since glaciers in the Mongolian Altai are located at high elevations they are supposed to receive considerable accumulation during summer, i.e. the time of the year where most of the precipitation falls, leading to simultaneous occurrence of the accumulation and ablation period (Dyurgerov and Meier, 1999). The sensitivity of such glaciers to climate warming is debated. Observations suggested that these glaciers are controlled by summer melt making them very vulnerable to temperature increase (Fujita and Ageta, 2000), whereas model studies predict smaller temperature dependence (Braithwaite et al., 2002). In the recent decades the investigations are in general constrained to the Russian Altai, with detailed mass balance observations of individual glaciers (Pattyn et al., 2003), or glacier change assessment for larger regions by means of satellite images and maps (Shahgedanova et al., 2010; Surazakov et al., 2007). Glaciers in this area, like most glaciers on Earth, have retreated significantly over the last century (Dyurgerov and Meier, 2000). It has been shown that they respond strongly to increased summer temperature and thus the remaining cold glaciers may change their regime from cold glaciers to a polythermal glaciers (Pattyn et al., 2003). This transition is of major importance regarding ice core science since a polythermal glacier may not preserve the climate signal and thus loses its suitability as climate archive. However, depending on the region the glaciers seem to respond in different ways to global warming. A further study based on satellite images and historical maps demonstrates diverging shrinkage rates between the Mongolian and the Russian/Chinese Altai for the period 1940 to 2000. While the Mongolian glaciers showed no or little shrinkage, the region north and west experienced steady shrinkage (Tsutomu and Davaa, 2007). However, the number and thickness of ice lenses identified in the Tsambagarav ice core increased during the last decades (see Chapter 6). This indicates changes in the mass balance of the glacier. Although, these changes cannot be directly linked to glacier variation and extrapolated to all Mongolian glaciers, they still suggest shrinkage of the glacier as observed for most of the glaciers on earth (Oerlemans, 2005). A comprehensive description of the current status of Altai glaciers and their changes in a future warmer climate, requires additional investigations, especially for the Chinese and Mongolian part of the mountain system.

During the melt season glaciers provide a permanent supply of fresh water. This is particularly important for the arid Mongolian Altai. The mountain range in its entirety acts as a watershed. In the Russian Altai the major rivers are Irtysh, Ob and Jenissei (Fig. 2.1). These very large rivers drain into the Arctic Ocean. The Irtysh flows into

the Ob in Chanty-Mansijsk, together they are among the longest rivers on earth. The annual discharge at the estuary is 12,759 m³/s (Yang et al., 2004). Although they collect water from different areas, their springs are located in the Altai. This makes the Altai the moated castle for a large part of Siberia and underlines the importance of the Altai glaciers on large areas thousands kilometers distant (Yang et al., 2004). In contrast, the Mongolian Altai has internal drainage systems into huge shallow lakes such as Uvs Nuur and Hyargas Nuur, located in western Mongolia (Fig. 2.3). The permanent supply of fresh water is very important in this arid climate. Lakes with no discharge are salty (e.g. Uvs Nuur, Hyargas Nuur) whereas others are freshwater reservoirs. The surroundings are often protected sites due to the occurrence of rare wildlife¹. These lakes provide the opportunity to extract paleoclimatic information through lake sediments as discussed in Section 2.4.

2.3 Climate of the Altai

The Altai experiences a continental climate with cold and dry winters and relative warm summers. Temperature differences between the two seasons are up to 40°C. The Siberian High (SH) is an anticyclone centered over Eurasia (40-65°N, 80-120°E) (Sahsamanoglou et al., 1991) and controls the winter weather in the Altai (Klinge et al., 2003). The SH is maintained by radiative cooling over snow-covered Asia, associated with large-scale descending motion (Ding and Krishnamurti, 1987). The anticyclone prevents winter precipitation in the Mongolian Altai, whereas few intrusions of Westerlies can result in precipitation in the Russian Altai (Klinge et al., 2003). Most of the precipitation occurs during summer.

The Altai acts as barrier for most of the humid air masses transported by the Westerlies, resulting in a strong northwest to southeast precipitation gradient (Klinge et al., 2003). Comparing weather station values (Fig. 2.4) and vegetation types on both sides of the mountain range illustrates this strong gradient.

In Barnaul on the northern side of the Altai annual precipitation is around 450 mm, whereas in Khovd only 120 mm are measured. In extreme cases the northwestern part receives more than 800 mm precipitation per year, whereas the driest part southeast (The Valley of the Great Lakes) receives less than 50 mm (Klinge et al., 2003). According to seasonal temperatures, winters in Western Mongolia are more rigorous than in the Siberian plains.

The mountain range acts as a watershed between the north and the south. This causes

¹<http://whc.unesco.org/en/list/769>

2 Regional setting

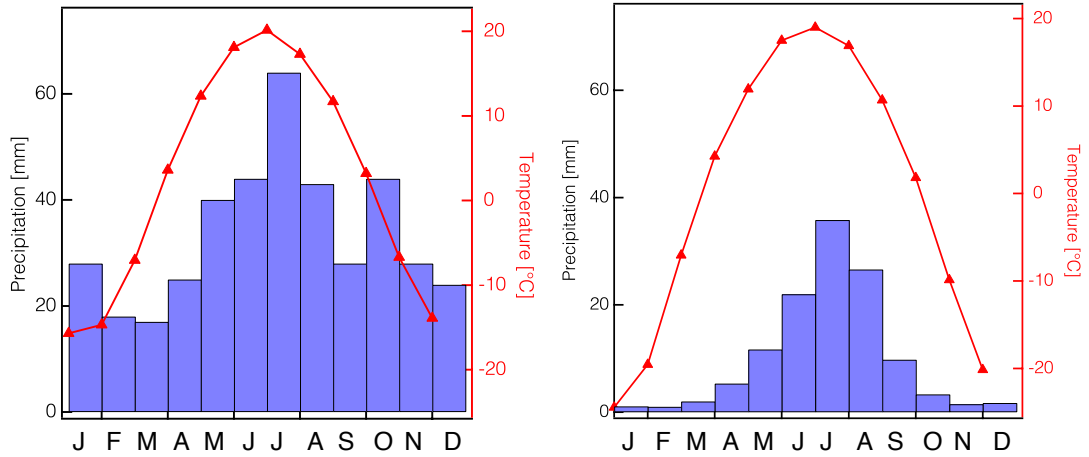


Figure 2.4: Climograph with temperature (red) and precipitation (blue bars) of the weather station Barnaul (1850-2000, *left*) and Khovd (1959-2008, *right*). Their locations are indicated in Fig.2.3.

the transition from the Siberian forest to the steppe-desert vegetation. Detailed comparison of water stable isotopes ($\delta^{18}\text{O}$ and δD) of a shallow ice core from the Belukha saddle with synoptic weather conditions allowed to attribute the origin of the air masses (Aizen et al., 2005). The degree of δD -excess and the $\delta^{18}\text{O}$ measured in the ice, were used for tracing the origin of the moisture. Thus the weather systems driving the precipitation in the Russian Altai could be attributed. Two thirds of the accumulation is of oceanic origin. More than 75% can be attributed to the Atlantic, whereas the remaining 25% are subdivided into Arctic and Pacific origins. The internal moisture component corresponds to one third and is related to the Aral-Caspian moisture basin (Aizen et al., 2005). On seasonal scale the contribution of the different sources varies. Summer precipitation is significantly correlated to stationary cyclones, which transport moisture from the Pacific Ocean to the Altai. The input of internal moisture sources such as the Caspian Sea increases during summer months. Fig. 2.5 illustrates the different trajectories of the moisture sources reaching the Altai (apart from the Indian Ocean).

The Mongolian Altai is located lee of the main moisture transport route (Fig. 2.5), thus precipitation attribution for the Russian Altai cannot be directly transferred. Additionally the seasonal distribution of precipitation is different between the northern and southern side of the Altai. In Khovd 70% of the precipitation is concentrated during the month June-July-August, whereas in Barnaul it is 37% (Fig. 2.4). A combined study using an isotope transport model and observations stipulates that the regions contributing to precipitation in Mongolia are central Asia and western Siberia (Sato et al., 2007),

corroborating findings of Aizen et al. (2005). The study excludes a monsoon influence on the water stable isotope signal in Mongolia. Compared to an intensively investigated area such as the Alps, where the origin of precipitation between the north and the south is still not fully understood (Sodemann and Zubler, 2009), the understanding of the synoptic systems controlling precipitation in the Mongolian Altai appears even more incomplete. Additional investigations are needed to understand the weather system in this region. An elaborate interpretation of the water stable isotopes from the Tsambagarav ice core might provide some further insights.

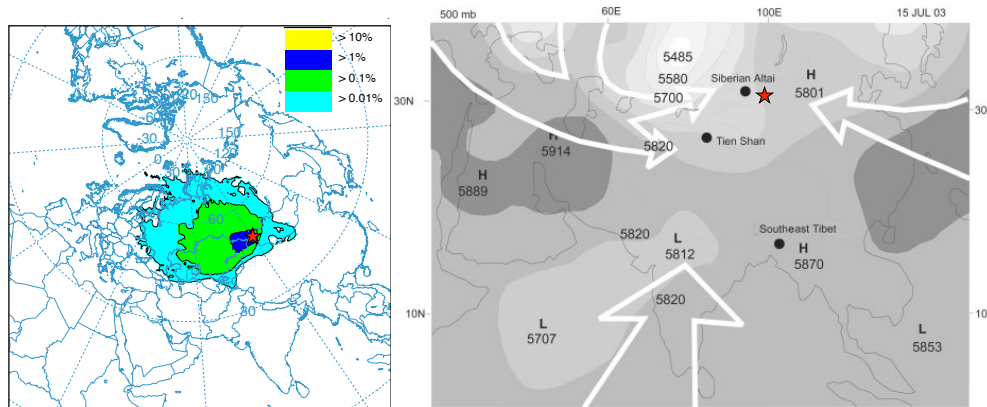


Figure 2.5: (left) Frequency plot of seven-day back trajectories for June, July, and August during the period 1991-2000 using HYSPLIT and the NCEP reanalysis data. Back trajectories were run every 6 hours. (right) Map of Central Asia with main trajectories of air masses bringing moisture to the Altai (apart from the Indian Ocean). Black points symbolize ice-coring sites. Graph from Aizen et al. (2006). Red stars symbolize the location of the Tsambagarav drill site.

2.4 Paleoclimatic studies from the Altai

The first scientific publications describing the formation of the Altai were geological studies to investigate mineral resources (Nechoroschew, 1966). In the following a variety of work has been published on Pleistocene glaciation especially related to the LGM in the Altai plus glacial lake outbursts or paleoshoreline fluctuations (e.g., Lehmkuhl et al., 2011; Rudoy, 2002; Komatsu et al., 2000). In this section the focus is on paleoclimate reconstructions dealing with the Holocene. Details of the different studies are presented in the references cited hereinafter. Three categories are introduced: Ice cores, lake sediment records, and tree-ring climate reconstructions.

2 Regional setting

2.4.1 Ice core

To our knowledge four ice cores have been retrieved in the Altai. At the Belukha mountain two ice cores have been drilled, the first in 2001 (hereinafter referred as BK01) at the saddle between the two summits (49°48'N, 86°34'E; 4062 m asl) (Olivier et al., 2003), the second in 2003 (hereinafter referred as BK03) at the West Plateau (49°49'N, 86°34'E; 4100 m asl) (Okamoto et al. (2011), Fig. 2.3). In 2008 a Chinese expedition drilled an ice core of 40.2 m in the Mongolian Altai (48°38'N, 90°58'E, H. Shugui personal communication²). The fourth ice core was collected during 2009 in the Tsambagarv massif and is the subject of this work.

Three temperature reconstructions have been proposed based on the two Belukha ice cores. Two are based on melt feature stratigraphy of the ice cores BK01 (AD 1815 to 2001) and BK03 (20th century, Henderson et al. (2006); Okamoto et al. (2011)). The comparison between the two ice cores shows high agreement in melt feature stratigraphy and confirms the representativeness of the melt features as temperature proxy in an ice core. Henderson et al. (2006) combined a $\delta^{18}\text{O}$ -record and the annual melt to show strong warming for the period AD 1816-2001. The third temperature reconstruction uses $\delta^{18}\text{O}$ as proxy (Eichler et al., 2009a). The study shows that there is a high correlation between $\delta^{18}\text{O}$ and solar forcing and suggests that the latter is a main driver for temperature variations during the period AD 1250-1850 (Fig. 2.6). For the industrial period this correlation holds no longer, indicating anthropogenically induced warming for this region.

The geochemical records of BK01 have been used to investigate past air composition, source variations and emission rates. The anthropogenic contribution to changes in air composition was reconstructed for the past centuries (Olivier et al., 2006; Eichler et al., 2009b). Emitted biogenic species are precursors of aerosols, which can significantly alter the regional radiation balance. Ice core records reconstructing aerosol composition beyond the observational period provide additional information to reduce uncertainties in the interaction between the climate and the different radiative forcing factors.

Ice core based reconstruction (BK01) of forest fire activity is a novel approach conducted by Eichler et al. (2011). With vast Siberian forest being located close to the drilling site, the geographical arrangement is appropriate for such reconstruction. A combination of geochemical records (K^+ & NO_3^-), pollen analysis and charcoal measurements were used to reconstruct the forest fire history of this region. A pronounced dry period (AD 1540-1600) preceded an interval of exceptionally high forest fire frequency (AD 1600-1689).

²http://news.xinhuanet.com/english/2008-08/28/content_9725932.htm

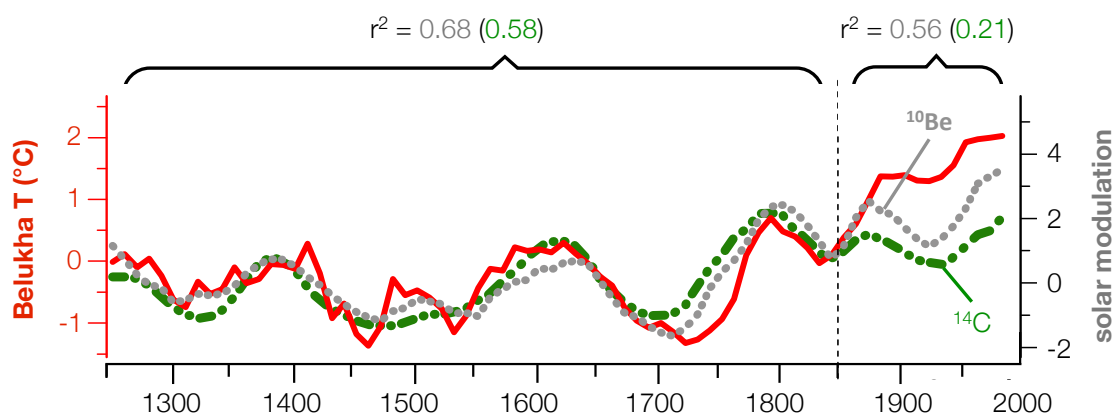


Figure 2.6: Comparison between reconstructed temperature from Belukha ice core (red) and solar modulation as proxy for solar activity inferred from ^{10}Be (grey) and ^{14}C (green) modified from Eichler et al. (2009a).

A teleconnection with the Pacific Decadal Oscillation (PDO) was suggested as trigger of this unprecedented combination. During the last 750 years the fire regime has been precipitation controlled and current global warming may affect this equilibrium (Eichler et al., 2011).

The reconstruction of mercury mining in Aktash was the initial motivation for the Belukha 2001 ice core project (Baeyens et al., 2003; Eyrikh et al., 2003). During the 18th century the Altai was the biggest silver supplier worldwide. The October Revolution 1917 and the subsequent U.S.S.R. initiated mining of Pb, Zn, Cu and Au (Nechoroschew, 1966). With the economic crisis towards the end of the U.S.S.R. the mining in the Russian Altai decreased substantially. With the collapse of the U.S.S.R., records of the history and quantity of extracted elements were lost. To investigate the magnitude of local former soil pollution environmental archives are required. A Pb concentration record from the BK01 for the period AD 1680-1995 is assumed to reflect Eastern European emissions (Eichler et al., 2012). The record shows an enhanced signal for AD 1935-1995 due to Pb additives in the gasoline. The subsequent decline was rather attributed to the economic crisis of the U.S.S.R. than a phase-out of the leaded gasoline. This record allowed to attribute 40% of the regional atmospheric Pb to the Rudny Altai mining (Eichler et al., 2012).

Several studies investigating biological parameters such as pollens, yeast or algae were conducted on the BK03 ice core. A method using small sample volume (10 ml) to analyze pollen species proved to be useful for dating by means of annual layer counting (ALC) (Nakazawa et al., 2004). The different species allow for precise separation of the sea-

2 Regional setting

sonal signal, facilitating the identification of the accumulation period (Nakazawa et al., 2011). DNA analysis of *Pinus* pollen deposited on the glacier demonstrate that they have the same origin as *Pinus* found in the immediate surroundings (Nakazawa et al., 2013). Yeast and algae on glacier surfaces may alter the radiative balance of the surface. Understanding the conditions facilitating their growth is crucial under current changing climate condition. Results from Uetake et al. (2011) suggest that surface melting is a major factor influencing yeast propagation. Detailed analysis of the alkanes allow to separate the different species in anthropogenic and biogenic sources (Miyake et al., 2006). Biological activity on the glacier surface is of major importance regarding the radiocarbon dating of the ice. As long as confined to the surface it will not alter the results, thereby an understanding of the processes is of the utmost importance.

Additionally, several shallow ice cores have been drilled on Belukha to test the suitability of the sites. Some have been used to derive the moisture source of the glaciers (see Section 2.3).

A shallow ice core was recovered at the summit of Tsast Uul (Fig. 2.2 and Fig. 2.3) during summer 1991 to investigate the isotopic composition of Mongolian glaciers (Schotterer et al., 1997). The study indicated that summer precipitation in the Mongolian Altai has a more important contribution of re-evaporated continental moisture sources than the Siberian Altai. This study and the work of Aizen et al. (2005) suggest that the water stable isotope signal bears hydrometeorological information that can be used to investigate the source of the atmospheric moisture.

2.4.2 Lake sediments

A variety of lakes have been cored in the surroundings of the Altai to examine their suitability for paleoclimate reconstruction. Lakes located within a reasonable perimeter of the Altai are presented together with their paleoclimatic interpretation. The focus is set on quantitative Holocene reconstructions. Pleistocene reconstructions such as from Lake Baikal (Prokopenko et al., 2006) are out of scope. The reconstructions are classified in two geographical regions, the Altai Mountains and the Northern Mongolian plateau (Wang and Feng, 2013).

Altai Mountains

The Holocene composite-lake-sediment-humidity record exhibits three phases: First rapid increase in humidity around 10 cal kyr BP, followed by wet conditions for four millennia. The third period (6 cal kyr BP to present) shows gradual decrease in humidity (Fig.

2.7, Wang and Feng 2013). The phases one and two give strong evidence through small uncertainties in the reconstruction. The records used to build this composite are briefly introduced in the following.

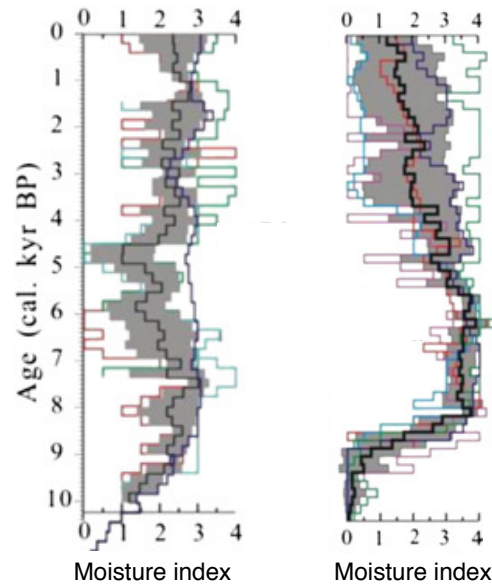


Figure 2.7: Moisture composite record from lake sediments in the Altai Mountains (*left*) and the Northern Mongolian Plateau (*right*). High moisture index corresponds to high moisture. Modified from Wang and Feng (2013).

Hoton-Nur ($48^{\circ}41'N$, $88^{\circ}19'E$, 2083 m asl) is a freshwater lake in the Mongolian Altai (Fig. 2.3), covering an area of 50.1 km^2 with an average depth of 26.6 m (Tarasov et al., 1994). A first core from 1980 analyzed with a coarse resolution suggests a warmer regional climate in the early-mid-Holocene followed by a shift towards drier environments during the late Holocene (Tarasov et al., 2000). A second core was retrieved during summer 2004 for fine-resolution palynological and diatom analyses to allow quantitative reconstructions of the Holocene lacustrine environments, vegetation and climate (Rudaya et al., 2009). The reconstruction suggests noticeable increase in precipitation from 200-250 mm/yr to 450-550 mm/yr at about 10 kyr BP. After 5 kyr BP precipitation decreased to 250-300 mm/yr. These findings agree well with the accumulation reconstruction from the Tsambagarav ice core (see Section 4.6). According to the two reconstructions the Mongolian Altai experienced relative wet conditions during the early Holocene (5-10 kyr BP), followed by dry conditions in the late Holocene (5 kyr to present). This trend coincides with a suggested shift of the intertropical convergence zone (ITCZ) during the

2 Regional setting

transition period (Wanner et al. (2008), Fig. 2.8).

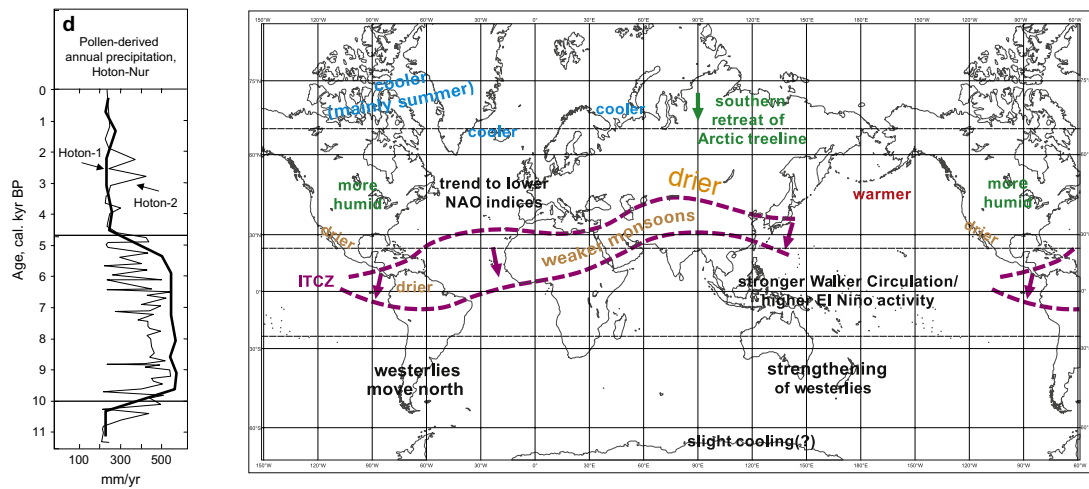


Figure 2.8: (left) Reconstruction of annual precipitation from pollen records of Hoton-Nuur (modified from Rudaya et al. 2009). (right) Global climate change for the preindustrial period (AD 1700) compared to the Mid Holocene (6 cal kyr BP) and suggested ITCZ-shift (modified from Wanner et al. 2008).

Akkol (50.25°N 89.62°E, 2204 m asl) and **Grusha** (50.38°N 89.42°E, 2413 m asl): The two lakes are less than 10 km apart (Fig. 2.3). Both are small lakes with areas smaller than 2 km². In the early Holocene (12 cal kyr BP) the pollen diagram of Lake Grusha suggests a dry and warm climate. This is supported with Lake Akkol being dry. At around 11 cal kyr BP both lakes show an increase in humidity. From 6 cal kyr BP onwards a cold and arid climate was dominating (Blyakharchuk et al., 2007).

Uzunkol (50.48°N 87.10°E, 1985 m asl) and **Kendegelukol** (50.50°N 87.63°E, 2050 m asl): The lakes are situated in the Russian Altai (Fig. 2.3). Coring was conducted during summer AD 2000. Based on pollen analysis the beginning of the Holocene (11 cal kyr BP) experiences a warm and wet climate. Changing pollen composition indicates a shift towards a cooler and drier climate from about 7.5 cal kyr BP onwards (Blyakharchuk et al., 2004).

Northern Mongolian Plateau

The composite lake sediment record compiled from sources from the Mongolian plateau, shows that both, the early Holocene and the late Holocene are characterized by relatively wet (and also probably cool) climates (Wang and Feng (2013), Fig. 2.7). The humidity trends are different from the Altai data. This illustrates the heterogeneity of the regional

climate and calls for additional data for a comprehensive understanding of the precipitation driving forces in Mongolia. For this region only the Lake Telmen record is further discussed, the other reconstructions being located far of the Altai Mountains.

Lake Telmen (48.83°N 97.33°E, 1789 m asl) has an average water depth of 13 m and a surface of 194 km² (Fig. 2.3). Palynological and sedimentological data allow a qualitative reconstruction of moisture changes for the mid to the late Holocene. The climate of the period 7.5-4.5 kyr ago was relatively arid. Maximum humidity is recorded between 4.5 and 1.6 cal kyr BP. The reconstruction suggests additional humid intervals during the Medieval Warm Period (AD 1000-1300) and the Little Ice Age (AD 1500-1900) (Fowell et al., 2003). Sedimentological and geomorphical evidence confirm those reconstructions (Peck et al., 2002).

Various records

Two additional records not considered in the composite record by Wang and Feng (2013) are discussed in the following. Uvs Nuur Lake (50.38°N 92.20°E, 759 m asl) is mentioned in this chapter because it is the largest lake of Mongolia. No sediment core is available from this shallow salty lake. Instead, shoreline fluctuations indicate changes in precipitation. Mid-Holocene shoreline elevation suggest a humid climate, falling lake levels during the second half of the Holocene point to lower temperatures and less precipitation from 5 ka BP onward (Grunert et al., 2000).

Lake Teletskoye is located in the Russian Altai (Fig. 2.3). With an average depth of 174 m (330 m at the deepest point), a length of 78 km and a width of only 3-5 km its properties are very different to the shallow Mongolian Altai lakes. Two cores were collected the first in 2001 and the second in 2002 from the deepest part of the lake. Using X-ray fluorescence and X-ray density, 800-year temperature and precipitation reconstructions were presented. These annual records show trends in climatic variability over the past 800 years similar to Northern hemispheric reconstructions (Kalugin et al., 2007). Pollen analysis of the same core documents climate-related vegetation history for the past millennium. Around AD 1020 climate conditions were similar to modern, followed by a short dry period with increased fire activity (AD 1100 to 1200). Climate became more humid with probably higher temperatures than present until AD 1410. Pollens suggest a decrease in precipitation for the period AD 1410 to 1560. During the Little Ice Age (AD 1560 and 1820) a cold and arid climate prevailed. From AD 1840 the pollen data is consistent with the instrumental data from the Barnaul meteorological station (Andreev et al., 2007).

2.4.3 Tree-rings

Tree-ring based paleoclimatic reconstructions have annual resolution and are therefore often used to extend instrumental data. For this reason they provide useful information for a region with temporally limited and spatially sparse instrumental data, such as Mongolia. The Mongolian American Tree Ring Project (MATRIP) is collecting tree-ring samples since 1995 and accelerated the paleoclimatic investigation in Mongolia. Different available reconstructions are presented in the following.

A tree-ring temperature chronology near Tarvagatay-Pass, Mongolia (48.29°N 98.93°E, 2450 m asl, Fig. 2.3) for the past 450 years shows strong temperature increase for recent decades (Jacoby et al., 1996). Relative to the past 450 years actual temperature evolution is unprecedented. This initial study demonstrated that annual ring width of trees in this region is sensitive to temperature variation and paved the way for further temperature reconstructions. A 1738 years-long temperature record inferred from tree-ring widths at Solongotyn Davaa (Sol Dav, 2420 m asl), suggests the warmest conditions of the past millennium during the recent decades; whereas the most severe cold occurred in the 19th century (D'Arrigo et al., 2001). A preliminary study for the Sayan-Altai Mountains contains the period AD 78 to 2006 (Mygland et al., 2008). The record is illustrated with the Sol Dav chronology in Fig. 2.9. The records are very similar, resulting in a coherent temperature reconstruction. The LIA appears temporally more extended but the temperature deficit is less pronounced than in the Sol Dav chronology. The cold interval around AD 540 is identifiable in both long-term records, indicating a severe cooling with regional effects. A regional-scale composite of four tree-ring width records from alpine sites in Mongolia for the period AD 1450 to 1998, confirms the accelerated warming in recent decades and corroborates indications of unusual warming during the twentieth century (D'Arrigo et al., 2000).

A drought reconstruction for Mongolia reveals the main summer moisture patterns of the past 470 years (Davi et al., 2010). The record is composed of chronologies, representing the different regions of the country. Actual measured droughts at the end of the 20th century are extreme relative to the past several hundred years, as shown by the Palmer Drought Severity Index (PDSI) reconstruction (Fig. 2.9). This drought reconstruction can be used to better understand climate variability in Mongolia and identify the major forcings of the climate.

Mongolian combined with North American tree-ring chronologies have been used to investigate the long-term variability of the Siberian High (D'Arrigo et al., 2005). The Siberian High (SH) index for the period AD 1599-1980 confirms the decline identified in

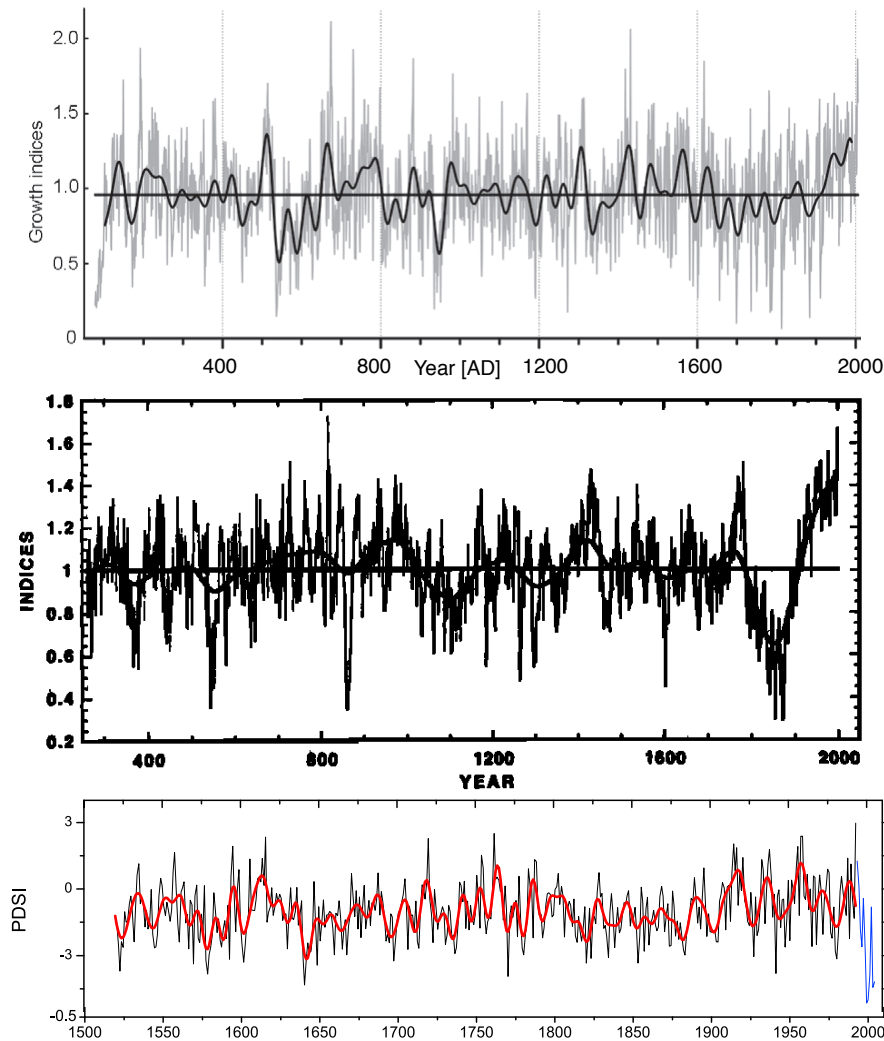


Figure 2.9: (*top*) Tree-ring chronology from the Sayan-Altai region: annual (grey) low-frequency smoothed (black) (modified from Mygland et al. 2008). (*middle*) Sol Dav record (modified from D’Arrigo et al. (2001)). (*bottom*) PDSI reconstruction of Mongolia based on tree rings combined with actual values (modified from Davi et al. 2010).

the instrumental SH index since the late 1970s, related to Eurasian warming. Teleconnections with different atmospheric features such as East Asian winter monsoon (EAWM) and the North Atlantic Oscillation (NAO) are expected but additional investigations are required for a complete understanding of the interactions.

Although a variety of records are available, a consistent understanding of the factors driving the climate of the Altai on the long-term is still missing. Asian temperature re-

2 Regional setting

constructions for the past two millennia are biased towards tree-ring widths (PAGES2k-Consortium, 2013). Additional studies can improve our understanding of the regional climate and help to put recent warming in a long-term perspective. This study is a step in this direction.

References

- Agatova, A., Nazarov, A., Nepop, R., 2012. Holocene glacier fluctuations and climate changes in the southeastern part of the Russian Altai (South Siberia) based on a radiocarbon chronology. *Quaternary Science Reviews* 43, 74–93.
- Aizen, V. B., Aizen, E., Fujita, K., Nikitin, S. A., Kreutz, K. J., Takeuchi, L. N., 2005. Stable-isotope time series and precipitation origin from firn-core and snow samples, Altai glaciers, Siberia. *Journal of Glaciology* 51 (175), 637–654.
- Aizen, V. B., Aizen, E. M., Joswiak, D. R., Fujita, K., Takeuchi, N., Nikitin, S. A., 2006. Climatic and atmospheric circulation pattern variability from ice-core isotope/geochemistry records (Altai, Tien Shan and Tibet). *Annals of Glaciology* 43 (1), 49–60.
- Andreev, A., Pierau, R., Kalugin, I., Daryin, A., Smolyaninova, L., Diekmann, B., 2007. Environmental changes in the northern Altai during the last millennium documented in Lake Teletskoye pollen record. *Quaternary Research* 67 (3), 394–399.
- Arendt, A., Bolch, T., Cogley, J., Gardner, A., Hagen, J.-O., Hock, R., Kaser, G., Pfeffer, W., Moholdt, G., Paul, F., Radic, V., Andreassen, L., Bajracharya, S., Beedle, M., Berthier, E., Bhambri, R., Bliss, A., Brown, I., Burgess, E., Burgess, D., Cawkwell, F., Chinn, T., Copland, L., Davies, B., De Angelis, H., Dolgova, E., Filbert, K., Forester, R., Fountain, A., Frey, H., Giffen, B., Glasser, N., Gurney, S., Hagg, W., Hall, D., Haritashya, U., Hartmann, G., Helm, C., Herreid, S., Howat, I., Kapustin, G., Khromova, T., Kienholz, C., Koenig, M., Kohler, J., Kriegel, D., Kutuzov, S., Lavrentiev, I., LeBris, R., Lund, J., Manley, W., Mayer, C., Miles, E., Li, X., Menounos, B., Mercer, A., Moelg, N., Mool, P., Nosenko, G., Negrete, A., Nuth, C., Pettersson, R., Racoviteanu, A., Ranzi, R., Rastner, P., Rau, F., Raup, H., Rich, J., Rott, H., Schneider, C., Seliverstov, Y., Sharp, M., Sigurdsson, O., Stokes, C., Wheate, R., Winsvold, S., Wolken, G., Wyatt, F., Zheltyhina, N., 2012. Randolph Glacier Inventory [v2.0]: A dataset of global glacier outlines. Global land ice measurements from space, Boulder Colorado, USA. Digital Media.

2.4 Paleoclimatic studies from the Altai

- Baeyens, W., Dehandschutter, B., Leermakers, M., Bobrov, V. A., Hus, R., Baeyens-Volant, D., 2003. Natural mercury levels in geological enriched and geological active areas: Case study of Katun river and Lake Teletskoye, Altai (Siberia). *Water air and soil pollution* 142 (1-4), 375–393.
- Blyakharchuk, T. A., Wright, H. E., Borodavko, P. S., van der Knaap, W. O., Ammann, B., 2004. Late Glacial and Holocene vegetational changes on the Ulagan high-mountain plateau, Altai Mountains, southern Siberia. *Palaeogeography, Palaeoclimatology, Palaeoecology* 209 (1-4), 259–279.
- Blyakharchuk, T. A., Wright, H. E., Borodavko, P. S., van der Knaap, W. O., Ammann, B., 2007. Late Glacial and Holocene vegetational history of the Altai Mountains (south-western Tuva Republic, Siberia). *Palaeogeography, Palaeoclimatology, Palaeoecology* 245 (3–4), 518–534.
- Bolch, T., Kulkarni, A., Kaab, A., Huggel, C., Paul, F., Cogley, J. G., Frey, H., Kargel, J. S., Fujita, K., Scheel, M., Bajracharya, S., Stoffel, M., 2012. The state and fate of Himalayan glaciers. *Science* 336 (6079), 310–314.
- Braithwaite, J. R., Zhang, Y., Raper, S. C. B., 2002. Temperature sensitivity of the mass balance of mountain glaciers and ice caps as a climatological characteristic. *Zeitschrift für Gletscherkunde und Glazialgeologie* 38 (1), 35–61.
- Bussemer, S., 2001. Jungquartäre Vergletscherung im Bergaltai und in angrenzenden Gebirgen—Analyse des Forschungsstandes. *Mitteilungen Geografische Gesellschaft München* 85, 45–64.
- D'Arrigo, R., Jacoby, G., Frank, D., Pederson, N., Cook, E., Buckley, B., Nachin, B., Mijiddorj, R., Dugarjav, C., 2001. 1738 years of Mongolian temperature variability inferred from a tree-ring width chronology of Siberian pine. *Geophysical Research Letters* 28 (3), 543–546.
- D'Arrigo, R., Jacoby, G., Pederson, N., Frank, D., Buckley, B., Nachin, B., Mijiddorj, R., Dugarjav, C., 2000. Mongolian tree-rings, temperature sensitivity and reconstructions of Northern Hemisphere temperature. *The Holocene* 10 (6), 669–672.
- D'Arrigo, R., Jacoby, G., Wilson, R., Panagiotopoulos, F., 2005. A reconstructed Siberian High index since A.D. 1599 from Eurasian and North American tree rings. *Geophysical Research Letters* 32 (5), L05705.

2 Regional setting

- Davi, N., Jacoby, G., Fang, K., Li, J., D'Arrigo, R., Baatarbileg, N., Robinson, D., 2010. Reconstructing drought variability for Mongolia based on a large-scale tree ring network: 1520–1993. *Journal of Geophysical Research* 115, 1–9.
- Ding, Y., Krishnamurti, T. N., 1987. Heat budget of the Siberian High and the winter monsoon. *Monthly Weather Review* 115 (10), 2428–2449.
- Dyurgerov, M. B., Meier, M. F., 1999. Analysis of winter and summer glacier mass balances. *Geografiska Annaler Series A-Physical Geography* 81A (4), 541–554.
- Dyurgerov, M. B., Meier, M. F., 2000. Twentieth century climate change: Evidence from small glaciers. *Proceedings of the National Academy of Science* 97 (4), 1406–1411.
- Eichler, A., Henderson, K., Olivier, S., Henderson, K., Laube, A., Beer, J., Papina, T., Gäggeler, H., Schwikowski, M., 2009a. Temperature response in the Altai region lags solar forcing. *Geophysical Research Letters* 36 (1), L01808.
- Eichler, A., Olivier, S., Brütsch, S., Papina, T., Schwikowski, M., 2009b. A 750 year ice core record of past biogenic emissions from Siberian boreal forests. *Geophysical Research Letters* 36 (18), L18813.
- Eichler, A., Tinner, W., Brütsch, S., Olivier, S., Papina, T., Schwikowski, M., 2011. An ice-core based history of Siberian forest fires since AD 1250. *Quaternary Science Reviews* 30 (9–10), 1027–1034.
- Eichler, A., Tobler, L., Eyrikh, S., Gramlich, G., Malygina, N., Papina, T., Schwikowski, M., 2012. Three centuries of Eastern European and Altai lead emissions recorded in a Belukha ice core. *Environmental Science and Technology* 46 (8), 4323–4330.
- Eyrikh, S., Schwikowski, M., Gäggeler, H. W., Tobler, L., Papina, T., May 2003. First mercury determination in snow and firn from high-mountain glaciers in the Siberian Altai by CV-ICP-MS. *Journal de Physique IV* 107 (Part 1), 431–434.
- Fowell, S. J., Hansen, B. C., Peck, J. A., Khosbayar, P., Ganbold, E., 2003. Mid to late holocene climate evolution of the lake Telmen basin, north central Mongolia, based on palynological data. *Quaternary Research* 59 (3), 353–363.
- Fujita, K., Ageta, Y., 2000. Effect of summer accumulation on glacier mass balance on the Tibetan Plateau revealed by mass-balance model. *Journal of Glaciology* 46 (153), 244–252.

2.4 Paleoclimatic studies from the Altai

- Ginot, P., Stampfli, F., Stampfli, D., Schwikowski, M., Gäggeler, H., 2002. FELICS, a new ice core drilling system for high-altitude glaciers. Proceedings of the workshop "Ice Drilling Technology 2000", Memoirs of National Institute of Polar Research, Special Issue 56, 38–48.
- Grunert, J., Lehmkuhl, F., Walther, M., 2000. Paleoclimatic evolution of theUvs Nuur basin and adjacent areas (Western Mongolia). *Quaternary International* 65–66, 171–192.
- Henderson, K., Laube, A., Gäggeler, H., Olivier, S., 2006. Temporal variations of accumulation and temperature during the past two centuries from Belukha ice core, Siberian Altai. *Journal of Geophysical Research* 111 (D3), D03104.
- Herren, P.-A., Eichler, A., Machguth, H., Papina, T., Tobler, L., Zapf, A., Schwikowski, M., 2013. The onset of Neoglaciation 6000 years ago in western Mongolia revealed by an ice core from the Tsambagarav mountain range. *Quaternary Science Reviews* 69 (C), 59–68.
- Jacoby, G., D'Arrigo, R., Davaajamts, T., 1996. Mongolian tree rings and 20th-century warming. *Science* 273 (5276), 771–773.
- Kalugin, I., Daryin, A., Smolyaninova, L., Andreev, A., Diekmann, B., Khlystov, O., 2007. 800-yr-long records of annual air temperature and precipitation over southern Siberia inferred from Teletskoye Lake sediments. *Quaternary Research* 67 (3), 400–410.
- Kaspari, S., Mayewski, P., Kang, S., Sneed, S., Hou, S., Hooke, R., Kreutz, K., Introne, D., Handley, M., Maasch, K., Qin, D., Ren, J., Jan. 2007. Reduction in northward incursions of the South Asian 1400 AD inferred from a Mt. Everest ice core. *Geophysical Research Letters* 34 (16), L16701.
- Klinge, M., 2001. Glazialgeomorphologische Untersuchungen im Mongolischen Altai als Beitrag zur jungquartären Landschafts- und Klimageschichte der Westmongolei. *Aachener Geographische Arbeiten* 35, Aachen, Deutschland, 125p.
- Klinge, M., Böhner, J., Lehmkuhl, F., 2003. Climate pattern, snow- and timberlines in the Altai Mountains, Central Asia. *Erdkunde* 57 (4), 296–308.
- Komatsu, G., Brantingham, P. J., Olsen, J. W., Baker, V. R., 2000. Paleoshoreline geomorphology of Böön Tsagaan Nuur, Tsagaan Nuur and Orog Nuur: the Valley of Lakes, Mongolia. *Geomorphology* 39 (3–4), 83–98.

2 Regional setting

- Kreutz, K. J., Sholkovitz, E. R., 2000. Major element, rare earth element, and sulfur isotopic composition of a high-elevation firn core: Sources and transport of mineral dust in central Asia. *Geochemistry Geophysics Geosystems* 1, 1–23.
- Lehmkuhl, F., 1998. Quaternary glaciations in central and western Mongolia. *Journal of Quaternary Science* 13 (6), 153–167.
- Lehmkuhl, F., 2012. Holocene glaciers in the Mongolian Altai: An example from the Turgen–Kharkhiraa Mountains. *Journal of Asian Earth Sciences* 52, 12–20.
- Lehmkuhl, F., Klinge, M., Strach, 2011. The extent and timing of Late Pleistocene Glaciations in the Altai and neighbouring mountain systems. In: Ehlers, J., Gibbard, P. L., Hughes, P. D. (Eds.), *Extent and Chronology – A Closer Look*. pp. 967–979.
- Miyake, T., Nakazawa, F., Sakugawa, H., Takeuchi, N., Fujita, K., Ohta, K., Nakawo, M., 2006. Concentrations and source variations of n-alkanes in a 21 m ice core and snow samples at Belukha glacier, Russian Altai mountains. *Annals of Glaciology* 43, 142–147.
- Mygland, V. S., Oidupaa, O. C., Kirilyanov, A. V., Vaganov, E. A., 2008. 1929-year tree-ring chronology for the Altai-Sayan region (Western Tuva). *Archaeology, Ethnology and Anthropology of Eurasia* 36 (4), 25–31.
- Nakazawa, F., Fujita, K., Uetake, J., Kohno, M., Fujiki, T., Arkhipov, S. M., Kameda, T., Suzuki, K., Fujii, Y., 2004. Application of pollen analysis to dating of ice cores from lower-latitude glaciers. *Journal of Geophysical Research* 109 (F4001), 1–6.
- Nakazawa, F., Miyake, T., Fujita, K., Takeuchi, N., Uetake, J., Fujiki, T., Aizen, V., Nakawo, M., 2011. Establishing the timing of chemical deposition events on Belukha glacier, Altai Mountains, Russia, using pollen analysis. *Arctic Antarctic and Alpine Research* 43 (1), 66–72.
- Nakazawa, F., Uetake, J., Suyama, Y., Kaneko, R., Takeuchi, N., Fujita, K., Motoyama, H., Imura, S., Kanda, H., 2013. DNA analysis for section identification of individual Pinus pollen grains from Belukha glacier, Altai Mountains, Russia. *Environmental Research Letters* 8 (1), 014032.
- Nechoroschew, W. P., 1966. *Geologie des Altai*. Fortschritte der sowjetischen Geologie, Akademie-Verlag Berlin 7.

- Oerlemans, J., 2005. Extracting a climate signal from 169 glacier records. *Science* 308 (5722), 675–677.
- Okamoto, S., Fujita, K., Narita, H., Uetake, J., Takeuchi, N., Miyake, T., Nakazawa, F., Aizen, V. B., Nikitin, S. A., Nakawo, M., 2011. Reevaluation of the reconstruction of summer temperatures from melt features in Belukha ice cores, Siberian Altai. *Journal of Geophysical Research* 116 (D2), D02110.
- Olivier, S., Blaser, C., Brüttsch, S., Frolova, N., Gäggeler, H., Henderson, K. A., Palmer, A. S., Papina, T., Schwikowski, M., 2006. Temporal variations of mineral dust, biogenic tracers, and anthropogenic species during the past two centuries from Belukha ice core, Siberian Altai. *Journal of Geophysical Research* 111 (D5), D05309.
- Olivier, S., Schwikowski, M., Brüttsch, S., Eyrikh, S., 2003. Glaciochemical investigation of an ice core from Belukha glacier, Siberian Altai. *Geophysical Research Letters* 30 (19), 1–3.
- PAGES2k-Consortium, 2013. Continental-scale temperature variability during the past two millennia. *Nature Geoscience* 6 (5), 339–346.
- Pattyn, F., De Smedt, P., De Brabander, S., Van Huele, W., Agatova, A., Mistrukov, A., Declerq, H., 2003. Ice dynamics and basal properties of Sofiyskiy glacier, Altai mountains, Russia, based on DGPS and radio-echo sounding surveys. *Annals of Glaciology* 37, 286–292.
- Peck, J. A., Khosbayar, P., Fowell, S. J., Pearce, R. B., Ariunbileg, S., Hansen, B. C., Soninkhishig, N., 2002. Mid to Late Holocene climate change in north central Mongolia as recorded in the sediments of Lake Telmen. *Palaeogeography, Palaeoclimatology, Palaeoecology* 183 (1–2), 135–153.
- Prokopenko, A. A., Hinnov, L. A., Williams, D. F., Kuzmin, M. I., 2006. Orbital forcing of continental climate during the Pleistocene: A complete astronomically tuned climatic record from Lake Baikal, SE Siberia. *Quaternary Science Reviews* 25 (23–24), 3431–3457.
- Rudaya, N., Tarasov, P., Dorofeyuk, N., Solovieva, N., Kalugin, I., Andreev, A., Daryin, A., Diekmann, B., Riedel, F., Tserendash, N., Wagner, M., 2009. Holocene environments and climate in the Mongolian Altai reconstructed from the Hoton-Nur pollen and diatom records: a step towards better understanding climate dynamics in Central Asia. *Quaternary Science Reviews* 28 (5–6), 540–554.

2 Regional setting

- Rudoy, A. N., 2002. Glacier-dammed lakes and geological work of glacial superfloods in the Late Pleistocene, Southern Siberia, Altai Mountains. *Quaternary International* 87 (1), 119–140.
- Rupper, S., Roe, G., Gillespie, A., 2009. Spatial patterns of Holocene glacier advance and retreat in Central Asia. *Quaternary Research* 72 (3), 337–346.
- Sahsamanoglou, S. H., Makrogiannis, T. J., Kallimopoulos, P. P., 1991. Some aspects of the basic characteristics of the Siberian anticyclone. *International Journal of Climatology* 11 (8), 827–839.
- Sato, T., Tsujimura, M., Yamanaka, T., Iwasaki, H., Sugimoto, A., Sugita, M., Kimura, F., Davaa, G., Oyunbaatar, D., 2007. Water sources in semiarid northeast Asia as revealed by field observations and isotope transport model. *Journal of Geophysical Research* 112 (D17), D17112.
- Schotterer, U., Fröhlich, K., Gäggeler, H. W., Sandjordj, S., Stichler, W., 1997. Isotope records from Mongolian and Alpine ice cores as climate indicators. *Climatic Change* 36 (3), 519–530.
- Shahgedanova, M., Nosenko, G., Khromova, T., Muraveyev, A., 2010. Glacier shrinkage and climatic change in the Russian Altai from the mid-20th century: An assessment using remote sensing and PRECIS regional climate model. *Journal of Geophysical Research* 115 (D16), D16107.
- Shi, F., 1992. Glaciers and glacial geomorphology in China. *Zeitsch. Geomorphol.* 86, 51–63.
- Sodemann, H., Zubler, E., 2009. Seasonal and inter-annual variability of the moisture sources for Alpine precipitation during 1995–2002. *International Journal of Climatology* 30 (7), 947–961.
- Surazakov, A. B., Aizen, V. B., Aizen, E. M., Nikitin, S. A., Apr. 2007. Glacier changes in the Siberian Altai Mountains, Ob river basin, (1952-2006) estimated with high resolution imagery. *Environmental Research Letters* 2 (4), 045017–1–7.
- Tarasov, P., Dorofeyuk, N., TSEVA, E. M., 2000. Holocene vegetation and climate changes in Hoton-Nur basin, northwest Mongolia. *Boreas* 29 (2), 117–126.
- Tarasov, P. E., Harrison, S. P., Saarse, L., Pushenko, M. Y., Andreev, A., Aleshinskaya, Z., Davydova, N., Dorofeyuk, N., Efremov, Y. V., Khomutova, I., Sevastyanov, D.,

2.4 Paleoclimatic studies from the Altai

- Tamosaitis, J., Uspenskaya, N., Yakushko, F., Tarasova, I. V., 1994. Lake status records from the former Soviet Union and Mongolia: data base documentation. World Data Center-A for Paleoclimatology, NOAA-NGDC Paleoclimatology Program.
- Thompson, L. G., 2000. A high-resolution millennial record of the South Asian Monsoon from Himalayan ice cores. *Science* 289 (5486), 1916–1919.
- Tsutomu, K., Davaa, G., 2007. Recent glacier variations in Mongolia. *Annals of Glaciology* 46 (1), 185–188.
- Uetake, J., Kohshima, S., Nakazawa, F., Takeuchi, N., Fujita, K., Miyake, T., Narita, H., Aizen, V., Nakawo, M., 2011. Evidence for propagation of cold-adapted yeast in an ice core from a Siberian Altai glacier. *Journal of Geophysical Research* 116 (G1019), 1–8.
- Wang, W., Feng, Z., 2013. Holocene moisture evolution across the Mongolian Plateau and its surrounding areas: A synthesis of climatic records. *Earth-Science Reviews* 122 (0), 38–57.
- Wanner, H., Beer, J., Bütikofer, J., Crowley, T. J., Cubasch, U., Flückiger, J., Goosse, H., Grosjean, M., Joos, F., Kaplan, J. O., Küttel, M., Müller, S. A., Prentice, I. C., Solomina, O., Stocker, T. F., Tarasov, P., Wagner, M., Widmann, M., 2008. Mid- to Late Holocene climate change: an overview. *Quaternary Science Reviews* 27 (19-20), 1791–1828.
- Yang, D., Ye, B., Shiklomanov, A., 2004. Discharge characteristics and changes over the Ob river watershed in Siberia. *Journal of Hydrometeorology* 5 (4), 595–610.

3 Methods

In general the methods used for this thesis can be separated in two categories. The first category involves techniques needed to assign an age to a certain depth, so called dating methods. The second category is used to reconstruct past climatic conditions. To date the Tsambagarav ice core the following parameters were analyzed: Tritium (^3H), ^{210}Pb and radiocarbon (^{14}C). For climate reconstruction the concentration of major ions, the stable isotope composition ($\delta^{18}\text{O}$) and ^{10}Be were measured. Diatom and pollen analyses were as well performed for the period ranging from AD 1934 to 2009. This is an ongoing project of Elena Mitrofanova (IWEF, SB RAS, Barnaul, Russia) and is not included in this work.

This chapter introduces the different methods and instruments applied in this project. First, the sample preparation is described in detail. This is followed by dating methods chronologically ordered by the the half-lives of the respective isotopes. At the end the climate proxy methods are introduced. A summary of the species analyzed in this project is given in Table 3.1. Indication of time resolution is only reasonable for species not analyzed close to bedrock, since strong thinning induces a very large time span (for details see Chapter 4).

Table 3.1: Species, number of samples and mean resolution in cm of the Tsambagarav ice core. The two values in the ^3H row correspond to two different measurement batch (for details see section 3.2). (*) close to bedrock strong thinning of annual layers induce very large time span, thus no range is indicated. (†) on going project, more samples will be processed.

Species	Number of samples	Depth-resolution [cm]	time-resolution [year]
^3H	20 & 21	66.7 & 22	1.45 & 0.48
^{210}Pb	38	132	6.33
^{14}C	19	15	*
major ions	2944	2.25	*
$\delta^{18}\text{O}$	2944	2.25	*
^{10}Be	130†	†	†

3.1 Sample processing

The 72 meter surface-to-bedrock ice core was drilled in summer 2009 with the electromechanical drill FELICS, resulting in 112 segments of 70 cm length with diameter of 8.25 cm. On site the 112 segments were packed in polyethylene bags and transported frozen to the PSI, where they were processed in the cold room (-20°C). Prior to cutting, each ice segment was backlit and photographed to establish a precise stratigraphy. Features observed were: dust layers, single large particles and melt layers (they appear bright and bubble-free when backlit). Samples for analysis of contamination sensitive species were collected from the inner part of the core (e.g. major ion). For species less sensitive to contamination (e.g. ^{210}Pb) the outer part of the core was used. The ice was processed using a band saw with a Teflon coated tabletop according to the procedure described in Eichler et al. (2000). Fig. 3.1 illustrates the cutting scheme, showing the attribution of the ice to the different analysis. All the handling and cutting of the ice cores was performed wearing polyethylene gloves to avoid contamination.

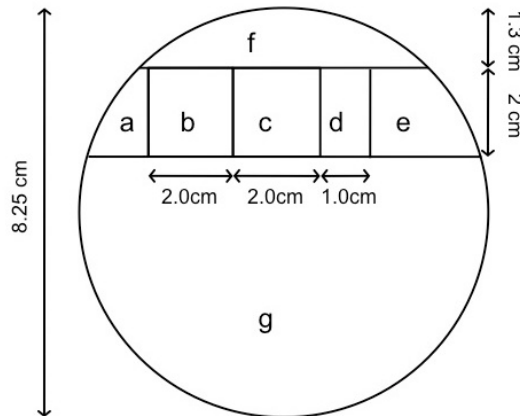


Figure 3.1: (*left*) Cross-section of the Tsambagarav ice core with cutting scheme. (a) was used for pollen and diatom measurements. (b) and (c) for major ion analyses. Section (d) for tritium measurements. The ^{10}Be samples were taken from (e). The slice (f) was used for ^{210}Pb analysis. The remaining part (g) was used for discrete ^{14}C analysis or few selected segments and still available or partly used to complete measurements.

3.2 Liquid scintillation counting (^3H)

The isotope tritium (^3H) has a half-life of 12.3 years and is the third frequent natural isotope of hydrogen (MacMahon, 2006). It is a low-energy β -emitter ($E_{\text{max}} = 18.6$ keV) and decays to ^3He . The natural background of ^3H is produced through bombardment of ^{14}N by fast neutrons ($n(\text{fast}) + ^{14}\text{N} \longrightarrow ^{12}\text{C} + ^3\text{H}$).

Through its interaction with stratospheric oxygen (O_2) it is incorporated in the water cycle. The residence time in the atmosphere is 1.6 years (Craig and Lal, 1961). With a production rate of $0.25 \text{ atoms} \cdot \text{cm}^{-2} \cdot \text{s}^{-1}$ the natural occurrence of ^3H is low (Craig and Lal, 1961) and negligible compared to the input by thermonuclear weapon tests initiated in the 1950's. The anthropogenically produced ^3H accumulated in the stratosphere until 1963, the year of the US-Soviet Test Ban Treaty. Since then the concentration is decreasing approximately at the rate of its half-life (Cook et al., 2004). This peak in activity can be used in ice core dating as time marker for the year 1963.

The analysis of ^3H was conducted with the outer part of the ice core since ^3H is less sensitive to contamination. Two series of ^3H activity measurements were performed. A first set at low-resolution (60 cm) for an approximate location and a second set at high-resolution (20 cm) for a refined location of the horizon within the ice core. The method applied was liquid scintillation counting (LSC).

The mass required for one measurement is 10 g. The samples are melted and suspended in a scintillator "cocktail" containing a solvent and placed in a TriCarb 2770 SLL/BGO counter (Packard SA, Meriden, II, USA). The β -particles emitted from the sample transmit energy to the scintillator, which converts the absorbed energy into photons. The fluorescence of the photons hits the photomultiplier tube (PMT) producing an electrical pulse proportional to the number of photons. This pulse is converted into a digital value. The counting time was 1200 min with a blank value of 0.95 counts per minute (cpm). The detection limit is 8.98 Tritium Units ($1 \text{ TU} = [^3\text{H}]/[\text{H}] = 10^{-18}$) and is related to the natural radioactivity in the instrument's construction materials, natural radioactivity in the vial walls or caps, cosmic ray interactions with the vial walls and vial contents, and thermal ionization in the PMTs (Cook et al., 2004). The activity is decay-corrected to the year 1963 for easier comparison with other records.

The analysis was conducted by Jost Eikenberg and Max R uthi from the Radioanalytic laboratory at the Paul Scherrer Institut.

3.3 α -spectroscopy (^{210}Pb)

^{210}Pb is part of the uranium-238 (^{238}U)-decay chain. It is formed in the atmosphere as a decay product of ^{222}Rn , which emanates constantly from the earth crust (Fig. 3.2). The ^{210}Pb isotope interacts with aerosols and reaches the glacier by dry or wet deposition (Gäggeler et al., 1983). Its residence time in the atmosphere ranges from days to weeks. To calculate the age of the ice constant accumulation is assumed. The datable time period datable is mainly controlled by the half-life of 22.3 years. However, favorable conditions such as high initial activity and low blank values, allow dating of more than 150 years. ^{210}Pb is indirectly measured by its decay product ^{210}Po ($T_{1/2} = 138$ d), which is an alpha-emitter. The ice core is supposed to rest several month in order to allow the ^{210}Po and ^{210}Pb activities to be in equilibrium.

To avoid large scattering of the data, due to varying transport and deposition, two core segments were combined for one measurement. Being not sensitive to contamination about 200 g of the outer part of the ice core were processed (Fig. 3.1). Before melting the sample, hydrochloric acid (HCl) is added together with a ^{209}Po ($T_{1/2} = 102$ y) standard. The melted sample is then bubbled for 3 min with sulfur dioxide at 90-95°C to adjust the pH. Then a silver plate is placed into the sample for 7 hours at 90-93°C to deposit the ^{210}Po on the plate. Finally the plate is rinsed with ultrapure water and dried. Samples are analyzed by α -spectrometry (Euertec Schlumberger, Typ 7164 with PIPS detector) to measure the α -activities of the two isotopes ^{209}Po and ^{210}Po . Energies of the α -lines analyzed are 4.9 MeV for ^{209}Po and 5.3 MeV for ^{210}Po . For one kg of ice the background activity is 2.2 mBq. The surface activity is required, to convert the decreasing activity into a timescale. In this study the surface activity was obtained by applying a linear regression to the upper 20 m weq and defining the y intercept as surface activity (272 mBq l⁻¹). The measured activities with the corresponding ages are discussed in Section 4.4.

Edith Vogel from the Laboratory of Radio- and Environmental Chemistry conducted the deposition on silver plates. Leo Tobler at the PSI performed the α -spectroscopy.

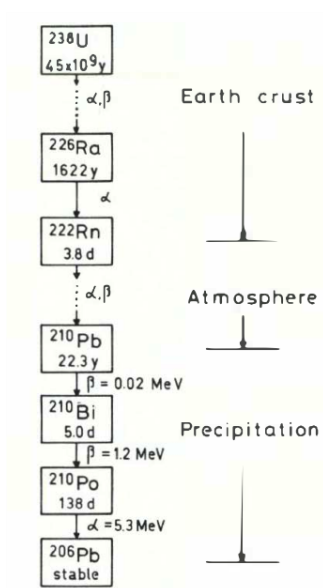


Figure 3.2: Decay chain of ^{210}Pb . Products in the decay chain of ^{238}U of importance in the ^{210}Pb dating method (from Gägger et al. (1983)).

3.4 Accelerator mass spectrometry (^{14}C)

Carbonaceous aerosol particles are deposited on the glacier with snow and embedded into the ice matrix. Measuring the $^{14}\text{C}/^{12}\text{C}$ ratio of those particles allows attributing an age to the glacier ice. This method becomes most relevant for the lower part of the ice core, where other dating techniques do not allow any age attribution (Zapf et al., 2013 in press). Prior to AD 1800 the organic carbon in the atmosphere was purely of biogenic origin and is thereby appropriate for radiocarbon dating of glacier ice (Jenk et al., 2007). With a half-life of 5730 years ^{14}C allows dating of up to 50'000 year old ice.

Developing a method to date glacier ice with particulate organic carbon (POC) was a demanding task. It involved a special design of a CO_2 trapping system and an accelerator mass spectrometer (AMS) with a gas ion source. The technique is shortly introduced, since the ^{14}C measurements had a major contribution to the dating of the lower part of the ice core and to the corresponding conclusions of Chapter 4.

To avoid contamination the inner part of the ice core is used and rinsed with ultrapure water (Fig. 3.1). After melting, the sample is filtered through preheated quartz fiber filters (Pallflex Tissuquartz, 2500 QAO-UP) and acidified (three times $5 \mu\text{l}$ 0.2 M HCl) to remove carbonates. The filter is stepwise combusted in a pure oxygen flow, first at 350°C (10 min) and later at 680°C (12 min) to separate the organic carbon (OC) from

3 Methods

the elemental carbon (EC) fraction. The emanating CO₂ is cryogenically trapped, manometrically quantified and sealed in a glass tube for AMS measurement. The glass ampules are introduced to the gas handling system of the 200 kV AMS system 'MICADAS' for the measurement of ¹⁴C. The technique allows measurement of very small carbon samples (> 3 μg C). For one sample, the procedure blank input ($m_{C,proc.blank}$) is 1.17±0.41 μg C with a fraction of modern ($f_{m,proc.blank}$) of 1.15±0.09. The correction applied to the AMS value is given by:

$$f_{m.corrected} = \frac{m_{C,sample} \cdot f_{m,sample} - m_{C,proc.blank} \cdot f_{m,proc.blank}}{m_{C,sample} - m_{C,proc.blank}} \quad (3.1)$$

where $m_{C,sample}$ is the measured carbon mass and $f_{m,sample}$ the measured fraction of modern of the sample. Details for the OC/EC separation conducted at the University of Berne are presented in Szidat et al. (2004) and Sigl et al. (2009), whereas details of the 'MICADAS' and its gas inlet system are described in Svalbu et al. (2007) and Ruff et al. (2007). The AMS measurements were performed at the ETH Zürich in the Laboratory of Ion Beam Physics. The OxCal software and the IntCal 09 calibration curve (Bronk Ramsey, 2001; Reimer et al., 2009) were used to calibrate the data. Ages are given in calibrated radiocarbon ages (cal years BP = years before 1950).

Compared to other sites the Tsambagarav ice core allowed for analysis of relative small samples. The average ice mass of the total 18 samples is 178 g. Samples with very high carbon concentration were portioned into two separate glass ampules (for details and complete analysis results see Table 9.1). Values with high dust input were excluded to derive the age-depth relationship presented in Chapter 4 (see Table 4.1). Alexander Zapf carried out all the sample preparation and the AMS measurement.

3.5 Ion chromatography (major ions)

The temporal distribution of the concentration of major ions in an ice core can be used to reconstruct the air composition and to identify changing source regions of air masses reaching the glacier. The 13 species analyzed and hereinafter called major ions are: 5 cations (Na⁺, NH₄⁺, K⁺, Mg²⁺ and Ca²⁺) and 8 anions (F⁻, CH₃COO⁻, HCOO⁻, CH₃SO₃⁻, Cl⁻, NO₃⁻, SO₄²⁻, C₂O₄²⁻). Only dissolved species have been analyzed within this study.

In total 2944 samples were processed in the cold room and measured with ion chromatography (IC). The initial resolution of 2.5 cm was increased to 2 cm from 50.68 m depth

(38.89 m weq) to account for the thinning of the annual layers in a glacier (Nye, 1963). The major ions present in trace concentrations are very sensitive to contamination and thus require very careful preparation. The 50 ml polypropylene vials are placed in ultrapure water during 24 hours which is repeated five times. To control the procedure blank frozen ultrapure water is processed identical to the ice core sample. Only the inner part of the ice core is used (see Fig. 3.1). To avoid contamination with gaseous compounds in the laboratory air, the sample containers are flushed with N_2 prior to melting and then directly placed in the autosampler of the instrument. The system used is the *850 Professional IC* combined with *872 Extension Module* from Metrohm. Details of the compounds and parameters are given in Table 3.2. The species-specific detection limits are given in Table 3.3. Concentrations are determined by external calibration with different dilutions of in-house reference solutions of 10 ppm, for each measurement batch. To control the calibration, a reference solution and an in-house standard (Jungfraujoch snow) are systematically measured. Raw data is evaluated with the MagICNet 1.1 software.

Table 3.2: Components of the Metrohm *850 Professional IC* & *872 Extension Module* ion chromatography system, for the analysis of the ionic species.

Component	cations	anions
Eluent	2.8 mM HNO_3	A: 1.5 mM Na_2CO_3 / 0.3 mM NaHCO_3 B: 8 mM Na_2CO_3 / 1.7 mM NaHCO_3
Flow rate	1 ml/min	0.9 ml/min
Loop	500 μl	500 μl
Autosampler	858 Professional Sample Processor	
Separation column	Metrosep C4	Metrosep A Supp 10
Guard column		Metrosep A Supp 5
Suppression	-	H_2SO_4 0.05 M
Detection	Conductivity detection	Conductivity detection
Software	IC MagicNet IC 1.1	IC MagicNet IC 1.1

3.6 Mass spectrometry ($\delta^{18}\text{O}$)

In certain regions of the globe, stable isotope ratio of oxygen ($^{16}\text{O}/^{18}\text{O}$) and hydrogen ($^1\text{H}/^2\text{H}$) in precipitation is related to temperature and can therefore be used as temperature proxy (Araguás-Araguás et al., 2000). During phase changes, such as evaporation or condensation the heavier stable isotopes enrich in one phase and deplete in the other.

3 Methods

Table 3.3: Detection limit for measured anions and cations with the Metrohm 850 Professional IC & 872 Extension Module system in ppb.

Anions	F⁻	CH₃COO⁻	HCOO⁻	CH₃SO₃⁻	Cl⁻	NO₃⁻	SO₄²⁻	C₂O₄²⁻
	0.1	0.7	0.8	0.5	0.6	0.6	1.0	0.8
Cations	Na⁺	NH₄⁺	K⁺	Mg²⁺	Ca²⁺			
	0.4	0.3	0.8	0.4	0.9			

This fractionation process is temperature dependent and thus the stable isotope ratio can be used to reconstruct temperature (Eichler et al., 2009; Johnsen et al., 1997).

The scientific notation used is $\delta^{18}\text{O}$ and it describes the ‰ deviation of the isotope ratio to an international accepted standard (Vienna Standard Mean Ocean Water, VSMOW).

The notations are described by:

$$\delta^{18}\text{O}(\text{‰}) = \frac{r_{\text{sample}} - r_{\text{VSMOW}}}{r_{\text{VSMOW}}} \quad (3.2)$$

with

$$r_{\text{VSMOW}} = \left(\frac{^{18}\text{O}}{^{16}\text{O}} \right)_{\text{VSMOW}} = (2005.2 \pm 0.45) \cdot 10^{-6} \quad (3.3)$$

$$r_{\text{sample}} = \left(\frac{^{18}\text{O}}{^{16}\text{O}} \right)_{\text{sample}} \quad (3.4)$$

The value r_{VSMOW} was proposed by Baertschi (1976).

The stable isotope ratio ($^{18}\text{O}/^{16}\text{O}$) was analyzed using isotope ratio mass spectrometry (IRMS). For $\delta^{18}\text{O}$ determination 1 ml aliquots of the samples prepared for IC analysis transferred in glass vials. One analysis consists of a threefold injection of 0.6 μl . To prevent memory effects, the first injection was omitted. Samples with large differences between the second and third injection ($\sigma > 0.2$) were re-measured. The sample is pyrolyzed in a glassy carbon reactor (High Temperature Combustion Elemental Analyzer TC/EA, Thermo Finnigan, Bremen, Germany) at 1450°C to decompose the water (H_2O) into hydrogen (H_2) and carbon monoxide (CO) ($\text{H}_2\text{O} + \text{C} \rightarrow \text{H}_2 + \text{CO}$). The gases are carried in a helium stream to the mass spectrometer (Delta plus XP, Thermo Finnigan,

Bremen) using a gas chromatography column for separation. The isotopes are determined by the mass charge ratio m/z of the CO^+ gas, 28 for C^{16}O^+ and 30 for C^{18}O^+ . To control the stability and potential drifts of the instrument every fifteenth measurement was an in-house standard (Haus: $\delta^{18}\text{O} = -9.82\text{‰}$). At the start and the end of each sample batch a sequence of standard was additionally measured to monitor the stability of the instrument (Haus & Miki: $\delta^{18}\text{O} = -20\text{‰}$). The overall precision of the measurement is $<0.2\text{‰}$ for $\delta^{18}\text{O}$.

3.7 Accelerator mass spectrometry (¹⁰Beryllium)

Different methods exist to reconstruct the variability of the sun. In this work Beryllium-10 (¹⁰Be) is used as proxy since its production is controlled by galactic cosmic ray (Bard and Frank, 2006). These measurements are ongoing, but a precise description of the procedure is given here for an interpretation of the data in future.

The analysis was performed in three distinct steps: At PSI the ice is processed, and the sample loaded on a ion exchange column. The elution to extract the ¹⁰Be from the column is performed at Aarhus University (Denmark) at the Department of Physics and Astronomy. Finally the samples are measured at the AMS-facility in Uppsala (Sweden). In the following the different procedures are described in details. ¹⁰Be is not sensitive to contamination. However, ¹⁰Be is also contained in mineral dust, but with unknown age of production. Thus, mineral dust has to be separated from the water sample containing the soluble (fresh) ¹⁰Be. After various tests a minimum sample size of 200 g was defined. Prior to melting, 100 μl of ⁹Be carrier (Scharlau BE03450100, 1000 mg/l) are added to each sample. The melted sample is filtered (Whatman 0.45 μm , D = 50 mm) and run through the column (BIO-RAD, AG 50W-X8 resin) to extract the ¹⁰Be from the water. The filter is weighted to determine the amount of dust. All containers are rinsed three times with ultrapure water before use. The loaded columns together with the filter are then shipped to Aarhus for the chemical extraction. The ¹⁰Be is extracted by pouring 25 ml HCl (4 M) through a quartz tube fixed at the top of the column and collected in the centrifuge tube located underneath. 10 ml NH₃ (25%) is added to the extracted liquid and carefully stirred. The BeO produced overnight is then centrifuged to be separated from the HCl-NH₃ solution. The BeO is transferred to a quartz tube and centrifuged again. The extra liquid is waste and the tube backed overnight at 800°C. The sample is then placed in an exsiccator. After cooling down at room temperature the sample is weighted and 1 mg of niobium is added. The grinded sampled is moved into a cathode used for AMS measurements. Consecutively Nb powder and Al-thread

3 Methods

is added and the sample is pressed. After sealing the cathode, the sample is ready for AMS measurement. Details about the AMS measurement in Uppsala can be found under <http://www.physics.uu.se/en/page/ion-physics>.

These analyses were performed in collaboration with Fadil Inceoglu and Mads Faurschou Knudsen from the Department of Geoscience at Aarhus University, Denmark. Preliminary results are presented in Chapter 7.

References

- Araguás-Araguás, L., Froehlich, K., Rozanski, K., 2000. Deuterium and oxygen-18 isotope composition of precipitation and atmospheric moisture. *Hydrological Processes* 14 (8), 1341–1355.
- Baertschi, P., 1976. Absolute ^{18}O content of standard mean ocean water. *Earth and Planetary Science Letters* 31 (3), 341–344.
- Bard, E., Frank, M., 2006. Climate change and solar variability: What's new under the sun? *Earth and Planetary Science Letters* 248 (1–2), 1–14.
- Bronk Ramsey, C., 2001. Development of the radiocarbon calibration program. *Radiocarbon* 43 (2A, Part 1), 355–363.
- Cook, G. T., Passo, Jr, C. J., Carter, B., 2004. 6 - Environmental Liquid Scintillation Analysis. In: L'Annunziata, M. F. (Ed.), *Handbook of Radioactivity Analysis* (Second Edition). Academic Press, San Diego, pp. 537–607.
- Craig, H., Lal, D., 1961. The production rate of natural tritium. *Tellus* 13 (1), 85–105.
- Eichler, A., Olivier, S., Henderson, K., Laube, A., Beer, J., Papina, T., Gaggeler, H., Schwikowski, M., 2009. Temperature response in the Altai region lags solar forcing. *Geophysical Research Letters* 36 (1), L01808.
- Eichler, A., Schwikowski, M., Gaggeler, H., 2000. Glaciochemical dating of an ice core from upper Grenzgletscher (4200 m asl). *Journal of Glaciology* 46 (154), 507–515.
- Gaggeler, H., von Gunten, H., Rössler, E., Oeschger, H., 1983. ^{210}Pb -dating of cold Alpine firn/ice cores from Colle Gnifetti, Switzerland. *Journal of Glaciology* 29 (101), 165–177.

- Jenk, T., Szidat, S., Schwikowski, M., Gäggeler, H., Wacker, L., Synal, H.-A., Saurer, M., 2007. Microgram level radiocarbon (^{14}C) determination on carbonaceous particles in ice. *Nuclear Instruments and Methods in Physics Research Section B: Beam Interactions with Materials and Atoms* 259 (1), 518–525.
- Johnsen, S. J., Clausen, H. B., Dansgaard, W., Gundestrup, N. S., Hammer, C. U., Andersen, U., Andersen, K. K., Hvidberg, C. S., Dahl-Jensen, D., Steffensen, J. P., Shoji, H., Sveinbjörnsdóttir, Á. E., White, J., Jouzel, J., Fisher, D., 1997. The $\delta^{18}\text{O}$ record along the Greenland Ice Core Project deep ice core and the problem of possible Eemian climatic instability. *Journal of Geophysical Research* 102 (C12), 26397–26410.
- MacMahon, D., 2006. Half-life evaluations for ^3H , ^{90}Sr , and ^{90}Y . *Applied Radiation and Isotopes* 64 (10-11), 1417–1419.
- Nye, J., 1963. Correction factor for accumulation measured by the thickness of the annual layers in an ice sheet. *Journal of Glaciology* 4 (36), 785–788.
- Reimer, P. J., Baillie, M. G. L., Bard, E., Bayliss, A., Beck, J. W., Blackwell, P. G., Ramsey, C. B., Buck, C. E., Burr, G. S., Edwards, R. L., Friedrich, M., Grootes, P. M., Guilderson, T. P., Hajdas, I., Heaton, T. J., Hogg, A. G., Hughen, K. A., Kaiser, K. F., Kromer, B., McCormac, F. G., Manning, S. W., Reimer, R. W., Richards, D. A., Southon, J. R., Talamo, S., Turney, C. S. M., van der Plicht, J., Weyhenmeyer, C. E., 2009. Intcal09 and marine09 radiocarbon age calibration curves, 0-50,000 years cal bp. *Radiocarbon* 51 (4), 1111–1150.
- Ruff, M., Wacker, L., Gäggeler, H., Suter, M., Synal, H.-A., Szidat, S., 2007. A gas ion source for radiocarbon measurements at 200 kV. *Radiocarbon* 49 (2), 307–314.
- Sigl, M., Jenk, T., Kellerhals, T., Szidat, S., 2009. Towards radiocarbon dating of ice cores. *Journal of Glaciology* 55 (194), 985–996.
- Synal, H.-A., Stocker, M., Suter, M., 2007. MICADAS: A new compact radiocarbon AMS system. *Nuclear Instruments and Methods in Physics Research Section B: Beam Interactions with Materials and Atoms* 259 (1), 7–13.
- Szidat, S., Jenk, T. M., Gäggeler, H. W., Synal, H.-A., Hajdas, I., Bonani, G., Saurer, M., 2004. THEODORE, a two-step heating system for the EC/OC determination of radiocarbon (^{14}C) in the environment. *Nuclear Instruments and Methods in Physics Research Section B: Beam Interactions with Materials and Atoms* 223–224, 829–836.

3 Methods

Zapf, A., Nesje, A., Szidat, S., Wacker, L., Schwikowski, M., 2013 in press. ^{14}C measurements of ice samples from the Juvfonne Ice Tunnel, Jotunheimen, Southern Norway- Validation of a ^{14}C dating technique for glacier ice. *Radiocarbon* 55 (3-4), 518–525.

4 The onset of Neoglaciation 6000 years ago in western Mongolia revealed by an ice core from Tsambagarav mountain range

Pierre-Alain Herren^{a,b}, Anja Eichler^{a,b}, Horst Machguth^{c,d}, Tatyana Papina^e, Leonhard Tobler^{a,b}, Alexander Zapf^{a,b} and Margit Schwikowski^{a,b,f,*}

^aPaul Scherrer Institut, 5232 Villigen PSI, Switzerland

^bOeschger Centre for Climate Change Research, University of Bern, 3012 Bern, Switzerland

^cGlaciology and Geomorphodynamics, University of Zürich, 8057 Zürich, Switzerland

^dGeological Survey of Denmark and Greenland, 1350 Copenhagen, Denmark

^eInstitute for Water and Environmental Problems, 656038 Barnaul, Russia

^fDepartment of Chemistry and Biochemistry, University of Bern, 3012 Bern, Switzerland

*Corresponding author

Published in Quaternary Science Reviews 69 (2013) 59-68

Abstract

Glacier highstands since the Last Glacial Maximum are well documented for many regions, but little is known about glacier fluctuations and lowstands during the Holocene. This is because the traces of minimum extents are difficult to identify and at many places are still ice covered, limiting the access to sample material. Here we report a new approach to assess minimal glacier extent, using a 72-meter long surface-to-bedrock ice core drilled on Khukh Nuru Uul, a glacier in the Tsambagarav mountain range of the Mongolian Altai (4130 m asl, 48°39.338'N, 90°50.826'E). The small ice cap has low ice temperatures and flat bedrock topography at the drill site. This indicates minimal lateral glacier flow and thereby preserved climate signals. The upper two-thirds of the ice core contain 200 years of climate information with annual resolution, whereas the lower third is subject to strong thinning of the annual layers with a basal ice age of approximately 6000 years before present (BP). We interpret the basal ice age as indicative of ice-free conditions in the Tsambagarav mountain range at 4100 m asl prior to 6000 years BP. This age marks the onset of the Neoglaciation and the end of the Holocene Climate Optimum. The ice-free conditions allow for adjusting the Equilibrium Line Altitude (ELA) and derive the glacier extent in the Mongolian Altai during the Holocene Climate Optimum. Based on the ELA-shift, we conclude that most of the glaciers are not remnants of the Last Glacial Maximum but were formed during the second part of the Holocene. The ice core derived accumulation reconstruction suggests important changes in the precipitation pattern over the last 6000 years. During formation of the glacier, more humid conditions than presently prevailed followed by a long dry period from 5000 years BP until 250 years ago. Present conditions are more humid than during the past millennia. This is consistent with precipitation evolution derived from lake sediment studies in the Altai.

4.1 Introduction

The Holocene can be divided into three phases; the early deglaciation period (11,600 to 9000 years BP), the Holocene Climate Optimum (HCO, 9000 to 6000-5000 years BP) and the Neoglaciation period (6000-5000 years BP to preindustrial time). Discussions about amplitude, duration, and causes of the different phases have initiated numerous studies and generated new paleoclimatic records. The hypothesis of a relative stable Holocene climate (Johnsen et al., 1997) compared to glacial interglacial changes has been contested and recurring cold events (so called “Bond cycles”) with a periodicity of 1470 ± 500 years

have been proposed for the Holocene (Bond et al., 1997; Mayewski et al., 2004). However, Wanner et al. (2011) did not observe periodic cold relapses during the last 10 kyr and contradicts the occurrence of “Bond cycles” for the Holocene. Additionally, the current debate about anthropogenic climate change raises the question if during the past 10 kyr temperatures higher or similar than today may have occurred. Generation and analysis of proxy data covering the Holocene epoch is thus of major importance in order to better understand the current climate change. In this context, glacier fluctuations can be used to study trends of temperature and precipitation during the Holocene (Oerlemans, 2005; Solomina et al., 2008; Davis et al., 2009; Owen, 2009). Most approaches rely on distinctive features such as terminal moraines or exposure dating to reconstruct maximum glacier extents. The current retreat of glaciers provides a unique opportunity to collect ancient embedded organic particles (Miller et al., 2012), wood fragments (Ivy-Ochs et al., 2009), or archeological remnants (Grosjean et al., 2007; Nesje et al., 2012). Artifacts exposed at the front of the glacier tongues are dated and allow for reconstructing glacier fluctuation chronologies.

However, for inferring minimum extent of glaciers such specific features are difficult to identify and the access to potential sample material is often hindered by ice coverage. Consequently, little is known about glacier lowstands and the discussion is ongoing which high-mountain glaciers and ice caps have persisted throughout the Holocene and which have disappeared at some point. A promising approach to overcome the lack of evidence is the use of high-resolution ice core records extracted from alpine glaciers. They may provide insight in former climate conditions (Thompson et al., 1998; Eichler et al., 2011) and may give access to datable material in the basal ice itself or from the bedrock.

The Intergovernmental Panel on Climate Change (IPCC, 2007) projection of total disappearance of Himalayan glaciers by 2035, a statement finally recalled, had the merit to increase the public awareness about glacier changes in Asia, their importance, and impacts on society. Most investigations dealing with Asian quaternary glacier fluctuations have focused on the Himalaya and the Tibetan Plateau (Lehmkuhl and Owen, 2005; Davis et al., 2009), likewise the ice core drilling projects. The adjacent mountain ranges including the Pamir, Tien Shan, and Altai have received less attention and were thereby investigated in less detail. For a complete understanding of glacier fluctuations in Asia, more research in these regions is required. Here we date an ice core from the Altai Mountains to examine glacier behavior and reconstruct accumulation rates during the Holocene. This work is a step towards an improvement in understanding the climate of Central Asia. We present a multi-proxy approach using an ice core covering approximately the last 6000 years and provide a larger perspective on the Holocene climate in

the Mongolian Altai, than has been provided up to now.

4.2 Regional setting

The Altai Mountains, a complex mountain system in Central Asia, form the borders between Russia, Kazakhstan, China, and Mongolia. The maximum elevation is 4500 m asl and the range extends over approximately 1200 km (Rudaya et al., 2009). According to the Randolph Glacier Inventory (RGI, Arendt et al. (2012)) and Landsat imagery used to manually correct the RGI, the Altai has a glaciated area of roughly 1300 km² including, approximately 500 km² of Mongolian glaciers. From northwest (Russian Altai) to southeast (Mongolian Altai) where the foothills reach the Gobi desert, the mountain range serves as watershed between the Arctic Ocean and the basin of central Asia. The location and extent imply a major role in the Asian climate system and thus, requires thorough paleoclimate investigations, all the more since instrumental data is limited and spatially sparse.

The mountain chain acts like a barrier and intercepts air masses originating from the west, leading to a strong northwest to southeast precipitation gradient. In the Russian Altai, mean annual precipitation is around 800 mm and decreases to less than 200 mm in the floor of the intermountain depressions of the Mongolian Altai (Klinge et al., 2003). The Siberian High controls the winter climate with cold and dry conditions. Most of the precipitation is related to the Westerlies and occurs mainly during the months June, July, and August (Klinge et al., 2003).

Glacier fluctuation studies dealing with the Altai mountain range are mainly limited to the late Pleistocene (Lehmkuhl et al., 2011), whereas knowledge for the Holocene period is rare. A detailed discussion of glacier fluctuations from (Agatova et al., 2012) refutes the former general concept of a gradual retreat of the Würm glaciers in the Russian Altai by summarizing former work and presenting new data. For the period 7000 years BP to present, temperature and humidity reconstructions are presented based on lichenometry, geomorphological methods, and further radiocarbon dates from formerly buried pieces of wood. Forest regrowth in presently glaciated areas during interstage mild periods suggest strong glacier retreat or even complete disappearance especially during the HCO. Additionally, the recovery of wood fragments originating from the HCO above the modern tree line indicates warmer temperatures than nowadays. After a glacier-hostile climate, glaciers started to regrow around 5000 years BP. Periods of glacier advances (8300, 5700, 4000, and 400 years BP) have been proposed for western China (Zhou et al., 1991) adjacent to the Mongolian Altai. Glacier advances detected around 5700 years BP in

western China, occurred slightly earlier than in the Russian Altai and can be interpreted as the end of the HCO and the onset of the Neoglaciation.

Lake sediment cores collected in Hoton-Nur lake (northwestern Mongolia, Fig. 4.1 show distinct variations in the precipitation. A major shift from wet to present dry conditions occurred 5000 years BP (Rudaya et al., 2009; Mackay et al., 2012). Information about glacier fluctuations and past temperature is, however, not available. Long-term Holocene climate records for the Mongolian Altai are thus incomplete and biased towards lake sediment data.

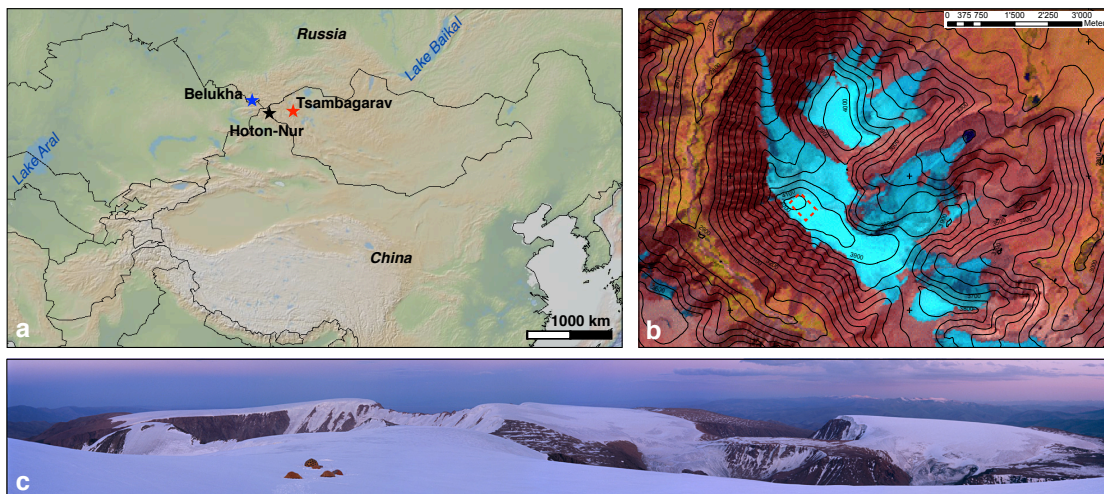


Figure 4.1: (a) Location of the Tsambagarav mountain range (red star), lake sediment Hoton-Nur (black star) in Mongolia, and Belukha glacier in the Siberian Altai (blue star; <http://www.geomapapp.org>). (b) Landsat images with SRTM DTM elevations (solid lines 100 m intervals), the red rectangle corresponds to the area of detailed glaciological survey. (c) Landscape of the Tsambagarav mountain range in the southern Mongolian Altai with typical small ice caps. View to the southeast from close to the drill site toward the campsite. Photo: H. Machguth.

For the Mongolian Altai, high-resolution climate reconstructions on a millennial scale are based on tree-ring chronologies. Most studies provide records for few centuries only, the longest currently available covers 1700 years (D'Arrigo et al., 2001; Loader et al., 2010). The reconstruction suggests that the coldest and warmest conditions of the last millennia occurred during the 19th and 20th century. Further back in time the different records show less coherent behavior and thus require more data for accurate past climate information. The only alternative reconstructions originate from an ice core drilled in the Russian Altai spanning 750 years (Eichler et al., 2009b,a). For the Siberian Altai, a correlation between solar forcing and temperature was found for the period 1250 to 1850 AD. In addition, the biogenic emissions from the Siberian forests are closely related to temperature changes.

However, no long-term reconstructions of Holocene glacier fluctuations in the Mongolian Altai exist.

4.3 Experimental Methods

4.3.1 Ice core drilling

In July 2009 a joint Russian-Swiss expedition collected a 72 m surface-to-bedrock ice core and an adjacent 52 m parallel core in the Tsambagarav mountain range situated in the Mongolian Altai (4130 m asl, 48°39.338'N, 90°50.826'E). This mountain range is dominated by small ice caps, with the ice margin varying between 3000 and 3800 m asl (Fig. 4.1) strongly depending on the orientation. The total glaciated area in 2008 was 73.2 km² (Demberel, 2011). The equilibrium line altitude (ELA) is estimated to be at 3700 m asl (Lehmkuhl et al., 2011). Prior to the expedition, the drill site was selected based on satellite imagery (Landsat 7/ 8.8.2002 <http://landsat.usgs.gov/index.php>) and the Shuttle Radar Topography Mission Digital Elevation Model (SRTM DEM, 90 m horizontal resolution). Two peaks of similar elevation dominate the mountain massive: Tsast Uul (4190 m asl) and Khukh Nuru Uul (4130 m asl, elevations derived from SRTM DEM). While the glaciation of Tsast Uul has a larger area extent, the ice cap appeared less suitable for drilling because of being strongly asymmetric with a steep ice face directly north of the summit. Although slightly lower, Khukh Nuru Uul was chosen because of its rather symmetric ice cap, which promised ideal conditions for undisturbed layering of accumulation

For drilling the lightweight electromechanical device FELICS (Ginot et al., 2002) was used. Based on previous work by Schotterer et al. (1997) and snow accumulation estimations by Lehmkuhl (1998), an ice core covering the last two millennia was expected. Ice segments of 0.7 m in length and 8.25 cm in diameter were packed and sealed on-site in polyethylene bags and transported in frozen condition to Switzerland, where they were processed. Drilling and transportation of the fragile ice cores required major logistical efforts involving helicopter flights from Russia to Mongolia and back, since the region has poor infrastructure, most of the roads are unpaved and freezing facilities are scarce. In the following we use the term Tsambagarav ice core when referring to the ice core from Khukh Nuru Uul glacier.

4.3.2 Glaciological survey

Ice thickness measurements were performed with radar echo sounding (Malå Ground Penetrating Radar system with 100 and 200 MHz unshielded antennas), combined with a GPS survey. In total 2030 m of radar profiles were measured with roughly half of the profiles located on the summit of Khukh Nuru Uul to construct a detailed map of bed topography around the drill site. Interpretation of the radar signals shows very clear reflections from the bedrock with weak internal reflections from the glacier ice (Fig. 4.2). The undisturbed signal points towards the absence of any liquid water in the glacier ice. Measured two-ways travel time of the radar signal was converted to ice thickness using a velocity of 0.175 m ns^{-1} , yielding a glacier thickness of $70.7 \pm 0.5 \text{ m}$ at the drilling site.

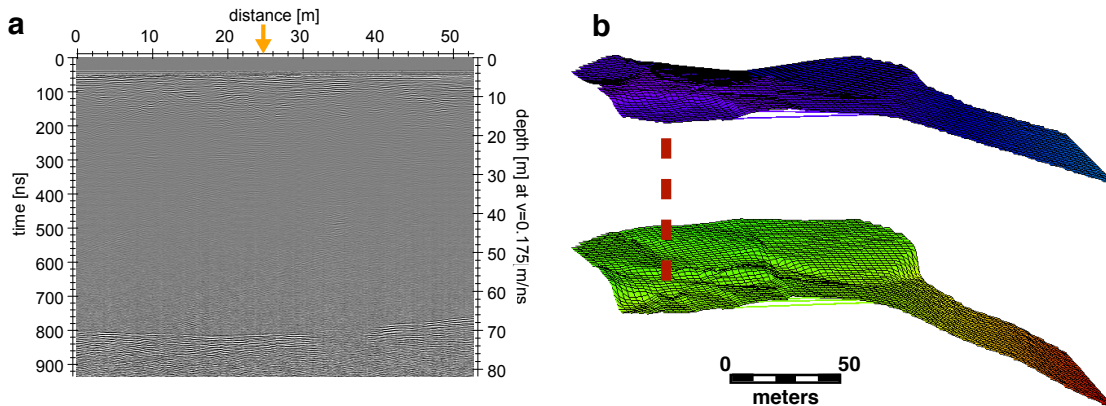


Figure 4.2: (a) Radar profile recorded at Khukh Nuru Uul with clearly identifiable bedrock at 70 m depth (yellow arrow shows drilling location). (b) Surface and bed topography at the drill site; the core is indicated by the dashed red line.

The detailed array of radar profiles around the drill site shows a flat bed topography (Fig. 4.2). The surface and bedrock geometry suggest minimal ice flow implying an undisturbed chronology within the ice core. After drilling, a thermistor chain was lowered into the borehole to measure the glacier temperature. Borehole temperatures were relatively low, ranging from -13.8 to -12.6°C (Fig. 4.3). Thus, the glacier is frozen to the underlying bedrock. With such low temperatures, meltwater produced occasionally at the surface during summer months refreezes mainly within the annual accumulation, creating melt features and preserving the environmental signal stored in the ice. Melt features are bubble-free ice lenses with higher density than the surrounding firn (Henderson et al., 2006), thus identifiable in the density profile. Higher summer temperatures during the last decades have led to an aggregation of these melt features within the upper 12 meters,

4 Onset of Neoglaciation in Mongolia

clearly visible in the density profile (Fig. 4.3). To account for increasing density towards bedrock, all depth values are in the following given in meters water equivalents (m weq), where not stated differently. The 72-meter long ice core corresponds to 58 m weq.

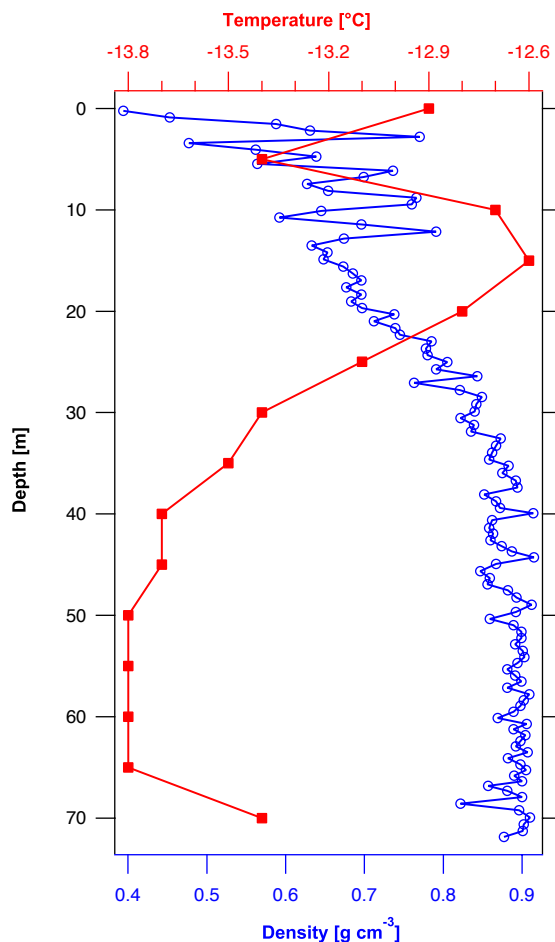


Figure 4.3: Density (blue) and temperature (red) profile of Khukh Nuru Uul glacier.

4.3.3 Analytical methods

Ice core sampling was performed at the cold room of the Paul Scherrer Institut (PSI) at -20°C . Prior to processing, ice core segments were backlit in the darkened cold room to observe dust horizons and ice lenses. A specially designed stainless steel band saw with Teflon coverage on the tabletop was used for sample preparation. For contamination-sensitive species, such as major ions (e.g. calcium, formate, ammonium, and sulfate), the inner part of the ice core was used and analyzed by standard ion chromatography

4.4 Dating of the ice core archive for the period AD 1815-2009

techniques. The resolution ranged from 2.5 cm at the top to 2 cm from 50 m depth downwards. For measurements of tritium (^3H) and ^{210}Pb , the outer part of the ice core was used since those are less sensitive to contamination. Two series of ^3H activity measurements were performed by liquid scintillation counting: A first set at low-resolution (60 cm) and a second set at high-resolution (20 cm) for a refined location of the horizon within the ice core (Eichler et al., 2000). The ^{210}Pb was measured by α -spectroscopy (Gäggeler et al., 1983) with a resolution ranging from 1.0 to 1.4 meters. Ten samples of the lower 20 m weq of the ice core were prepared for ^{14}C analysis of the particulate organic carbon fraction, according to the procedure described in Jenk et al. (2009) and Sigl et al. (2009). In comparison to other sites the carbon concentrations at Tsambagarav allowed relative small sample volumes ranging from 143 to 278 ml, resulting in carbon amounts varying between 19 and 58 μg . For decontamination purposes, the outer part of the ice core segment was removed with the band saw and the inner part was rinsed with ultra-pure water. To extract the particulate carbon, ice samples were melted, filtered, and acidified with HCl to remove carbonates. A two-step combustion at 340°C and 650°C separates filtered particulate carbon into the organic (OC) and elemental carbon (EC) fraction (Szidat et al., 2004). The generated CO_2 was cryogenically trapped and sealed in glass tubes for accelerator mass spectrometry (AMS) measurements. The 200 kV 'MICADAS' AMS system with a gas ion source (Ruff et al., 2007; Synal et al., 2007) allows direct measurements of gas samples. Details about the samples and results are given in Table 4.1.

The ^{14}C values were calibrated using the OxCal software and the IntCal 09 calibration curve (Bronk Ramsey, 2001; Reimer et al., 2009). Ages are given in calibrated radio-carbon ages (cal years BP = years before 1950). Dates are given with their 1σ -range.

4.4 Dating of the ice core archive for the period AD 1815-2009

For obtaining high-resolution climate information based on ice core data, the establishment of an age-depth scale is crucial. The dating of the upper 36 m weq was performed using a combination of several methods as described in the following.

4 Onset of Neoglaciation in Mongolia

Table 4.1: Summary of the ^{14}C results for the Tsambagarav 2009 ice core samples, analyzed at ETH Zürich. The fraction of modern (fM) is given with the corresponding 1σ -range. For the calibrated age, ranges are given with 68% probability. All the values correspond to the particulate organic carbon (POC) fraction of the sample.

Core segment #	Depth [m weq]	Ice Sample mass [kg]	Absolute carbon amount [μg]	AMS Lab Nr.	Radiocarbon fM	Calibrated age years BP = 1950
75	38.19	0.166	33	ETH43436.1.1	0.983 \pm 0.012	280-10
81	41.64	0.181	19	ETH43438.1.1	0.996 \pm 0.017	270-10
92	47.55	0.219	33	ETH42822.1.1	0.891 \pm 0.010	930-770
97	49.65	0.183	32	ETH42824.1.1	0.800 \pm 0.010	1860-1570
102	52.21	0.186	22	ETH42826.1.1	0.666 \pm 0.014	3720-3270
105-1	53.59	0.278	58	ETH42156	0.605 \pm 0.007	4800-4420
105-2	53.73	0.229	29	ETH42166	0.597 \pm 0.010	4850-4240
107	55.05	0.143	23	ETH42828.1.1	0.578 \pm 0.015	5440-4710
109	55.80	0.194	32	ETH42157	0.548 \pm 0.009	5710-5330
111	57.45	0.161	55	ETH42836.1.1	0.532 \pm 0.008	5920-5660

4.4.1 Identification of reference horizons

Thermonuclear bomb tests have accumulated ^3H in the atmosphere, reaching maximum concentrations in 1963, the year of the partial Test Ban Treaty. Identification of the ^3H peak in ice core records served as time marker in many previous investigations (Eichler et al., 2000; Knüsel et al., 2003; Olivier et al., 2004). Maximum activity of 6202 ± 62 Tritium Units (TU, decay corrected to the year 1963) is located at a depth of 15.4 m weq (Fig. 4.4) which is comparable to the maximum activity of 8000 TU detected at Belukha glacier, 350 km to the northwest (Olivier et al., 2004), for location see Fig. 4.1. Similar high values at both sites are due to enhanced stratosphere-troposphere transport of ^3H in spring/summer, the seasons when precipitation is occurring.

Major volcanic eruptions have large climatic impacts through the emission of sulfur dioxide into the stratosphere, where it is oxidized to sulfate aerosols which influence the earth radiative balance (Robock and Jianping, 1995). These eruptions are often used as time markers in ice cores (Robock and Jianping, 1995; Zielinski, 1995). However, sulfate has various sources, the major ones being anthropogenic sulfur dioxide emissions from fossil fuel combustion and natural emissions of mineral dust containing gypsum. In order to correct for the mineral sulfate input an alternative non-dust sulfate record is required. Calcium was used as tracer for mineral dust and by regression analysis of sulfate and calcium concentrations prior to significant fossil fuel emissions (AD 1945), a ratio of 0.22 was obtained (concentration in $\mu\text{eq l}^{-1}$). This value is very similar to the value 0.21 deduced at Belukha (Olivier et al., 2006). As long as other sources are negligible, maxima

4.4 Dating of the ice core archive for the period AD 1815-2009

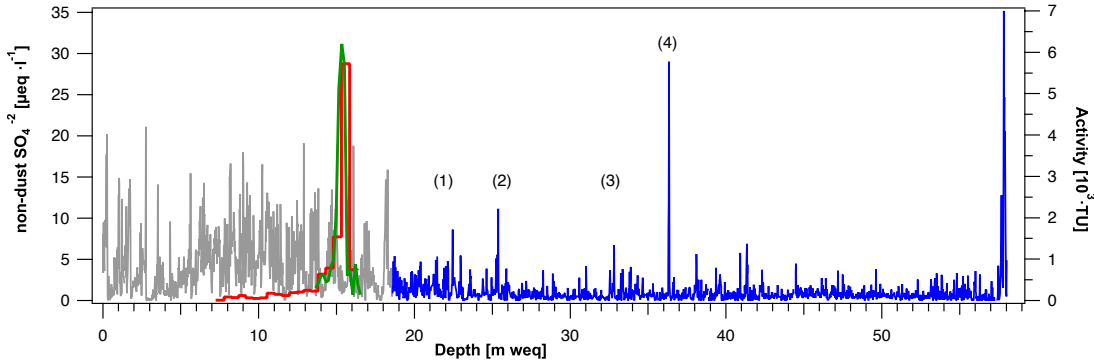


Figure 4.4: Evolution of the ^3H activity in Tritium Units (TU) with depth in the Tsambagarav ice core for coarse (red) and fine (green) resolution decay corrected for the year 1963. Non-dust sulfate record in $\mu\text{ eq l}^{-1}$ (blue) with the corresponding volcanic eruptions, 1933 Kharimkotan (1), 1912 Katmai (2), 1854 Shiveluch (3), and 1815 Tambora (4). The elevated concentrations in the upper 19 m weq are due to anthropogenic fossil fuel combustion (grey curve).

in the non-dust sulfate ($[\text{non-dust sulfate}] = [\text{sulfate}] - 0.22[\text{calcium}]$) can be related to volcanic eruptions (Zielinski, 1995) as shown in Fig. 4.4. Strong anthropogenic sulfate concentrations prevent an unambiguous identification of volcanic eruptions in the upper 20 m weq, corresponding to the period AD 2009 to 1941. Hence, potential signals of the Pinatubo (1991), El Chichon (1982), and Agung (1963) eruptions could not be attributed. Four eruptions were identified in the non-dust sulfate record: Kharimkotan (1933), Katmai (1912), Shiveluch (1854), and Tambora (1815). Remarkable is the strength of the 1815 Tambora eruption with its signal even exceeding the anthropogenic emissions. A similarly pronounced 1815 Tambora signal was observed at the Belukha glacier in the Siberian Altai (Olivier et al., 2006), reinforcing the dating for both ice cores. Older eruptions could not be clearly identified, which requires more than one sample with elevated sulfate concentration, due to an attenuation of the signal by annual layer thinning. Elevated concentrations in non-dust record for the lowest cm are not attributed to a volcanic eruption but rather an artifact of the nearby bedrock. The same is seen for the other ion records.

4.4.2 Annual layer counting

To obtain a continuous age-depth relation and to account for interannual accumulation variations, annual layer counting (ALC) was performed using the record of seasonally varying parameters ($\delta^{18}\text{O}$, concentration of formate and ammonium). This method has been successfully applied before in ice core science (Cole-Dai et al., 1997; Olivier et al.,

2006). On average one year contains 9 to 10 samples, ranging from 30 at the top to 2 samples at 36 m weq, the year 1815. Below this depth recognition of annual cycles and allocation of volcanic eruptions was not possible since the sampling resolution could not be increased further for adjusting to the strong annual-layer thinning. The uncertainty of ALC was established through repeated counting. Within one decade of an identified horizon an error of ± 1 year was estimated increasing to $\pm 2-3$ years outside of these ranges (1998-1974, 1952-1944, 1902-1865, 1843-1826). Chemical tracers are independent of the $\delta^{18}\text{O}$ record, which further increases the robustness of the ALC.

4.4.3 Radioactive dating with ^{210}Pb

To obtain an additional and independent timescale, ^{210}Pb activity was analyzed in the ice. This technique allows dating on a centennial timescale determined by the half-life of ^{210}Pb ($t_{1/2} = 22.3$ years) and has been applied before for ice cores (Gäggeler et al., 1983; Eichler et al., 2000). The decreasing activity with depth was used to establish an age-depth relation, assuming constant input of ^{210}Pb and no post-depositional alteration. Fig. 4.5 shows the decrease of ^{210}Pb activity concentration and the corresponding age increase with depth. The values range from 1.7 to 387 mBq l^{-1} with an error of 1.7 to 14.6% depending on the counting statistics. The scatter of the data in the uppermost 15 m weq can partly be explained by deviation of the assumed constant input. With increasing depth the nonlinear activity-depth relation confirms the annual-layer thinning for the lower part of the glacier. The ^{210}Pb surface activity in the Tsambagarav mountain range is 272 mBq l^{-1} , obtained by applying a linear regression to the upper 20 m weq and defining the y intercept as surface activity. This approach neglects compaction of the annual layers for this section. The value is identical with the surface activity at the Belukha glacier (280 mBq l^{-1} , Olivier et al. (2006), but much higher than in less continental areas such as the Alps (85 mBq l^{-1} , Eichler et al. (2000)). High surface activity allowed dating back to AD 1853 \pm 5. The period AD 1815-2009 was thus dated by four independent techniques, which agree well. The ^3H fallout in 1963, major volcanic eruptions and ALC dates are all located within the uncertainty of the ^{210}Pb values (see Fig. 4.5).

4.4 Dating of the ice core archive for the period AD 1815-2009

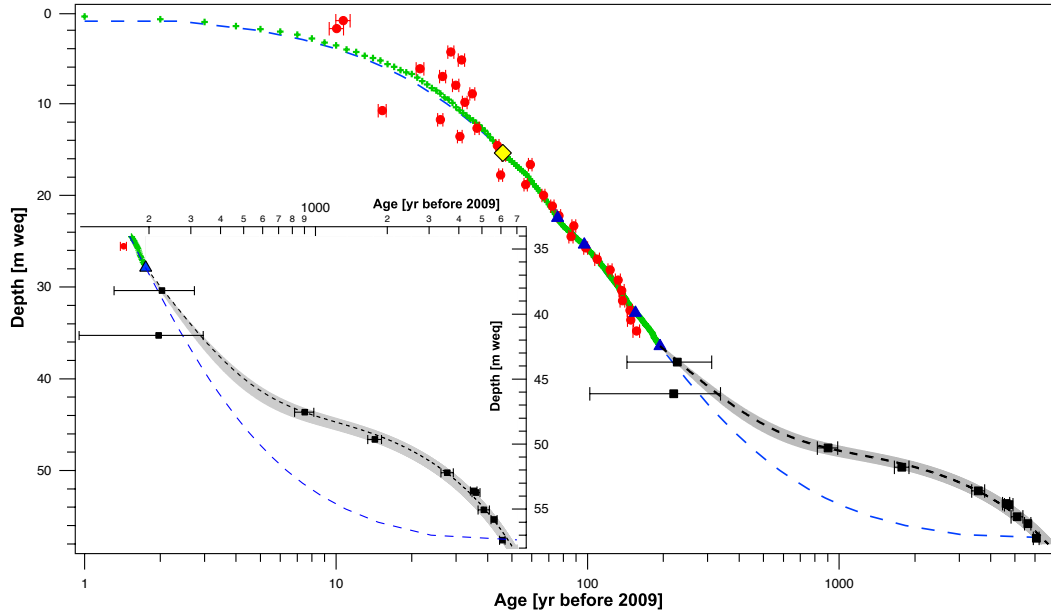


Figure 4.5: Age-depth relationship for the Tsambagarav ice core. Annual layer counting (green crosses), tritium peak (yellow diamond), volcanic eruptions (blue triangle), ^{210}Pb activity with analytical uncertainties (red circles), glacier flow model (blue dashed line), exponential equation (black dashed line) with upper and lower limit of the equation (grey shaded area) and ^{14}C values with the 1σ -range (black squares). Insert: magnification of the lower 36 m weq with identical symbols.

4.4.4 Glacier flow model

A further method to establish an age-depth scale is the application of a simple glacier flow model given by

$$z(t) = H \left[1 - \left(\frac{t \cdot b \cdot p}{H} - 1 \right)^{1/p} \right] \quad (4.1)$$

where H is the glacier thickness (58 m weq), z the depth in water equivalent, t the time, b the modeled averaged accumulation rate, and p a constant (Thompson et al., 1998). Dated horizons and ALC were used to fit b and p in Equation 4.1 ($R^2=0.998$). The flow model reproduces well the timescale derived by the combination of the different dating methods (Fig. 4.5). Thus, the upper 36 m weq of the Tsambagarav ice core give a consistent age-depth relation with annual resolution.

4.5 Millennial ice from the Mongolian Altai

4.5.1 Complex age-depth relation derived from ^{14}C data

To establish a timescale for the lower part of the ice core, a radiocarbon method for dating ice developed by our group was applied (Jenk et al., 2009; Kellerhals et al., 2010). From a total of ten radiocarbon samples, the uppermost two were analyzed to investigate a possible offset in the transition from the upper to the lower part of the ice core caused by an initial age of the carbonaceous particles (inbuilt ^{14}C). The eight remaining samples were used to date the ten meters weq above bedrock. The age ranges of the top two samples (ETH43436.1.1, ETH43438.1.1) at 38.19 and 41.64 m weq are 280 to 10 and 270 to 10 cal years BP, respectively. This large relative uncertainty has two reasons: First, the ages are at the upper boundary of the radiocarbon method (<500 cal years BP, Jenk et al. (2009)), which is determined by the potential influence from fossil fuel emissions, and second the scattering of the radiocarbon calibration curve in this period. Because of this large uncertainty, the two ages cannot be distinguished. Nevertheless, the horizon at the 1815 Tambora eruption lies within the 1σ -range of the ^{14}C ages, making a dating offset between the methods used in the upper and lower part of the ice core unlikely. Therefore the ^{14}C values seem to be suitable to establish an age-depth relation for the lower part of the ice core.

Given that, the ^{14}C ages show a steady increase for the section 36 m weq down to bedrock (Table 4.1), reinforcing the suitability of the method. The 68% range is relatively small, due to good AMS measurement performance, little scatter in the calibration curve, and large sample sizes. The concentrations of particulate organic carbon varied from 116 to 340 $\mu\text{g l}^{-1}$, resulting in absolute carbon amounts well above the limit of the method (3 μg , Sigl et al. (2009)). For the sections 36 to 52 m weq, the values indicate faster layer thinning than predicted by commonly used age-depth models (Nye (1963), Thompson et al. (1990); see 4.4.4, Fig. 4.5). This characteristic has been noticed before for other mid-latitude glaciers frozen to bedrock (Thompson et al., 1998; Knüsel et al., 2003). An alternative age-depth model is thus required to fit the discrete ^{14}C ages and obtain a continuous timescale. Analogous to the approach used in Thompson et al. (1998), an empirical exponential equation given by

$$z(t) = a \cdot e^{b \cdot t} + c \cdot e^{d \cdot t} \quad (4.2)$$

was derived, where z is the depth in m weq, t the time in years BP, and a - d are constants.

The equation 4.2 has been applied for the lower part of the ice core and therefore only valid for $z > 36$ m weq. Nine horizons were used to fit the equation, including the 1815 Tambora eruption and the eight lower ^{14}C ages. The considered horizons are well reproduced by the equation ($R^2=0.997$) with an almost perfect match of the 1815 Tambora eruption leading to a smooth transition from the upper to the lower part of the ice core (Fig. 4.5). The model uncertainty was determined by two alternative datasets. The lower (upper) limit of the model was calculated by fitting Equation 4.2 with the 1815 Tambora eruption and the ^{14}C ages minus (plus) one standard deviation. The empirical exponential equation 4.2 provides a monotonic age-depth model and avoids constant layer thickness between two time horizons, which would lead to a stepwise function implying abrupt changes in layer thickness. Since the glacier flow model (Equation 4.1) approaches asymptotically the depth of 58 m weq, the intersection with the empirically derived timescale (Equation 4.1) is located at 57.6 m weq predicting identical age at bedrock.

4.5.2 Neoglacial ice at bedrock

The ^{14}C dates revealed a basal age of 5920 to 5660 cal years BP. Sufficient carbon content gives a confident value with a small relative uncertainty. This age of the deepest ice close to bedrock suggests ice-free conditions prior to approximately 6000 years BP at 4100 m asl on the summit of Khukh Nuru Uul. Complete disappearance of glaciers during the HCO has been identified in various glaciated areas of the globe (Solomina et al., 2008; Davis et al., 2009). The disappearance of the tropical glaciers in the Andes has been explained through a combination of increasing temperatures and most notably a decrease in precipitation (Abbott et al., 2003). Also in Scandinavia most of the glaciers melted away during the mid Holocene mainly because of increased summer temperatures (Nesje, 2009) and there is evidence that also in the High Arctic ice caps had disappeared (Madsen and Thorsteinsson, 2001).

The maximal ice age of 6000 years BP can be interpreted as glacier advance following the HCO and provides indication for the onset of the Neoglaciation. The timing is consistent with glacier waxing in northwestern China (5680 years BP, Zhou et al. (1991)), implying that this feature of Neoglaciation is more than only a local phenomenon of the Mongolian Altai, and corroborating the findings of this study. Complete glacier vanishing was also suggested for the Russian Altai by 7000 years BP, however the advance occurred later, around 5000 years BP (Agatova et al., 2012).

This is the first study documenting the end of the HCO and the onset of Neoglaciation

in the Mongolian Altai. There is strong evidence that the top of Khukh Nuru Uul was ice free until roughly 6000 years BP, pointing towards glacier-hostile climatic conditions during the HCO, inducing a minimum ELA-shift of 430 m from 3700 to 4130 m. Extrapolating this increase in ELA to the surrounding glaciated areas results in a complete degradation of the Mongolian glaciers south of the Tsambagarav mountain range where the altitude difference between ELA and summit is today smaller than 430 m. To the north glaciers must at least have declined severely, as an ELA increase of 430 m would in the present conditions not be sufficient for complete degradation. This approach is conservative since the upper limit of the ELA-shift is defined by the elevation of Khukh Nuru Uul and might have been larger. Nevertheless the possibility remains that glaciers located on north facing slopes survived the ELA increase.

Pollen records from lake sediments about 200 km north of drilling site suggest a timberline rise of 400 m during the HCO, implying a temperature increase of approximately 5°C (Blyakharchuk et al., 2007). Assuming constant accumulation and a lapse rate of 2°C per 300 m results in a positive ELA-shift of 750 m. This value is reasonably close to the ice core derived data.

This study together with previously published records therefore suggests that most of the current glaciers in the Mongolian Altai are not remnants of the Last Glacial Maximum, but have been formed during the second part of the Holocene.

4.6 Accumulation reconstruction

4.6.1 Accumulation rates for the period AD 1815 to 2009

Annual accumulation rates can be reconstructed based on ALC combined with flow models to correct for the nonlinear thinning. The flow model used to date the upper part of the ice core (Equation 4.1, Thompson et al. (1990)) provides an adequate thinning rate. The accumulation was calculated from the ratio of the measured annual layer thickness obtained by ALC to the modeled thickness multiplied by the surface accumulation rate. Neglecting lateral flow within the upper 3.35 m weq (covering a period of 10 years) yields an annual surface accumulation rate of 335 mm. For the period AD 1815 to 2009 the reconstructed mean annual accumulation rate is 329 mm weq with a standard deviation of 91 mm. The profile shows no trend although drier decades are identifiable around AD 1950 and 1910 (Fig. 4.6). The mean value is in good agreement with the annual surface accumulation of 335 mm and appears plausible in comparison with annual precipitation in the lowlands of less than 200 mm. This is the first study providing glacier accumula-

tion estimates for the last 200 years in the Mongolian Altai.

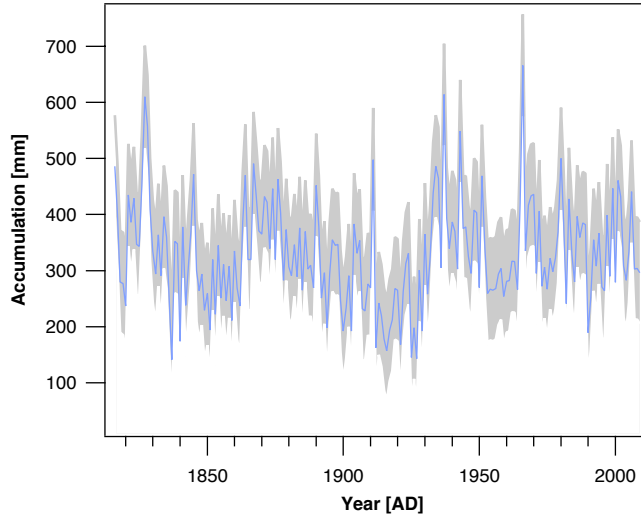


Figure 4.6: Accumulation profile for the period AD 1825 to 2009 in m weq with 1σ uncertainties.

Other studies (Ovchinnikov, 2004; Kalugin et al., 2005) investigated high-resolution climate records from the Russian Altai. A comparison with this study showed no common trends in aridity or humidity and therefore suggests a pronounced north-south precipitation pattern in Altai regarding short-term changes.

4.6.2 Accumulation trends for the past 6 kyr

For the lower 20 m weq, another approach was required to reconstruct the accumulation since the derived age-depth relation (Equation 4.1) deviates from the age-depth model (Equation 4.2; Fig. 4.5). Within the section 45 to 52 m weq, the age-depth function suggests a more rapid thinning relative to the lowest six m weq. Changes in the accumulation rate are one possible explanation for this characteristic. To account for these fluctuations another approach was applied by a stepwise calculation of the accumulation rate (b_{ij}) between two dated horizons i and j resulting in a function given by

$$b_{ij} = \frac{1}{\Delta t_{ij}} \cdot \int_i^j \left(1 - \frac{z}{H}\right)^{-p} dz \quad (4.3)$$

where Δt_{ij} is the number of years between z_i and z_j analogous to (Thompson et al., 1998). In order to better describe the observed fluctuation in layer thinning, different

4 Onset of Neoglaciation in Mongolia

parameters p (0.7, 1.1 and 1.3) were used representing weak, medium, and strong thinning resulting in three time series of accumulation according to (Thompson et al., 1998). The reconstructed accumulation rates differ largely with varying p yet following a similar trend. Fig. 4.7 shows three distinct phases of high, low, and again high accumulation rates. The ice core data does not allow identification of short-term accumulation changes in the lower part. There, the resolution is given by the time difference between two ^{14}C ages, which is on average 700 years (see Table 4.1).

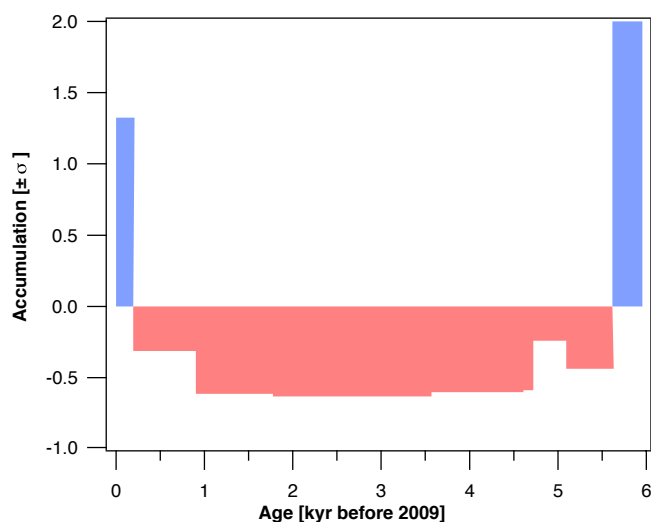


Figure 4.7: Accumulation reconstruction presented as anomaly from the mean for the past 6 kyr. The three age-depth models representing weak, medium, and strong thinning were combined and presented as deviation from the mean.

For the interval AD 1815 to 2009 an average accumulation rate of 329 ± 91 mm was reconstructed (see section 6.1). The preceding 4500 years were significantly drier with considerably lower accumulation rates (40 ± 30 mm) compared to the period before and after. Data close to bedrock suggest an increase in humidity from 4800 to 6000 years BP (460 ± 410 mm). The thinning parameter p of Equation 4.3 becomes more important with increasing depth, resulting in substantial uncertainties.

The changes in accumulation could also be caused by a hiatus. However, the stratigraphy did not reveal visible features in the ice such as pronounced dust layers. Additionally the geochemical records (not shown) did not exhibit any peculiar concentration increase, indicating a continuous record without a hiatus.

A precipitation reconstruction from the Karakorum claims the period 1850 AD to present to be the wettest within the past millennia (Treydte et al., 2006), a conclusion supporting

the elevated accumulation rates from 1800 to 2009 AD in Mongolia. Humidity reconstruction of lake sediment records from the northern and southern Altai (Tarasov et al., 2000; Blyakharchuk et al., 2004, 2007; Rudaya et al., 2009) show similar trends as the ice core data. Wet conditions during the period 5 to 10 cal ky BP were followed by dry conditions until present. This spatial and temporal consistence of reconstructed precipitation pattern indicates a regional phenomenon. The sampling resolution of the lake sediment data prevents the identification of the short-term increase during the last 200 years as observed in the ice core data. While short-term precipitation changes did not show common features between northern and southern Altai, the pronounced long-term changes are clearly recorded on both sides of the mountain range. Thereby the intensity and occurrence of those identified changes are confirmed.

In accordance with our accumulation reconstruction (Wanner et al., 2011) proposed a shift of the Intertropical Convergence Zone (ITCZ) between the HCO and the Neoglaciation to explain drastic changes in the precipitation pattern north of the Himalaya. Dry conditions for the same period have also been suggested for the Russian and Mongolian Altai (Rudaya et al., 2009; Agatova et al., 2012). Noticeable is the persistence of dry conditions, lasting until the beginning of the Medieval Warm Period (AD 950 to 1250).

4.7 Conclusions

The Tsambagarav ice core was dated with a variety of methods, including identification of reference horizons, annual layer counting, nuclear dating with ^{210}Pb , and a novel ^{14}C technique. This gives confidence in the obtained chronology. The upper 36 m weq embody 200 years of climate information, suitable for climate reconstruction with annual resolution. Strong annual layer thinning characterizes the lower 20 m weq. To obtain a continuous age-depth profile, an empirical equation was implemented, linking the upper and lower part of the ice core.

The accumulation reconstruction indicates changes in the precipitation pattern over the last 6000 years. The most recent 200 years are influenced by relative humid conditions, preceded by an arid period beginning around 5000 years BP. During the build-up phase of the glacier 6000 years BP, the derived accumulation suggests an increase in precipitation. This is in agreement with other reconstructions, pointing to a consistent precipitation evolution for the Altai region.

As dating of the basal ice revealed a build-up of the glacier at roughly 6000 years BP, this suggests complete glacier disappearance during the HCO as observed in various other places of the globe. The waxing of the glacier provides benchmarks for the end of

the HCO and the onset of the Neoglaciation at around 6000 years BP. The total glacier disappearance indicates higher temperatures at that time compared to present, especially since the period preceding the Neoglaciation experienced humid climatic conditions. High accumulation during the build-up of the glacier combined with decreasing temperatures is a plausible hypothesis for the onset of the glaciers in the Tsambagarav mountain range. A minimal ELA-shift of 430 m on Khukh Nuru Uul is seen as a strong indication that most glaciers in the Mongolian Altai had also disappeared. Accordingly, most glaciers in the Mongolian Altai are not remnants from the Last Glacial Maximum, but instead they were formed during the second part of the Holocene. This provides new insight into the glacialiation/deglaciation process of the Mongolian Altai.

Acknowledgements

This project was supported by the Swiss National Science Foundation (200021_119743) and the Russian Academy of Sciences (Integration project No. 92 of SB RAS and project 16.12 of Presidium RAS). We are much indebted to Sergey Mironov, Chairman of the Council of the Federal Assembly of the Russian Federation for assistance in organizing our expedition and to the Federal Security Service of the Russian Federation for flying us safely to the glacier. The support of Dr Beket from the Social Economy Research Center in Bayan-Ulgii, Mongolia, and Veronica Morozova from IWEP is highly acknowledged. We thank Beat Rufibach, Michael Sigl, Manuel Schläppi, and Heinz Gäggeler for their help in drilling the ice core. Jost Eikenberg (Paul Scherrer Institut) for ^3H analysis, Edith Vogel (University of Bern) for ^{210}Pb sample preparation, Sönke Szidat (University of Bern) for access to the Theodore system, and Lukas Wacker (ETH Zürich) for help with the AMS analysis are highly acknowledged. We thank the two reviewers Olga Solomina and Atle Nesje for their valuable comments.

References

- Abbott, M. B., Wolfe, B. B., Wolfe, A. P., Seltzer, G. O., Aravena, R., Mark, B. G., Polissar, P. J., Rodbell, D. T., Rowe, H. D., Vuille, M., 2003. Holocene paleohydrology and glacial history of the central Andes using multiproxy lake sediment studies. *Palaeogeography, Palaeoclimatology, Palaeoecology* 194 (1-3), 123–138.
- Agatova, A., Nazarov, A., Nepop, R., 2012. Holocene glacier fluctuations and climate

changes in the southeastern part of the Russian Altai (South Siberia) based on a radiocarbon chronology. *Quaternary Science Reviews* 43 (0), 74–93.

Arendt, A., Bolch, T., Cogley, J., Gardner, A., Hagen, J.-O., Hock, R., Kaser, G., Pfeffer, W., Moholdt, G., Paul, F., Radic, V., Andreassen, L., Bajracharya, S., Beedle, M., Berthier, E., Bhambri, R., Bliss, A., Brown, I., Burgess, E., Burgess, D., Cawkwell, F., Chinn, T., Copland, L., Davies, B., De Angelis, H., Dolgova, E., Filbert, K., Forester, R., Fountain, A., Frey, H., Giffen, B., Glasser, N., Gurney, S., Hagg, W., Hall, D., Haritashya, U., Hartmann, G., Helm, C., Herreid, S., Howat, I., Kapustin, G., Khromova, T., Kienholz, C., Koenig, M., Kohler, J., Kriegel, D., Kutuzov, S., Lavrentiev, I., LeBris, R., Lund, J., Manley, W., Mayer, C., Miles, E., Li, X., Menounos, B., Mercer, A., Moelg, N., Mool, P., Nosenko, G., Negrete, A., Nuth, C., Pettersson, R., Racoviteanu, A., Ranzi, R., Rastner, P., Rau, F., Raup, H., Rich, J., Rott, H., Schneider, C., Seliverstov, Y., Sharp, M., Sigurdsson, O., Stokes, C., Wheate, R., Winsvold, S., Wolken, G., Wyatt, F., Zheltyhina, N., 2012. Randolph Glacier Inventory [v2.0]: A dataset of global glacier outlines. Global land ice measurements from space, Boulder Colorado, USA. Digital Media.

Blyakharchuk, T. A., Wright, H. E., Borodavko, P. S., van der Knaap, W. O., Ammann, B., 2004. Late Glacial and Holocene vegetational changes on the Ulagan high-mountain plateau, Altai Mountains, southern Siberia. *Palaeogeography, Palaeoclimatology, Palaeoecology* 209 (1-4), 259–279.

Blyakharchuk, T. A., Wright, H. E., Borodavko, P. S., van der Knaap, W. O., Ammann, B., 2007. Late Glacial and Holocene vegetational history of the Altai Mountains (southwestern Tuva Republic, Siberia). *Palaeogeography, Palaeoclimatology, Palaeoecology* 245 (3-4), 518–534.

Bond, G., Showers, W., Cheseby, M., Lotti, R., Almasi, P., de Menocal, P., Priore, P., Cullen, H., Hajdas, I., Bonani, G., 1997. A pervasive millennial-scale cycle in North Atlantic Holocene and glacial climates. *Science* 278 (5341), 1257–1266.

Bronk Ramsey, C., 2001. Development of the radiocarbon calibration program. *Radiocarbon* 43 (2A, Part 1), 355–363.

Cole-Dai, J., Mosley-Thompson, E., Thompson, L., 1997. Annually resolved southern hemisphere volcanic history from two Antarctic ice cores. *Journal of Geophysical Research* 102 (D14), 16761–16771.

4 Onset of Neoglaciation in Mongolia

- D'Arrigo, R., Frank, D., Jacoby, G., Pederson, N., 2001. Spatial Response to Major Volcanic Events in or about AD 536, 934 and 1258: Frost Rings and Other Dendrochronological Evidence from Mongolia and Northern Siberia: Comment on R. B. Stothers, 'Volcanic dry fogs, climate cooling, and plague pandemics in Europe and the Middle East' (Climatic Change, 42, 1999). *Climatic Change* 49 (1-2), 239–246.
- Davis, P. T., Menounos, B., Osborn, G., 2009. Holocene and latest Pleistocene alpine glacier fluctuations: a global perspective. *Quaternary Science Reviews* 28 (21-22), 2021–2033.
- Demberel, O., 2011. Sovremennoe Oledenje Gornogo Uzla Tsambagarav Ul (Mongolskiy Altay) (Present day glaciation of the Tsambagarav mountain massive, Mongolian Altai). *Vestnik Tomskogo Gosudarstvenogo Universiteta* 348.
- Eichler, A., Brütsch, S., Olivier, S., Papina, T., Schwikowski, M., 2009a. A 750 year ice core record of past biogenic emissions from Siberian boreal forests. *Geophysical Research Letters* 36 (18), L18813.
- Eichler, A., Olivier, S., Henderson, K., Laube, A., Beer, J., Papina, T., Gäggeler, H., Schwikowski, M., 2009b. Temperature response in the Altai region lags solar forcing. *Geophysical Research Letters* 36 (1), L01808.
- Eichler, A., Schwikowski, M., Gäggeler, H., 2000. Glaciochemical dating of an ice core from upper Grenzgletscher (4200 m asl). *Journal of Glaciology* 46 (154), 507–515.
- Eichler, A., Tinner, W., Brütsch, S., Olivier, S., Papina, T., Schwikowski, M., 2011. An ice-core based history of Siberian forest fires since AD 1250. *Quaternary Science Reviews* 30 (9–10), 1027–1034.
- Gäggeler, H., von Gunten, H., Rössler, E., Oeschger, H., 1983. ^{210}Pb -Dating of cold Alpine firn/ice cores from Colle Gnifetti, Switzerland. *Journal of Glaciology* 29 (101), 165–177.
- Ginot, P., Stampfli, F., Stampfli, D., Schwikowski, M., Gäggeler, H., 2002. FELICS, a new ice core drilling system for high-altitude glaciers. Proceedings of the workshop "Ice Drilling Technology 2000", *Memoirs of National Institute of Polar Research, Special Issue* 56, 38–48.
- Grosjean, M., Suter, P. J., Trachsel, M., Wanner, H., 2007. Ice-borne prehistoric finds in the Swiss Alps reflect Holocene glacier fluctuations. *Journal of Quaternary Science* 22 (3), 203–207.

- Henderson, K., Laube, A., Gäggeler, H., Olivier, S., 2006. Temporal variations of accumulation and temperature during the past two centuries from Belukha ice core, Siberian Altai. *Journal of Geophysical Research* 111 (D3), D03104.
- IPCC, 2007. *Climate Change 2007 - The Physical Science Basis: Working Group I Contribution to the Fourth Assessment Report of the IPCC*. Cambridge University Press, Cambridge, UK and New York, NY, USA.
- Ivy-Ochs, S., Kerschner, H., Maisch, M., Christl, M., Kubik, P. W., Schlüchter, C., 2009. Latest Pleistocene and Holocene glacier variations in the European Alps. *Quaternary Science Reviews* 28 (21–22), 2137–2149.
- Jenk, T. M., Szidat, S., Bolius, D., Sigl, M., Gäggeler, H., Wacker, L., Ruff, M., Barbante, C., Boutron, C. F., Schwikowski, M., 2009. A novel radiocarbon dating technique applied to an ice core from the Alps indicating late Pleistocene ages. *Journal of Geophysical Research* 114 (D14), D14305.
- Johnsen, S. J., Clausen, H. B., Dansgaard, W., Gundestrup, N. S., Hammer, C. U., Andersen, U., Andersen, K. K., Hvidberg, C. S., Dahl-Jensen, D., Steffensen, J. P., Shoji, H., Sveinbjörnsdóttir, Á. E., White, J., Jouzel, J., Fisher, D., 1997. The $\delta^{18}\text{O}$ record along the Greenland Ice Core Project deep ice core and the problem of possible Eemian climatic instability. *Journal of Geophysical Research* 102 (C12), 26397–26410.
- Kalugin, I. A., Selegei, V., Goldberg, E., Seret, G., 2005. Rhythmic fine-grained sediment deposition in Lake Teletskoye, Altai, Siberia, in relation to regional climate change. *Quaternary International* 136 (1), 5–13.
- Kellerhals, T., Brütsch, S., Sigl, M., Knüsel, S., Gäggeler, H., Schwikowski, M., 2010. Ammonium concentration in ice cores: A new proxy for regional temperature reconstruction? *Journal of Geophysical Research* 115 (D16), D16123.
- Klinge, M., Böhner, J., Lehmkuhl, F., 2003. Climate pattern, snow- and timberlines in the Altai Mountains, Central Asia. *Erdkunde* 57 (4), 296–308.
- Knüsel, S., Ginot, P., Schotterer, U., Schwikowski, M., Gäggeler, H., Francou, B., Petit, J., Simoes, J., Taupin, J., 2003. Dating of two nearby ice cores from the Illimani, Bolivia. *Journal of Geophysical Research* 108 (D6), 4181.
- Lehmkuhl, F., 1998. Quaternary glaciations in central and western Mongolia. *Journal of Quaternary Science* 13 (6), 153–167.

4 Onset of Neoglaciation in Mongolia

- Lehmkuhl, F., Klinge, M., Strach, 2011. The extent and timing of Late Pleistocene Glaciations in the Altai and neighbouring mountain systems. In: Ehlers, J., Gibbard, P. L., Hughes, P. D. (Eds.), *Extent and Chronology – A Closer Look*. pp. 967–979.
- Lehmkuhl, F., Owen, L., 2005. Late Quaternary glaciation of Tibet and the bordering mountains: a review. *Boreas* 34 (2), 87–100.
- Loader, N., Helle, G., Los, S., Lehmkuhl, F., 2010. Twentieth-century summer temperature variability in the southern Altai Mountains: A carbon and oxygen isotope study of tree-rings. *The Holocene* 20 (7), 1149–1156.
- Mackay, A. W., Bezrukova, E. V., Leng, M. J., Meaney, M., Nunes, A., Piotrowska, N., Self, A., Shchetnikov, A., Shilland, E., Tarasov, P., Wang, L., White, D., 2012. Aquatic ecosystem responses to Holocene climate change and biome development in boreal, central Asia. *Quaternary Science Reviews* 41 (0), 119–131.
- Madsen, K., Thorsteinsson, T., 2001. Textures, fabrics and meltlayer stratigraphy in the Hans Tausen ice core, North Greenland - indications of late Holocene ice cap generation? In: (U.C. Hammer, ed.) *The Hans Tausen Ice Cap Glaciology and Glacial Geology*. Meddelelser om Grønland, Geoscience, pp. 97–114.
- Mayewski, P. A., Rohling, E. E., Curt Stager, J., Karlén, W., Maasch, K. A., David Meeker, L., Meyerson, E. A., Gasse, F., van Kreveland, S., Holmgren, K., Lee-Thorp, J., Rosqvist, G., Rack, F., Staubwasser, M., Schneider, R. R., Steig, E. J., 2004. Holocene climate variability. *Quaternary Research* 62 (3), 243–255.
- Miller, G. H., Geirsdóttir, Á., Zhong, Y., Larsen, D. J., Otto-Bliesner, B. L., Holland, M. M., Bailey, D. A., Refsnider, K. A., Lehman, S. J., Southon, J. R., Anderson, C., Björnsson, H., Thordarson, T., 2012. Abrupt onset of the Little Ice Age triggered by volcanism and sustained by sea-ice/ocean feedbacks. *Geophysical Research Letters* 39 (2), L02708.
- Nesje, A., 2009. Latest Pleistocene and Holocene alpine glacier fluctuations in Scandinavia. *Quaternary Science Reviews* 28 (21–22), 2119–2136.
- Nesje, A., Pilo, L. H., Finstad, E., Solli, B., Wangen, V., Odegard, R. S., Isaksen, K., Storen, E. N., Bakke, D. I., Andreassen, L. M., 2012. The climatic significance of artefacts related to prehistoric reindeer hunting exposed at melting ice patches in southern Norway. *The Holocene* 22 (4), 485–496.

- Nye, J., 1963. Correction factor for accumulation measured by the thickness of the annual layers in an ice sheet. *Journal of Glaciology* 4 (36), 785–788.
- Oerlemans, J., 2005. Extracting a climate signal from 169 glacier records. *Science* 308 (5722), 675–677.
- Olivier, S., Bajo, S., Fifield, L. K., Gägger, H., Papina, T., Santschi, P. H., Schotterer, U., Schwikowski, M., Wacker, L., 2004. Plutonium from global fallout recorded in an ice core from the Belukha glacier, Siberian Altai. *Environmental Science & Technology* 38 (24), 6507–6512.
- Olivier, S., Blaser, C., Brüttsch, S., Frolova, N., Gägger, H., Henderson, K. A., Palmer, A. S., Papina, T., Schwikowski, M., 2006. Temporal variations of mineral dust, biogenic tracers, and anthropogenic species during the past two centuries from Belukha ice core, Siberian Altai. *Journal of Geophysical Research* 111 (D5), D05309.
- Ovchinnikov, D. V., 2004. Reconstruction of glacier mass balance of the Malii Aktru (Altay), according to maximum density of tree-rings. *Proceedings of the RGS* 134 (1), 37–45.
- Owen, L. A., 2009. Latest Pleistocene and Holocene glacier fluctuations in the Himalaya and Tibet. *Quaternary Science Reviews* 28 (21–22), 2150–2164.
- Reimer, P. J., Baillie, M. G. L., Bard, E., Bayliss, A., Beck, J. W., Blackwell, P. G., Ramsey, C. B., Buck, C. E., Burr, G. S., Edwards, R. L., Friedrich, M., Grootes, P. M., Guilderson, T. P., Hajdas, I., Heaton, T. J., Hogg, A. G., Hughen, K. A., Kaiser, K. F., Kromer, B., McCormac, F. G., Manning, S. W., Reimer, R. W., Richards, D. A., Southon, J. R., Talamo, S., Turney, C. S. M., van der Plicht, J., Weyhenmeyer, C. E., 2009. Intcal09 and marine09 radiocarbon age calibration curves, 0–50,000 years cal bp. *Radiocarbon* 51 (4), 1111–1150.
- Robock, A., Jianping, M., 1995. The volcanic signal in surface temperature observations. *Journal of Climate* 8, 1086–1103.
- Rudaya, N., Tarasov, P., Dorofeyuk, N., Solovieva, N., Kalugin, I., Andreev, A., Daryin, A., Diekmann, B., Riedel, F., Tserendash, N., Wagner, M., 2009. Holocene environments and climate in the Mongolian Altai reconstructed from the Hoton-Nur pollen and diatom records: a step towards better understanding climate dynamics in Central Asia. *Quaternary Science Reviews* 28 (5–6), 540–554.

4 Onset of Neoglaciatioin in Mongolia

- Ruff, M., Wacker, L., Gäggeler, H., Suter, M., Synal, H.-A., Szidat, S., 2007. A gas ion source for radiocarbon measurements at 200 kV. *Radiocarbon* 49 (2), 307–314.
- Schotterer, U., Fröhlich, K., Gäggeler, H. W., Sandjordj, S., Stichler, W., 1997. Isotope records from Mongolian and Alpine ice cores as climate indicators. *Climatic Change* 36 (3), 519–530.
- Sigl, M., Jenk, T., Kellerhals, T., Szidat, S., 2009. Towards radiocarbon dating of ice cores. *Journal of Glaciology* 55 (194), 985–996.
- Solomina, O., Haeberli, W., Kull, C., Wiles, G., 2008. Historical and Holocene glacier–climate variations: General concepts and overview. *Global and Planetary Change* 60 (1–2), 1–9.
- Synal, H.-A., Stocker, M., Suter, M., 2007. MICADAS: A new compact radiocarbon AMS system. *Nuclear Instruments and Methods in Physics Research Section B: Beam Interactions with Materials and Atoms* 259 (1), 7–13.
- Szidat, S., Jenk, T. M., Gäggeler, H. W., Synal, H.-A., Hajdas, I., Bonani, G., Saurer, M., 2004. THEODORE, a two-step heating system for the EC/OC determination of radiocarbon (^{14}C) in the environment. *Nuclear Instruments and Methods in Physics Research Section B: Beam Interactions with Materials and Atoms* 223–224, 829–836.
- Tarasov, P., Dorofeyuk, N., TSEVA, E. M., 2000. Holocene vegetation and climate changes in Hoton-Nur basin, northwest Mongolia. *Boreas* 29 (2), 117–126.
- Thompson, L. G., Davis, M. E., Mosley-Thompson, E., Sowers, T. A., Henderson, K., Zagorodnov, V., Lin, P.-N., Mikhaleiko, V. N., Campen, R. K., Bolzan, J. F., Cole-Dai, J., Francou, B., 1998. A 25,000-year tropical climate history from Bolivian ice cores. *Science* 282 (5395), 1858–1864.
- Thompson, L. G., Mosley-Thompson, E., Davis, M., Bolzan, J. F., Dai, J., Klein, L., Gundestrup, N., Yao, T., Wu, X., Xie, Z., 1990. Glacial stage ice core records from the subtropical Dunde ice cap, China. *Annals of Glaciology* 14, 288–297.
- Treydte, K. S., Schleser, G. H., Helle, G., Frank, D. C., Winiger, M., Haug, G. H., Esper, J., 2006. The twentieth century was the wettest period in northern Pakistan over the past millennium. *Nature* 440 (7088), 1179–1182.
- Wanner, H., Solomina, O., Grosjean, M., Ritz, S., 2011. Structure and origin of Holocene cold events. *Quaternary Science Reviews* 30 (21–22), 3109–3123.

4.7 Conclusions

- Zhou, S., Chen, F., Pan, B., Cao, J., Li, J., Derbyshire, E., 1991. Environmental change during the Holocene in western China on a millennial timescale. *The Holocene* 1 (2), 151–156.
- Zielinski, G. A., 1995. Stratospheric loading and optical depth estimates of explosive volcanism over the last 2100 years derived from the Greenland Ice Sheet Project 2 ice core. *Journal of Geophysical Research* 100 (D10), 20937–20955.

5 Late-Holocene temperature reconstruction for Siberia

Pierre-Alain Herren^{a,b}, Anja Eichler^{a,b}, Tatyana Papina^c, and Margit Schwikowski^{a,b,d}

^aPaul Scherrer Institut, 5232 Villigen PSI, Switzerland

^bOeschger Centre for Climate Change Research, University of Bern, 3012 Bern, Switzerland

^cInstitute for Water and Environmental Problems, 656038 Barnaul, Russia

^dDepartment of Chemistry and Biochemistry, University of Bern, 3012 Bern, Switzerland

To be submitted to Nature Geoscience

Abstract

Current climate change has strong regional patterns. To investigate the spatio-temporal differences, regionally resolved paleoclimate records are required. Here we reconstructed temperature for the past 3,200 years based on concentration of biogenic species measured in an ice core from the Altai. This novel temperature record of the Siberian forests together with two tree-ring chronologies located north and south on the Asian continent, suggest elevated temperature at the start of the current era (CE) 2,000 years ago. This period can be assigned to the Roman Warm Period (RWP). The occurrence within individual records considered for comparison differ in time and in magnitude yet all show the same pattern. We argue that Siberia experienced a pronounced RWP. The agreement with other Asian records indicates a pronounced continental occurrence. The rapid transition to colder climate is consistent with the Migration period. Due to resolution issues and boundary effects, comparison to present warming is difficult. On a long-term perspective (100 years) current temperatures in Siberia are at least as warm as any time during the past 3,200 years.

5.1 Importance of regionally resolved paleoclimate records for northern Asia

Current climate change has diverse spatial and temporal consequences (IPCC, 2007). Changes in precipitation or temperature affect the continents differently. Regionally resolved long-term perspectives are required to distinguish internal variability from human induced changes. Especially millennial reconstructions are important to investigate centennial climate fluctuations not captured by the instrumental data. This applies in particular for remote areas such as Siberia. This region experienced enhanced warming during the industrial period (Hansen et al., 1998; Bradley et al., 2003; Hansen, 2006) but understanding of its internal climate variability is lacking. The embedding of the Siberian climate into the global atmospheric teleconnections is still insufficient. Siberia and Central Asia are strongly influenced by the Siberian-High (SH), an anticyclone located during wintertime over Eurasia and with larger pressure differences than the well studied Icelandic Low in the Atlantic or Aleutian Low in the Pacific (Sahsamanoglou et al., 1991). Changes in the SH intensity have been related to Asian temperature changes, autumn snow cover, precipitation and the Arctic oscillation (Gong and Ho, 2002; Wu and Wang, 2002; Cohen et al., 2001; D'Arrigo et al., 2005). During summer 2003 forest fires in Siberia contributed to a strong increase of the CO₂ concentrations mea-

5.1 Importance of regionally resolved paleoclimate records for northern Asia

sured at Mauna Loa (Huang et al., 2009). These two examples illustrate the regional complexities of the Siberian climate system with impacts on a global scale. Thereby regional paleoclimatic records are required for a long-term perspective. The Past Global Changes (PAGES) 'PAGES 2k' project aims to produce a global array of regional climate reconstructions for the past 2000 years. Regarding Asia, the reconstruction consists exclusively of tree-rings records and covers the period AD 800-1989 (PAGES2k-Consortium, 2013). Additional long-term paleoclimatic records from different archives are necessary for a broader support of the Asian temperature reconstruction. Two ice cores from the Altai Mountain Range, located on the southern border of Siberia, provide the unique opportunity to contribute in reconstructing the regional climate. This part of the globe experiences strong continental conditions (Lydolph, 1977) and lacks high-resolution paleoclimate records other than tree-ring reconstructions. The first ice core drilled in 2001 at the Belukha saddle, Russia (4062 m asl., 49°48'26"N, 86°34'43"E, Fig. 5.1) is situated on the northern side of the Altai (Olivier et al., 2003). It covers the period AD 1250 to 2000 (Eichler et al., 2009b). The second ice core was collected during summer 2009 in the Tsambagarav Mountains, Mongolia (4130 m asl., 48°39'20"N, 90°50'50"E, Fig. 5.1), located on the southern side of the massif (Herren et al., 2013). This ice core contains Mid-Holocene climate information reaching back 6,000 years BP (Herren et al., 2013). Both ice cores were dated using ^{210}Pb activity record, a three-parameter annual layer-counting methodology and reference horizons, such as the maximum of nuclear weapons testing 1963 (Maximum in ^3H activity) and different volcanic eruptions (Eichler et al., 2009b; Herren et al., 2013). In the lower part of the Tsambagarav ice core particulate organic carbon was used to derive radiocarbon ages. For the period AD 1250 to 2009 the mean dating uncertainty for the Belukha is ± 10 years. Strong thinning of annual layers in the Tsambagarav ice core induce an mean uncertainty of ± 75 years for the last 750 years, rising to ± 150 years for the preceding millennia.

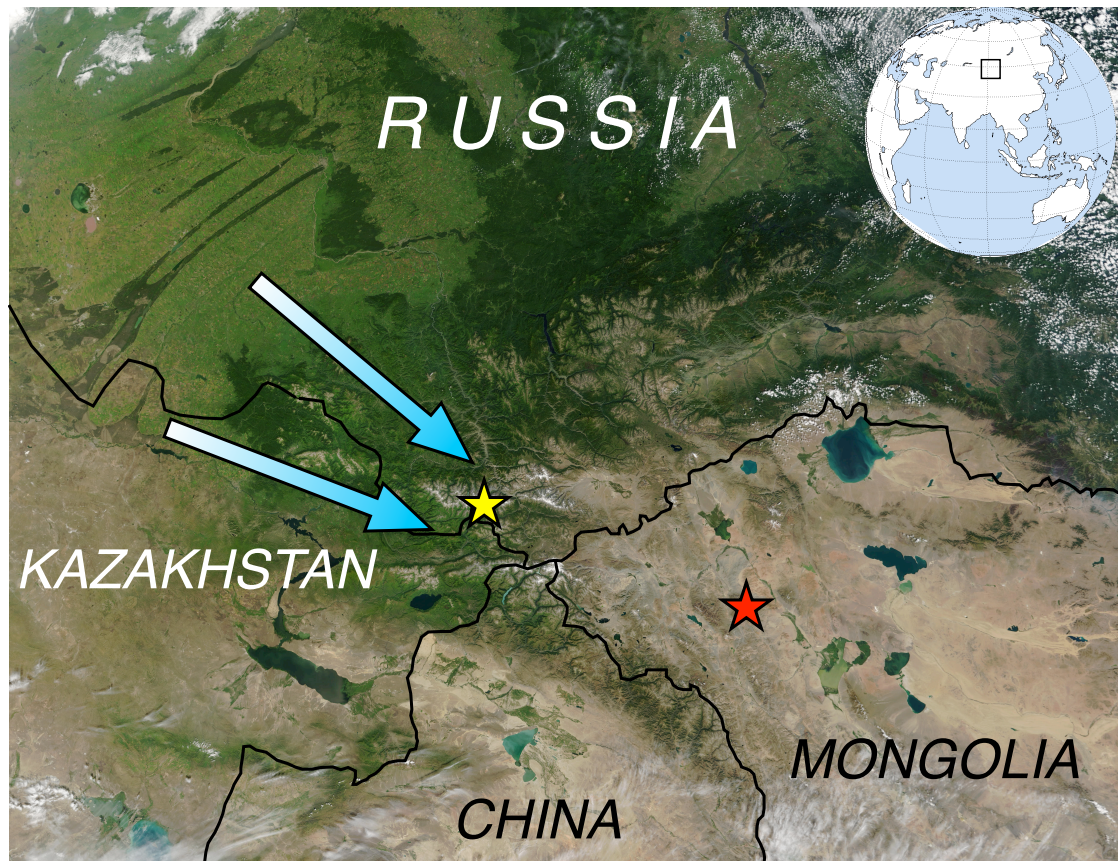


Figure 5.1: Location of the Belukha (yellow star) and Tsambagarav (red star) ice core sites in the Altai Mountain range. Blue arrows indicate the dominant direction of moisture transport to the glacier, based on seven-day back trajectories for June, July, and August in the period 1991-2000 using HYSPLIT and the NCEP reanalysis. Back trajectories were run every 6 hours. Background is true-color image from the Moderate Resolution Imaging Spectroradiometer (MODIS) on the Terra satellite (Jacques Descloitres, MODIS Land Rapid Response Team, NASA/GSFC) of south-central Russia. It shows the marked change in vegetation between Russia and northern Mongolia (bottom right) and northern China (bottom center).

5.2 Biogenic emissions as temperature proxy

Here we used the second principle component (PC2) of the geochemical records measured in the Tsambagarav ice core as temperature proxy for Siberia. Principal Component Analysis (PCA) was performed for 20-year means of 9 major ions over the period BC 1200 to AD 1940 to investigate the main sources of the chemical species (Table 5.1). After AD 1940 anthropogenic NH_3 limiting the paleoclimate reconstruction up to the pre-industrial period. The first three principle components explain 86% of the total data

5.3 Calibration and assessment of a new temperature proxy

variance. The first principal component (PC1) with high loadings of most ions, explains more than 63% of the total data variance. It is attributed to the transport of mineral dust-related species to the glacier. PC2 with high loadings of ammonium (NH_4^+) and formate (HCOO^-) reflects exclusively to biogenic emissions upwind the drilling site. We argue that the PC3 with high loadings in K^+ can be associated with the forest fire history, however the low loading in NO_3^- weakens the representativeness (Song et al., 2005). In this study we focus on the interpretation of PC2 and its relation to biogenic activity. The natural sources of NH_3 (precursor of NH_4^+) are mainly vegetation and soil emissions (Dentener and Crutzen, 1994; Langford and Fehsenfeld, 1992), while HCOOH (precursor of HCOO^-) emanates directly from the vegetation or is produced through oxidation of species like isoprene and monoterpenes (Chebbi and Carlier, 1996). A positive link between emission rates of various biogenic species and temperature was shown for different biogenic species and regions of the globe (Fuentes et al., 1996; Dentener and Crutzen, 1994; Rinne et al., 2002; Guenther et al., 1995; Monson et al., 1992). Air masses reaching the Tsambagarav glacier mainly originate from the northwest (Aizen et al. (2006), Fig. 5.1). During transport over the taiga belt they collect precursors gases of biogenic emission, which are deposited onto the glacier during snowfall. In the Altai biogenic emissions and precipitation peak in the summer months (Lydolph, 1977), resulting in an archive of the biogenic activity in the Taiga belt not diluted through winter precipitation. Ice core studies from the Andes, Himalaya and Altai confirmed this relation by correlating temperature changes to variations in the concentration of biogenic species measured in the ice (Kellerhals et al., 2010; Eichler et al., 2009a; Kang et al., 2002). Natural emissions are low compared to anthropogenic, thus extended source areas are required for a sensitive proxy.

The Siberian forest within Russia accounts for approximately 17 million km^2 corresponding two thirds of Earth's boreal forest (Wooster and Zhang, 2004).

Similar to an ice core study from tropical South America (Kellerhals et al., 2010), we argue that sources of those biogenic species are emanation from soil and vegetation in the Siberian plains.

5.3 Calibration and assessment of a new temperature proxy

Limited and spatially sparse regional instrumental data impede direct calibration. After AD 1940 anthropogenic NH_3 emissions changed the atmospheric mixing ratios in Siberia, making temperature reconstruction for the industrial period impossible (Herren et al.,

5 Late-Holocene temperature reconstruction for Siberia

Table 5.1: Loadings of the Tsambagarav PCA performed on the normalized 20-year means of the 9 major ions and the variance explained by each component for the time period 1200 BC to AD 1940.

	PC1	PC2	PC3
Ca ²⁺	0.90	-0.30	-0.10
Na ⁺	0.89	-0.32	-0.10
Mg ²⁺	0.88	-0.29	0.01
Cl ⁻	0.88	-0.33	-0.10
NO ₃ ⁻	0.81	0.22	0.17
SO ₄ ²⁻	0.81	0.10	-0.17
NH ₄ ⁺	0.75	0.62	-0.06
HCOO ⁻	0.72	0.52	-0.11
K ⁺	0.43	-0.03	0.89
<i>Variance explained</i>	<i>64%</i>	<i>12%</i>	<i>10%</i>
	Mineral dust	Biogenic emissions	Biomass burning

2013). The sample size is further reduced through the 20-year resolution, given by the thinning of annual layer with increasing glacier depth (Nye, 1963; Herren et al., 2013). For this study we take advantage of the $\delta^{18}\text{O}$ based March-November temperature reconstruction from the Belukha ice core located in the Siberian Altai (Eichler et al., 2009b) (Fig. 5.1). The PC2 reflecting biogenic concentrations of the Tsambagarav ice core is significantly correlated with reconstructed temperature from Belukha ($r = 0.70$, $n = 19$, $p < 0.001$; Fig. 5.2 9.3). Considering smoothed data enhances the correlation coefficient significantly, pointing towards a relation on longer timescales (Fig. 5.2). This relation is used to derive a new temperature proxy for the Siberian forest located upwind of the Tsambagarav glacier. The good agreement between two independent parameters ($\delta^{18}\text{O}$ and PC2) of two ice cores 350 km distant (Fig. 5.1) indicates a robust temporal and spatial interconnection. To avoid a bias of the calibration by dating uncertainties, we choose the calibration period from AD 1590 to 1940. For the time interval AD 1270 to 1590 the two records have similar trends. However, in general the Belukha $\delta^{18}\text{O}$ record precedes the PC2 chronology by 20 to 60 years (Fig. 5.2). The lag between the two records is within the dating uncertainties (Herren et al., 2013; Eichler et al., 2009b). Because of strongly decreasing resolution due to thinning, the lowest 6 m weq of the ice core were not considered. The PC2 of the Tsambagarav ice core allows for a temperature reconstruction with 20-year resolution, for the period 1200 BC to AD 1940. Combination with the Belukha ice core enables to extend the temperature reconstruction to AD 1980.

To illustrate the spatial representativeness of this reconstruction, we correlated the tem-

5.3 Calibration and assessment of a new temperature proxy

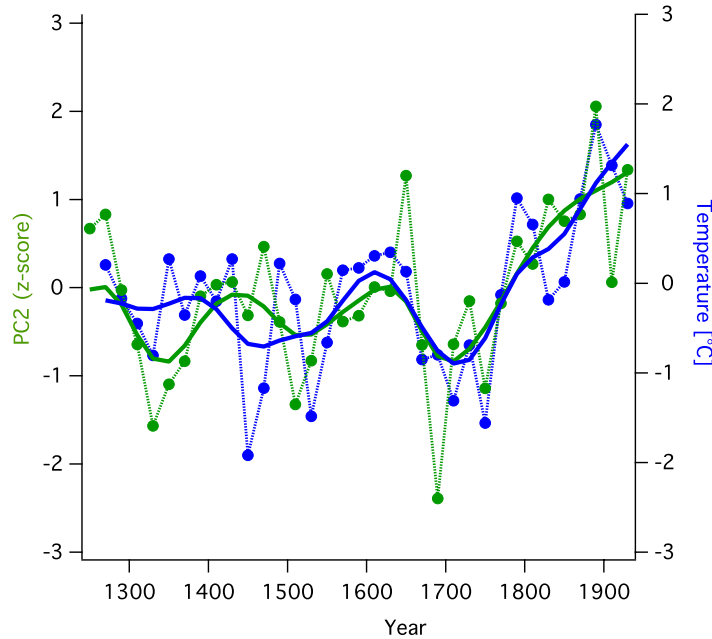


Figure 5.2: Calibration of the Tsambagarav PC2 as biogenic emission proxy (green) against $\delta^{18}\text{O}$ value from Belukha (blue). 20-year resolution values (thin line) smoothed with a 5-point binomial filter (bold curves).

perature record from Barnaul, used to calibrate the $\delta^{18}\text{O}$ record from Belukha, with gridded 20th century reanalysis data (Fig. 5.3). Although not entirely independent, since the Barnaul temperatures have been integrated in the gridded reconstruction, significant correlation ($p < 0.01$) is identifiable for large parts of Siberia.

Three independent humidity records were examined, to investigate the effect of varying precipitation on the concentration of biogenic species. The first record is directly derived from the Tsambagarav ice core through a glacier accumulation reconstruction (Herren et al., 2013). The second and third are composite records of lake sediments from the Altai and the Northern Mongolian Plateau (Wang and Feng (2013), Fig. 5.4). The Tsambagarav accumulation reconstruction shows steady dry conditions for the last 3,000 years, followed by an increase in accumulation from AD 1850 onwards. However, the low resolution does not allow for direct comparison, since temporal changes in the accumulation cannot be resolved with the accumulation record (Fig. 5.4). The two lake sediment composite records show different trends. The Altai experienced a relative dry climate during the Holocene, whereas precipitation in Northern Mongolian Plateau was above Holocene average. Trends of PC2 do not follow the humidity reconstructions. This

5 Late-Holocene temperature reconstruction for Siberia

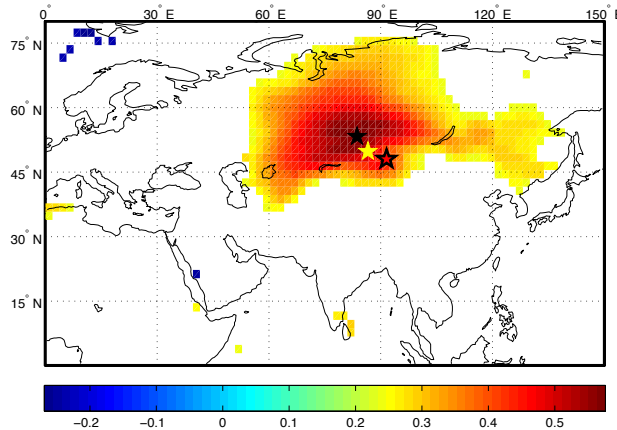


Figure 5.3: Spatial distribution of correlation coefficients between Barnaul March-November temperatures (<http://www.ncdc.noaa.gov/data-access/land-based-station-data/find-station>) and gridded 20th century Reanalysis March-November temperature (<http://climexp.knmi.nl>) shown for the period 1871-2000 ($p < 10\%$). Location of Barnaul (black star), Belukha (yellow star) and Tsambagarav (red star) are marked.

implies that precipitation changes over the past 3,200 years unlikely induced changes in the biogenic species concentration. Concentration of Ca^{2+} as mineral dust tracer is often used as precipitation proxy due to their anticorrelation (Knüsel et al., 2005). Dry conditions induce elevated dust emissions, inducing changes in Ca^{2+} concentration. For the Tsambagarav ice core this tracer cannot be used, since no common pattern was identified between humidity and Ca^{2+} concentration record (Fig. 9.1). With this we exclude a dilution effect on the biogenic species, they are assumed to be a robust temperature proxy. Fortiori since biogenic species in the Belukha ice core showed to be closely related to changes in temperature derived from the $\delta^{18}\text{O}$ record (Eichler et al., 2009a).

Despite the excellent correlation between the $\delta^{18}\text{O}$ values from Belukha and Barnaul temperature (Eichler et al., 2009b), the stable isotope record from Tsambagarav does not provide significant correlation with instrumental data of the surrounding weather stations and Reanalysis data. The 20-year resolutions of the $\delta^{18}\text{O}$ record circumvent any direct calibration. Additionally comparison of the $\delta^{18}\text{O}$ from Belukha and Tsambagarav show distinct differences for the period AD 1250 to 2000 (Fig. 9.2). Previous studies from the Altai indicate a variety of moisture sources including re-evaporation from continental moisture sources. Therefore the stable isotopes record is a combination of

moisture source and temperature (Aizen et al., 2006; Schotterer et al., 1997). Within the arid Mongolian Altai internal moisture sources have a larger contribution and thus can alter the isotope signal stronger than in the more humid north.

5.4 Late-Holocene temperature reconstruction for the Siberian plains

Fig. 5.4 shows the reconstructed temperature of the Siberian Taiga belt compared to other paleoclimate records. All following records are normalised to the overlapping period AD 1270 to 1930. The range of reconstructed temperature was calculated based on the 2σ -range of the calibration slope (Fig. 9.3). For the past 3,200 years the temperature anomalies fluctuated between -3.0 and 5.6°C with rapid transitions from warm to cold periods and vice versa, resulting in high frequency temperature changes. Smoothing the reconstruction helps to identify patterns and trends. The record allows for a characterization of different well-known climatic periods, such as the Roman Warm Period (RWP), the Dark Ages Cold Period (DACP), the Medieval Warm Period (MWP), the Little Ice Age (LIA) and the present warming. Suggested transitions between two periods are rough guides since clear identification is challenging. The thousand years preceding the current era are characterised by two pronounced cold periods ~ 530 - 710 BC and ~ 850 - 1030 BC interrupted by a warm interval. Around 650 BC our record suggests the coldest but brief period of the past 3,200 years. The RWP is the most striking feature of the record, especially regarding long-term changes. The period is long-lasting with temperatures 1.3°C above average from 130 BC to AD 310. The subsequent DACP does not show cold climate condition. The most noticeable pattern is the rapid transition around AD 310 from the RWP by a decrease in temperature of 2°C . This decrease coincides with the largest central Eurasian historical crisis, the Migration Period, a time marked by lasting political turmoil, cultural change, socioeconomic instability and westward migration of the Huns (Swain and Edwards, 2004; Hedeager, 2007). The period lasted for approximately 300 years with values fluctuating around the normalised mean. Similar to the DACP the MWP is only marginal perceptible. Temperatures are elevated by 0.5°C for slightly longer than 100 years. From around AD 890 the Siberian temperature fluctuate between 0 and -1°C . This period is the coldest of the past two millennia and confirms the occurrence of the LIA in Siberia. During this phase of permanent negative temperatures different colder dips are identifiable, with the most pronounced in the 18th century. Subsequent temperatures are steadily increasing until the end of the reconstruction in AD

5 Late-Holocene temperature reconstruction for Siberia

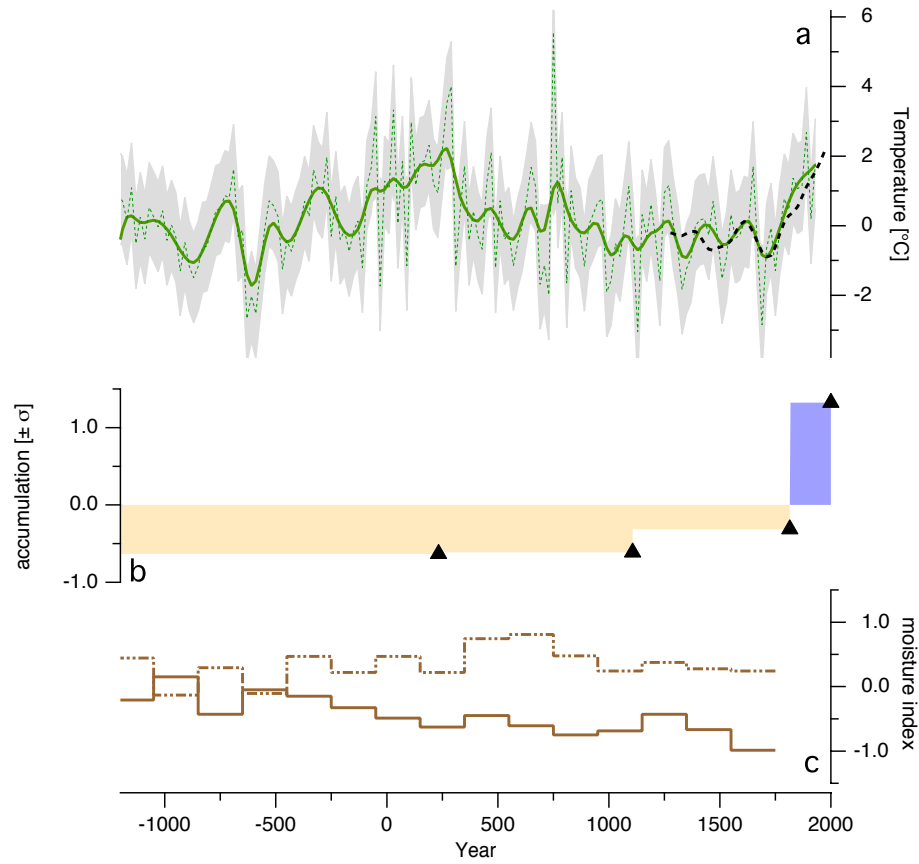


Figure 5.4: (a) Reconstructed Siberian temperature from Tsambagarav PC2 scores (normalized to the AD 1270 to 1930 period) for the last $\sim 3,200$ years (green dashed line) and smoothed with a 5-point binomial filter (bold green line) and Belukha $\delta^{18}\text{O}$ based temperature reconstruction (dashed black line). The shaded region envelops the uncertainty as described in the text. (b) Accumulation reconstruction presented as anomaly of the past $\sim 6,000$ years adapted from Herren et al. (2013). Black triangle are dating horizons to illustrate the resolution. (c) Regionally averaged moisture indices from lake sediment data for the Northern Mongolian Plateau (dashed curve) and Altai Mountains (bold curve) adapted from Wang and Feng (2013).

1980. The Belukha $\delta^{18}\text{O}$ values and the PC2 suggest identical amplitude in the warming. In Fig. 5.5 the reconstruction is compared to the instrumental data from Barnaul. The overlap time between the two records is short (AD 1860 to 1980). However, they coincide well and suggest current warming to be similar to the climate during the RWP.

5.5 Pronounced warm climate during the Roman Warm Period

For a representative chronology the ice core records from Belukha and Tsambagarav were combined. This composite temperature reconstruction covers the period 1200 BC to AD 1980 (Fig. 5.5) and is used in the following analysis as temperature record of Siberia.

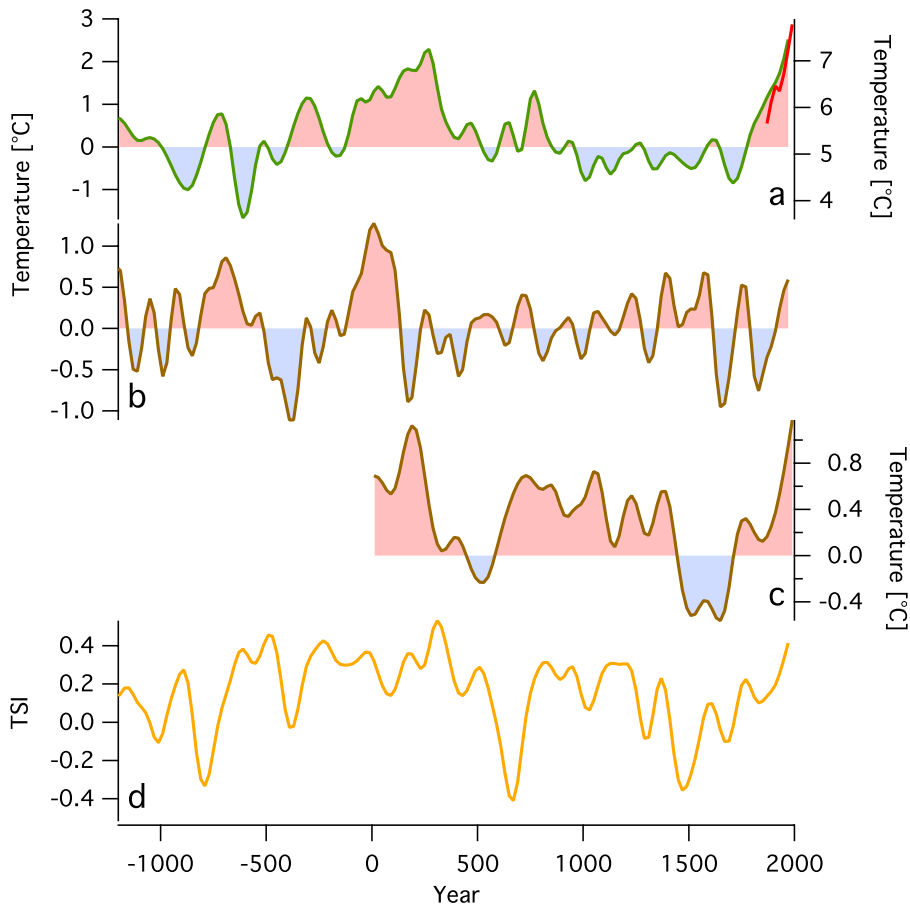


Figure 5.5: . (a) Reconstructed Siberian temperature from Tsambagarav PC2 scores and Belukha $\delta^{18}\text{O}$ values for the last $\sim 3,200$ years (bold green line) and 20-year resolution Barnaul temperature for the period AD 1870 to 1990 (red line). (b) Reconstructed southern Yamal summer temperature from tree-ring-width chronology (Hantemirov and Shiyatov, 2002). (c) China-wide temperature composites covering the last 2,000 years obtained from ice cores, tree rings, lake sediments and historical documents (Yang, 2002). (d) Total Solar Irradiance (TSI) composite from the cosmogenic radionuclide ^{10}Be measured in ice cores (Steinhilber et al., 2009). All records have 20-year resolution, are normalized to the AD 1270 to 1930 period (except Barnaul temperature) and smoothed with a 5-point binomial filter.

5 *Late-Holocene temperature reconstruction for Siberia*

In an ice core from Illimani in the eastern Bolivian Andes (Kellerhals et al., 2010), NH_4^+ concentrations were used to reconstruct Tropical South American temperature. With the Tropics being located close to the equator, limited temperature variations are predicted and accordingly changes in biogenic emissions are small. This is confirmed by the reconstruction values ranging from -0.8 to 0.4°C . However, the latitude of the Siberian Taiga is above 50°N where changes in climate are amplified compared to lower latitudes, resulting in larger temperature variations. For Tsambagarav this corresponds to changes of -1.7 to 2.9°C on centennial scale (Fig. 5.5). Model studies and measurements show that Siberia experienced enhanced warming during the past decades (Hansen et al., 1998; Hansen, 2006; Smith et al., 2007). This is corroborated by Barnaul instrumental temperature measurements increasing by 2°C in the period AD 1860 to 1980 (Fig. 5.5). Changes measured in Siberia exceed 2°C whereas in the Tropics they are around 0.4°C . This illustrates well the difference between the two sites. The difference in amplitude between the records from the Tropics and Siberia confirms the sensitivity of biogenic emissions on temperature changes.

To place this novel temperature reconstruction in perspective we consider available paleoclimatic records north and south of the Taiga belt. For this remote part of the globe the lack of data makes it difficult to find records covering identical period with similar resolution. Regarding lake sediments, a majority of the records cover the whole Holocene with low resolution that is inappropriate for comparison (Melles et al., 2012; Prokopenko et al., 2006). Thus tree-ring based climate reconstructions are most suitable for comparison. Here we take advantage of a 4000-year (2000 BC to AD 1996) tree-ring-width chronology, from which summer temperature variability in this region was estimated on annual to multidecadal timescales (Hantemirov and Shiyatov, 2002). The chronology consists of a multitude of trees located between $67^\circ00'$ and $67^\circ50'\text{N}$ and $68^\circ30'$ and $71^\circ00'\text{E}$ on the Yamal Peninsula. A conspicuous common feature is the noisiness of the temperature evolution. The region seems to experience sharp and pronounced temperature changes. The ice core data allows for identification of well-known warm and cold periods for instance the LIA or MWP. The Yamal tree-ring temperature reconstruction suggests high frequency changes from warm to cold conditions. Neither the LIA nor the MWP are identifiable. However, a distinctive period of enhanced temperatures occurred around 130 BC to AD 130 corresponding to the RWP. This interval fits best with the ice core derived data (Fig. 5.6). The difference to our record lasting approximately 150 years longer can be attributed to different effects: (i) The dating uncertainties of the ice core and tree-ring chronology. (ii) The glacier captures the signal of air masses traveling over large areas resulting in a regionally signal versus a more local from the tree-ring chronol-

5.6 Reconstructed 20th century temperature increase

ogy. Considering these two effects we suggest a regionally pronounced warm period for two and a half centuries at the beginning of the current era. The absence of recent warming in the tree-ring width chronology for the last centuries is a major difference to the ice core data. The discrepancy between observations and paleoclimate reconstructions is still not fully understood (Sidorova et al., 2011; Saurer et al., 2002).

To integrate our results in a more continental context, we compare them with 2,000 years of China temperature reconstruction located south (Fig. 5.5). The China chronology is a combination of multiple paleoclimate proxy records obtained from ice cores, tree rings, lake sediments and historical documents (Yang, 2002). Both records capture current warming, yet the highest agreement is obtained for the RWP (Fig. 5.6). The temporal occurrence of RWP coincides, with a narrower period in China ending around 100 years earlier than our Siberian record, but still within the dating uncertainty.

For the period AD 1250-1850 a strong correlation between reconstructed temperature from Belukha $\delta^{18}\text{O}$ values and solar activity was found (Eichler et al., 2009b). The new 3,200-year temperature record allows investigating this radiation interaction further back in time. For comparison we used the record derived from cosmogenic radionuclide ^{10}Be measured in ice cores (Steinhilber et al. (2009), Fig. 5.5). Prior to AD 1250 there are still common features as for the RWP, where elevated temperatures correspond to high solar irradiance. The long-term trends are similar with a general increase from 1200 BC to the RWP, followed by decrease until the end of the LIA. However, the overall correlation between temperature and solar forcing is lost. While discussing differences and similitudes between the two reconstructions, one should keep in mind the increased dating uncertainty towards longer timescales and the variability in solar reconstructions (Muscheler et al., 2007).

5.6 Reconstructed 20th century temperature increase

Most tree-ring-width chronologies from Siberia do not reflect warming since the end of the LIA. The temperature reconstruction presented in this study coincides in amplitude and timing with instrumental temperature measurements. The good agreement confirms Siberia as a fast warming region on the globe. The high sensitivity of the Taiga forests makes its especially vulnerable to temperature and precipitation changes. Atmospheric modification may trigger droughts thus increasing the risk of forest fires (Eichler et al., 2011) and induce major changes in the regional climate.

5 Late-Holocene temperature reconstruction for Siberia

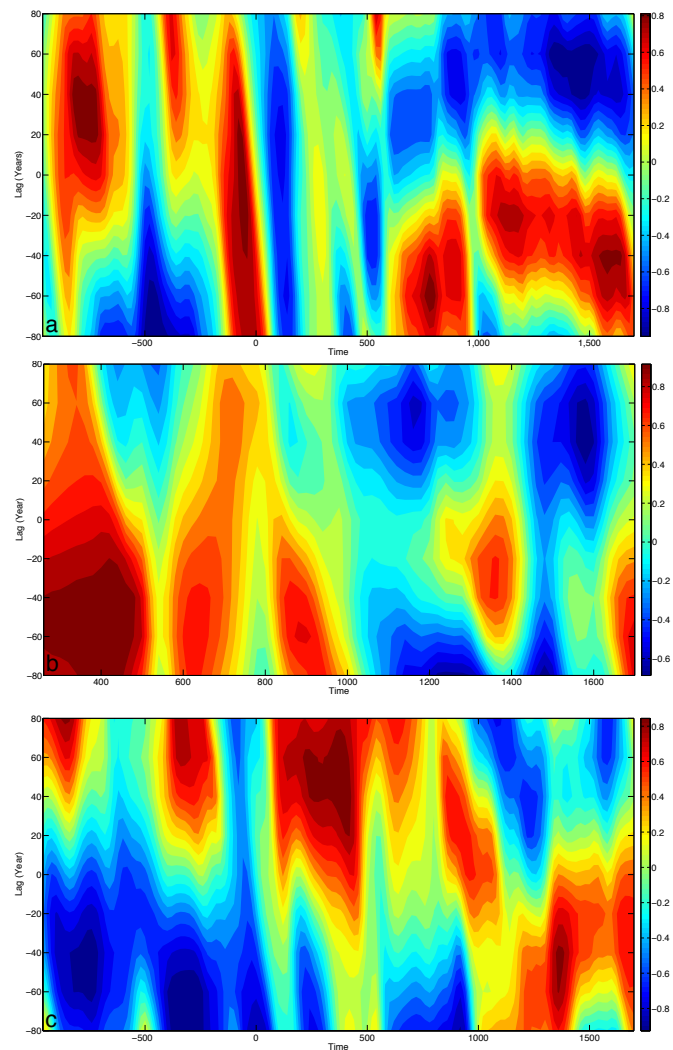


Figure 5.6: Cross correlation analyses with 420 years window moved through the data in steps of 20 years to obtain the temporal changes of the correlation coefficient between (a) Siberian temperature composite and Yamal tree ring chronology (b) Siberian temperature composite and China temperature composites (c) Siberian temperature composite and total solar irradiance (TSI).

References

- Aizen, V. B., Aizen, E. M., Joswiak, D. R., Fujita, K., Takeuchi, N., Nikitin, S. A., 2006. Climatic and atmospheric circulation pattern variability from ice-core isotope/geochemistry records (Altai, Tien Shan and Tibet). *Annals of Glaciology* 43 (1), 49–60.

5.6 Reconstructed 20th century temperature increase

- Bradley, R. S., Briffa, K. R., Cole, J., Hughes, M. K., Osborn, T. J., 2003. The Climate of the Last Millennium. In: Alverson, K., Pedersen, T., Bradley, R. (Eds.), *Global Change — The IGBP Series*. Springer Berlin Heidelberg, pp. 105–141.
- Chebvi, A., Carlier, P., 1996. Carboxylic acids in the troposphere, occurrence, sources, and sinks: A review. *Atmospheric Environment* 30 (24), 4233–4249.
- Cohen, J., Saito, K., Entekhabi, D., 2001. The role of the Siberian High in northern hemisphere climate variability. *Geophysical Research Letters* 28 (2), 299–302.
- D'Arrigo, R., Jacoby, G., Wilson, R., Panagiotopoulos, F., 2005. A reconstructed Siberian High index since A.D. 1599 from Eurasian and North American tree rings. *Geophysical Research Letters* 32 (5), L05705.
- Dentener, F., Crutzen, P., 1994. A three-dimensional model of the global ammonia cycle. *Journal of Atmospheric Chemistry* 19 (4), 331–369.
- Eichler, A., Brüttsch, S., Olivier, S., Papina, T., Schwikowski, M., 2009a. A 750 year ice core record of past biogenic emissions from Siberian boreal forests. *Geophysical Research Letters* 36 (18), L18813.
- Eichler, A., Olivier, S., Henderson, K., Laube, A., Beer, J., Papina, T., Gäggeler, H., Schwikowski, M., 2009b. Temperature response in the Altai region lags solar forcing. *Geophysical Research Letters* 36 (1), L01808.
- Eichler, A., Tinner, W., Brüttsch, S., Olivier, S., Papina, T., Schwikowski, M., 2011. An ice-core based history of Siberian forest fires since AD 1250. *Quaternary Science Reviews* 30 (9–10), 1027–1034.
- Fuentes, J. D., Wang, D., Neumann, H. H., Gillespie, T. J., DenHartog, G., Dann, T. F., 1996. Ambient biogenic hydrocarbons and isoprene emissions from a mixed deciduous forest. *Journal of Atmospheric Chemistry* 25 (1), 67–95.
- Gong, D. Y., Ho, C. H., 2002. The Siberian High and climate change over middle to high latitude Asia. *Theoretical and Applied Climatology* 72, 1–9.
- Guenther, A., Hewitt, C. N., Erickson, D., Fall, R., Geron, C., Graedel, T., Harley, P., Klinger, L., Lerdau, M., Mckay, W. A., Pierce, T., Scholes, B., Steinbrecher, R., Tallamraju, R., Taylor, J., Zimmerman, P., 1995. A global model of natural volatile organic compound emissions. *Journal of Geophysical Research* 100 (D5), 8873–8892.

5 *Late-Holocene temperature reconstruction for Siberia*

- Hansen, J., 2006. Global temperature change. *Proceedings of the National Academy of Sciences* 103 (39), 14288–14293.
- Hansen, J., Sato, M., Glascoe, J., Ruedy, R., 1998. A common-sense climate index: Is climate changing noticeably? *Proceedings of the National Academy of Sciences* 95 (8), 4113–4120.
- Hantemirov, R. M., Shiyatov, S. G., 2002. A continuous multimillennial ring-width chronology in Yamal, northwestern Siberia. *The Holocene* 12 (6), 717–726.
- Hedeager, L., 2007. Scandinavia and the Huns: An interdisciplinary approach to the Migration Era. *Norwegian Archaeological Review* 40 (1), 42–58.
- Herren, P.-A., Eichler, A., Machguth, H., Papina, T., Tobler, L., Zapf, A., Schwikowski, M., 2013. The onset of Neoglaciation 6000 years ago in western Mongolia revealed by an ice core from the Tsambagarav mountain range. *Quaternary Science Reviews* 69 (C), 59–68.
- Huang, X., Chen, F., Fan, Y., 2009. Dry late-glacial and early Holocene climate in arid central Asia indicated by lithological and palynological evidence from Bosten Lake, China. *Quaternary International* 194 (1-2), 19–27.
- IPCC, 2007. *Climate Change 2007 - The Physical Science Basis: Working Group I Contribution to the Fourth Assessment Report of the IPCC*. Cambridge University Press, Cambridge, UK and New York, NY, USA.
- Kang, S., Mayewski, P. A., Qin, D., Yan, Y., Zhang, D., Hou, S., Ren, J., 2002. Twentieth century increase of atmospheric ammonia recorded in Mount Everest ice core. *Journal of Geophysical Research* 107 (D21), 4595.
- Kellerhals, T., Brütsch, S., Sigl, M., Knüsel, S., Gäggeler, H., Schwikowski, M., 2010. Ammonium concentration in ice cores: A new proxy for regional temperature reconstruction? *Journal of Geophysical Research* 115 (D16), D16123.
- Knüsel, S., Brütsch, S., Henderson, K. A., Palmer, A. S., Schwikowski, M., 2005. ENSO signals of the twentieth century in an ice core from Nevado Illimani, Bolivia. *Journal of Geophysical Research* 110 (D1), D01102.
- Langford, A. O., Fehsenfeld, F. C., 1992. Natural vegetation as a source or sink for atmospheric ammonia: A case study. *Science* 255 (5044), 581–583.

5.6 Reconstructed 20th century temperature increase

- Lydolph, P. E., 1977. *Climates of the Soviet Union*. Vol. 7 of *World Survey of Climatology*. World Survey of Climatology, Amsterdam.
- Melles, M., Brigham-Grette, J., Minyuk, P. S., Nowaczyk, N. R., Wennrich, V., DeConto, R. M., Anderson, P. M., Andreev, A. A., Coletti, A., Cook, T. L., Haltia-Hovi, E., Kukkonen, M., Lozhkin, A. V., Rosen, P., Tarasov, P., Vogel, H., Wagner, B., 2012. 2.8 million years of Arctic climate change from Lake El'gygytgyn, NE Russia. *Science* 337 (6092), 315–320.
- Monson, R. K., Jaeger, C. H., Adams, W. W., Driggers, E. M., Silver, G. M., Fall, R., 1992. Relationships among isoprene emission rate, photosynthesis, and isoprene synthase activity as influenced by temperature. *Plant Physiology* 98 (3), 1175–1180.
- Muscheler, R., Joos, F., Beer, J., Mueller, S. A., Vonmoos, M., Snowball, I., 2007. Solar activity during the last 1000 yr inferred from radionuclide records. *Quaternary Science Reviews* 26 (1-2), 82–97.
- Nye, J., 1963. Correction factor for accumulation measured by the thickness of the annual layers in an ice sheet. *Journal of Glaciology* 4 (36), 785–788.
- Olivier, S., Schwikowski, M., Brüttsch, S., Eyrikh, S., Gäggeler, H. W., Luthi, M., Papina, T., Saurer, M., Schotterer, U., Tobler, L., Vogel, E., 2003. Glaciochemical investigation of an ice core from Belukha glacier, Siberian Altai. *Geophysical Research Letters* 30 (19), 2019.
- PAGES2k-Consortium, 2013. Continental-scale temperature variability during the past two millennia. *Nature Geoscience* 6 (5), 339–346.
- Prokopenko, A. A., Hinnov, L. A., Williams, D. F., Kuzmin, M. I., 2006. Orbital forcing of continental climate during the Pleistocene: a complete astronomically tuned climatic record from Lake Baikal, SE Siberia. *Quaternary Science Reviews* 25 (23-24), 3431–3457.
- Rinne, H. J. I., Guenther, A. B., Greenberg, J. P., Harley, P.C., 2002. Isoprene and monoterpene fluxes measured above Amazonian rainforest and their dependence on light and temperature. *Atmospheric Environment* 36 (14), 2421–2426.
- Sahsamanoglou, S. H., Makrogiannis, T. J., Kallimopoulos, P. P., 1991. Some aspects of the basic characteristics of the Siberian anticyclone. *International Journal of Climatology* 11 (8), 827–839.

5 *Late-Holocene temperature reconstruction for Siberia*

- Saurer, M., Schweingruber, F., Vaganov, E. A., Shiyatov, S. G., Siegwolf, R., 2002. Spatial and temporal oxygen isotope trends at the northern tree-line in Eurasia. *Geophysical Research Letters* 29 (9), 7-1-7-4.
- Schotterer, U., Fröhlich, K., Gäggeler, H. W., Sandjorj, S., Stichler, W., 1997. Isotope records from Mongolian and Alpine ice cores as climate indicators. *Climatic Change* 36 (3), 519-530.
- Sidorova, O. V., Saurer, M., Myglan, V. S., Eichler, A., Schwikowski, M., Kirilyanov, A. V., Bryukhanova, M. V., Gerasimova, O. V., Kalugin, I. A., Daryin, A. V., Siegwolf, R. T. W., 2011. A multi-proxy approach for revealing recent climatic changes in the Russian Altai. *Climate Dynamics* 38 (1-2), 175-188.
- Smith, D. M., Cusack, S., Colman, A. W., Folland, C. K., Harris, G. R., Murphy, J. M., 2007. Improved surface temperature prediction for the coming decade from a global climate model. *Science* 317 (5839), 796-799.
- Song, C. H., Ma, Y., Orsini, D., Kim, Y. P., Weber, R. J., 2005. An investigation into the ionic chemical composition and mixing state of biomass burning particles recorded during TRACE-P P3B Flight#10. *Journal of Atmospheric Chemistry* 51 (1), 43-64.
- Steinhilber, F., Beer, J., Fröhlich, C., 2009. Total solar irradiance during the Holocene. *Geophysical Research Letters* 36 (19), L19704.
- Swain, S., Edwards, M. J., 2004. Approaching late antiquity: the transformation from early to late Empire.
- Wang, W., Feng, Z., 2013. Holocene moisture evolution across the Mongolian Plateau and its surrounding areas: A synthesis of climatic records. *Earth-Science Reviews* 122, 38-57.
- Wooster, M. J., Zhang, Y. H., 2004. Boreal forest fires burn less intensely in Russia than in North America. *Geophysical Research Letters* 31 (20), L20505.
- Wu, B., Wang, J., 2002. Winter Arctic oscillation, Siberian High and East Asian winter monsoon. *Geophysical Research Letters* 29 (19), 3-1-3-4.
- Yang, B., 2002. General characteristics of temperature variation in China during the last two millennia. *Geophysical Research Letters* 29 (9), 1324.

6 Comparison of two ice cores from the Central Asian Altai mountain range

Pierre-Alain Herren^{a,b}, Anja Eichler^{a,b}, Tatyana Papina^c, and Margit Schwikowski^{a,b,d}

^aPaul Scherrer Institut, 5232 Villigen PSI, Switzerland

^bOeschger Centre for Climate Change Research, University of Bern, 3012 Bern, Switzerland

^cInstitute for Water and Environmental Problems, 656038 Barnaul, Russia

^dDepartment of Chemistry and Biochemistry, University of Bern, 3012 Bern, Switzerland

Manuscript to be submitted to Journal of Geophysical Research

Abstract

Investigating the spatial extent of ice core based climate reconstruction is challenging due to limited number of suitable sites within reasonable distance. Here we compare geochemical records and melt rate reconstructions of two ice cores 350 km apart, one from Belukha (4062 m asl, 49°48.433'N, 86°34.716'E) in the Siberian Altai and the other from Tsambagarav (4130 m asl, 48°39.338'N, 90°50.826'E) in the Mongolian Altai. Investigated are similarities and differences, to understand their importance in a geographical context exceeding the drill site. The melt rate records have similar long-term trends and point towards enhanced melting in recent decades, suggesting a modified glacier mass balance. Variations of the Tsambagarav melt record fits changes in radiation and can be related to atmospheric dimming and brightening observations. Principle component analysis of the geochemical records was performed to assign the sources of the different species. Both sites have different loadings in the mineral dust component, indicating local dust input. Reconstruction of biogenic emissions and biomass burning are very similar in both sites. The large area of the Siberian forests induces large emissions, which are archived in both sides of the Altai mountain range. Species associated to forest fires are recorded in both ice cores, suggesting a regional importance.

6.1 Introduction

In recent decades the geographical region of Siberia experienced enhanced warming (Hansen et al., 1998; Bradley et al., 2003; Hansen, 2006). During the first half decade of the 21st century temperature in the central part increased by 1.6 to 2.1°C (Hansen, 2006). Together with Alaska and Northern Greenland it belongs to the fastest warming regions of the globe. However, climate information for this region remains limited and spatially sparse. This region of central Asia is characterized by pronounced continental climate, due to the remoteness of the oceans (Lydolph, 1977). Seasonal differences are up to 40°C, with very cold and dry winters and relative warm summers (Klinge et al., 2003). The Siberian High controls winter climate preventing precipitation (Sahsamanoglou et al., 1991). In summer, humid air masses from the Atlantic Ocean as well as recycled moisture are the main sources of precipitation (Aizen et al., 2006). Regarding late-Holocene paleoclimate reconstructions, Asia and Central Asia are strongly biased towards tree-ring archives (PAGES2k-Consortium, 2013).

In this study we introduce historical trends in summer melt and geochemical records of an ice core drilled in the Altai Mountain Range, more specific in the Mongolian part

of the Altai close to the border to Siberia (Fig. 6.1). The results are compared with previous studies from a Belukha ice core in the Siberian Altai (Fig. 6.1) to investigate the geographic representativity of the records. Summer surface melt in glaciated regions causes the percolation of meltwater into the ice matrix where it refreezes in distinct layers. The distribution and extent of these melt features can be related to summer warmth (e.g., Koerner and Fisher, 1977; Fisher et al., 2012). Energy sources for melt are longwave incoming radiation, absorbed global radiation and sensible heat flux (Ohmura, 2001). Thus modification in the radiation balance can affect the surface melting of a glacier. Previous studies in the Altai showed a high industrial to preindustrial sulfate ratio with a maximum of the anthropogenic contribution of more than 80% (Olivier et al., 2006). Ice-core based reconstruction from other alpine regions suggest similar concentrations (Schwikowski et al., 1999; Kaspari et al., 2009). These anthropogenic emissions can modify the radiative balance on a regional scale (e.g., Charlson et al., 1992).

Here we present the results of a new ice core from the Mongolian Altai and investigate their geographical coverage.



Figure 6.1: Location of the Tsambagarav mountain range in Mongolia (red star), Belukha glacier in the Siberian Altai (blue star), and the GEBA stations (black stars; <http://www.geomapapp.org>).

6.2 Methods

The Belukha ice core was drilled during summer 2001 on the saddle between the West and East summit of Belukha, in the Russian Altai on the north side of the mountain range (4062 m asl, 49°48.433'N, 86°34.716'E, Fig. 6.1) (Olivier et al., 2003). The ice core is 139 m long, covers the period AD 1250 to 2001, with a mean annual accumulation rate of 0.56 m weq (Eichler et al., 2009a). The second ice core was drilled in July 2009 on the summit Khukh Nuru Uul glacier (4130 m asl, 48°39.338'N, 90°50.826'E, Fig. 6.1) (Herren et al., 2013). The glacier is located within the Tsambagarav Mountain massif in the Mongolian Altai on the south side of the mountain range. The surface-to-bedrock ice core is 72 m long and due to a low accumulation rate (0.32 m weq) contains Mid-Holocene ice (6'000 years BP, Herren et al. 2013). In the following we use the term Tsambagarav ice core when referring to the ice core from Khukh Nuru Uul glacier. Both ice cores were transported frozen to the Paul Scherrer Institut (PSI), where they were processed in the cold room at -20°C. A specially designed stainless steel band saw with Teflon coverage on the tabletop was used for sample preparation.

6.2.1 Dating

The dating of the two ice cores was performed applying a combination of different methods. For Belukha the timescale was derived using the ^{210}Pb activity record, a three-parameter annual layer-counting methodology, and a nonlinear regression (Haefeli, 1961) through reference horizons such as the maximum of nuclear weapons testing in 1963 (maximum in ^3H activity) and different volcanic layers (Olivier et al., 2006; Henderson et al., 2006; Eichler et al., 2009a). For the period AD 1815 to 2001 dating uncertainty was estimated to be smaller than three, increasing to five years between AD 1400 and 1815, and less than 10 years for the period AD 1250-1400 (Eichler et al., 2009a). The upper part of the Tsambagarav ice core (AD 1815 to 2009) was dated with identical methods (Herren et al., 2013). Within one decade of an identified horizon an error of ± 1 year was estimated increasing to $\pm 2-3$ years outside of these ranges. Strong annual-layer thinning in the lower part of the ice core prevents attributing an age scale with conventional dating methods, therefore radiocarbon dating of particulate organic carbon was conducted (Sigl et al., 2009; Jenk et al., 2009). For a continuous age-depth scale the ^{14}C results were fitted using an empirical exponential equation (Herren et al., 2013). With increasing depth the dating uncertainty becomes more important ± 17 years between 1815 and 1700, ± 55 years for AD 1700 to AD 1500 and ± 140 years for AD 1500 to 1250.

6.2.2 Chemical analysis

For both ice cores inner sections were used to analyze concentrations of the main water-soluble ionic species (Na^+ , NH_4^+ , K^+ , Ca^{2+} , Mg^{2+} , and Cl^- , NO_3^- , SO_4^{2-} , HCOO^-) using standard ion chromatographic techniques. The median and mean values of the different species are given in Table 6.1. For Tsambagarav the resolution ranged from 2.5 cm at the top to 2 cm from 50 m depth downwards, in total 2944 samples, whereas the Belukha ice core was processed with a resolution of 2-7 cm, resulting in a total of 3615 samples. Being very sensitive to contamination ^{14}C analyses were as well conducted with the inner part of the ice core segments and additionally rinsed with ultra-pure water prior melting. To extract the particulate carbon, samples were filtered and acidified to remove carbonates. Combustion of the filter generated CO_2 , which was cryogenically trapped and sealed in glass tubes for accelerator mass spectrometry (AMS) measurements (Szidat et al., 2004; Ruff et al., 2007; Synal et al., 2007; Jenk et al., 2009). For species less sensitive to contamination ($\delta^{18}\text{O}$, ^{210}Pb and ^3H) outer sections were used (Eichler et al., 2009a; Gäggeler et al., 1983; Olivier et al., 2003). To correct for increasing density with depth and alternating ice lenses, all the values have been converted to meter water equivalents (m weq).

Table 6.1: Mean (upper line) and Median (lower line) concentrations of major ions [ppb] in the Belukha and Tsambagarav ice cores from Altai.

	HCOO^-	Cl^-	NO_3^-	SO_4^{2-}	Na^+	NH_4^+	K^+	Mg^{2+}	Ca^{2+}	$\delta^{18}\text{O}$
Belukha	215	40	208	233	41	132	21	19	185	-14
	199	32	192	176	31	121	18	16	148	-14
Tsambagarav	303	50	273	283	36	191	16	25	212	-15
	301	38	254	210	25	177	15	21	162	-15

6.2.3 Ice core melt percent

The method introduced by Henderson et al. (2006) to calculate melt percent in the Belukha ice core was adapted to the requirements of the Tsambagarav ice core. Melt features were identified when the ice core segment is backlit in a darkened cold room for better contrast. Refrozen meltwater layers appear bright and bubble-free in such configuration. The layer extent and class was determined by visual evaluation. Here we assigned three classes I, II and III. Category I is the densest ice with very few air bubbles, it appears uniformly bright. To those layers 100% weight was attributed. Category II ice lenses have more air bubbles and are classified as icy layers. The layers are less bright

6 Comparison of two Altai ice cores

but are still clearly distinguishable to the surrounding glacier ice with high air bubble content. A weight of 80% was attributed. Category III is generally referred as icy firn, differences to glacier ice are small. They appear slightly brighter on the light table; a weight of 50% was attributed. The final melt percent profile is mainly controlled through the thickness of the layers. The attribution and weighting of the layers has thus only limited influence. Pipes and ice layers not continuous over the whole cross-section of the segment were intentionally omitted. Wedge-shaped or irregular layer thickness was measured on both sides of the core to calculate the mean thickness. Such techniques have been demonstrated to yield reproducible melt percent profiles independent of observer or classification scheme (Kotlyakov et al., 2004). With increasing depth identification of the ice lenses is precluded through convergence of the glacier ice and ice lens properties. The annual melt percent (AMP) was calculating according to

$$AMP = \frac{\sum(dz_i \cdot c)}{\lambda_i} \quad (6.1)$$

where dz_i is the thickness of individual ice lenses in one year, c is the attributed ice lens category and λ_i the reconstructed annual accumulation rate described by:

$$\lambda_i = \frac{\lambda_{ALC}}{\lambda_{Model}} \cdot 335 \text{ mm} \quad (6.2)$$

where λ_{ALC} is the annual layer thickness derived by a three-parameter annual layer counting, λ_{Model} is the modeled thickness according to Thompson et al. (1990). Neglecting lateral flow within the upper 3.35 m weq, corresponding to a period of 10 years in the Tsambagarav ice core, yields an annual surface accumulation rate of 335 mm (Herren et al., 2013). In order to avoid inconsistency in the depth profile, within one segment the average density was attributed to all ice lenses. The upper end of the ice lens was used to attribute the timescale. Thick lenses exceeding the annual accumulation rate can thus result in AMP larger than 100%.

Although the stratigraphy was recorded for the whole core only the last 200 years were used to derive a melt percent record. Strong thinning of the annual layers with increasing depth prevented annual layer counting (Herren et al., 2013). Thus reconstruction of annual accumulation rates was only possible for the period AD 1815 to 2009.

6.3 Results and Discussion

6.3.1 200-year melt percent record of the Mongolian Altai

Borehole temperature at the Tsambagarav drilling-site showed cold ice ranging from -13.8 to -12.6°C (Herren et al., 2013). Meltwater produced by high summer air temperatures and solar radiation mainly refreezes within the annual accumulation layer. However, for the past two centuries we reconstruct six events with AMP exceeding 100% (AD 1894, 1929, 1942, 1993, 1996, 2000, Fig. 6.2). The temporal interpretation of those strong melt events is challenging. Retrospectively different scenarios are plausible such as one strongly pronounced warm year or various consecutive events. Since the distinction is impossible, we choose to average with the preceding year because of the melt water flowing from more recent years to older layers. Fig. 6.2 illustrates the trend of AMP for the last 200 years. The distribution of melt features alters the density profile. The values at the depth of identified ice lenses exceed theoretical predictions from simple firn compaction (Reeh et al., 2005). The Tsambagarav ice core is almost free of melt features for the majority of the 19th century. Subsequent three distinct phases of enhanced melting (1884-1910, 1927-1952 and 1985-ongoing) were interrupted by periods of reduced melting. The latest increased in frequency of AMP peaks at the year AD 2000 and decreases in the following years.

6.3.2 Unprecedented melting in high altitude Altai

The Belukha AMP record was used to derive summer temperatures according to the empirical relation given by Tarussov (1992) and was discussed in details relative to the $\delta^{18}\text{O}$ values (Henderson et al., 2006). Later the melt percent-temperature relation was re-evaluated (Okamoto et al., 2011), showing that the study by Henderson et al. (2006) underestimated the temperature reconstruction. Additionally the variability of the AMP was adjusted downward. We do not relate the Tsambagarav AMP to temperature for two reasons. On the one hand values exceeding 100% circumvent a realistic temperature reconstruction. On the other hand, periods with no melting cannot be used to attribute a temperature. Here we compare the two AMP records 350 km apart in similarity and differences to identify local and regional patterns.

For the past two centuries the AMP derived from the Belukha ice core increases steadily (Fig. 6.2). The two records differ in amplitude and extent for individual periods, yet increasing until the last decade. Comparing specific time intervals the two melt records

6 Comparison of two Altai ice cores

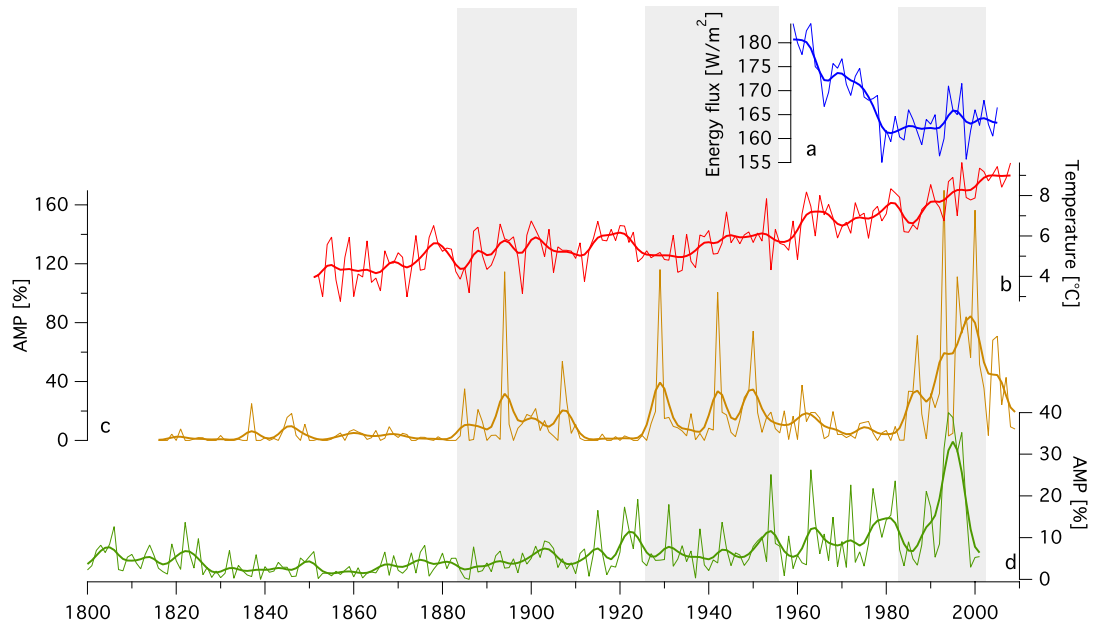


Figure 6.2: (a) Mean energy flux of three GEBA station (Table 6.2). (b) March-November averages of air temperature at Barnaul. (c) Annual melt percent (AMP) of the Tsambagarav and Belukha (d) ice core. Annual values (thin line) smoothed with a 5-point binomial filter (bold curves).

have opposite trends until common severe increase at the middle of the 1980's. Southern and northern Altai experienced unprecedented melting in the late 1990's pointing towards major regional climate changes. The maximal melt at Belukha is a narrow peak from 1993 to 1997 followed by a rapid decrease to little melt in the remaining 3 years of the ice core. The peak of maximal melting in the Tsambagarav record is broader (1993 to 2000). The duration of high AMP values in the Belukha ice core is difficult to establish, since it ends in 2001. The offset between the two maxima can rather be attributed to resolution and dating issues than different climatic conditions. Hence, during the last two centuries the two records suggest increased glacier-hostile climate conditions for the whole Altai and indicate severe changes in the mass balance of the glaciers. Although, these changes cannot directly be linked to changes in glacier extent, former studies showed that melt records from the accumulation area bears strong relationship to melting over the whole glacier (Koerner, 1990). The higher frequency of intense melt events towards present are in agreement with the identified shrinkage of Altai glaciers by former studies (Pattyn et al., 2003; Shahgedanova et al., 2010) and contradicts former work stipulating Tsambagarav massif experiencing no significant change in area since 1963 (Tsutomu and Davaa,

2007).

The long-term trend of the AMP corresponds to observation data that show pronounced warming for the period 1940 to 2008 (Bezuglova et al., 2012). Past decades present acceleration in rising temperature. Multi-proxy data set for the Russian Altai, consisting of tree-ring width, ice core and lake sediment records confirm an enhanced warming of Siberia (Sidorova et al., 2011).

6.3.3 Incident solar radiation archived in the melt record

Periods of low and high AMP in the Tsambagarav reconstruction appear to coincide with the general solar radiation pattern incident at the Earth's surface during the 20th century (Wild et al., 2005; Wild, 2009). Various studies suggest a widespread decrease in surface solar radiation between the 1950s and 1980s generally referred as 'global dimming' followed by a recovery designated as 'brightening'. Few records from the first half of the 20th century suggest an 'early brightening' additionally supported by diurnal temperature range and sunshine duration (Ohmura, 2007; Wild, 2009). The periods of enhanced annual melt (1927-1966 and 1985-ongoing) coincide well with the 'early brightening' and 'brightening' period, whereas the period of reduced melt intensity matches the 'dimming' interval. For the ongoing period the melt record peaks at around 2000 and decreases subsequently. This pattern reinforces the hypothesis of 'renewed dimming' in Eastern Asia due to tremendous emission increases in China after 2000 combined with the dimming in India (Streets et al., 2009; Wild, 2009).

We compared our record with data from the Global Energy Balance Archive (GEBA¹, Fig. 6.1). Three stations were selected Altay, Urumqi and Ulaangom (Table 6.2). The longest record barely spans a period of high and low radiation making comparison difficult. Other parameters such as sunshine duration or diurnal temperature range are not available to extent the records significantly. However, for the brief overlap the records confirm the coincidence of reduced (enhanced) radiation with low (elevated) melt rates. The three observation records differ in the moment of minimum values and their inter-annual variability. Considering different seasons did not improve the accordance between the stations nor with the melt record, we thus argue that small temporal differences between the melt record and the observation can be explained through local variability combined with lags due to dating uncertainties in the ice core timescale. Melt layers formed during the past two decades may be caused through a combination of radiation and increased temperatures. This is corroborated through the March-November Barnaul

¹http://www.iac.ethz.ch/groups/schaer/research/rad_and_hydro_cycle_global/geba

6 Comparison of two Altai ice cores

temperature, which does not reproduce the phases of low and high melting (Fig. 6.2). Changes in albedo as major driver of the melt is assumed to be minimal since the melt occurs during summer, the main accumulation period in the Altai (Dyurgerov and Meier, 1999). Thereby the glacier is constantly covered with fresh snow keeping the albedo high. These results provide further evidence (Wild et al., 2005) of the radiative changes during the past decades in the Altai region and introduce a potential new proxy to investigate the anthropogenic influence on the earth's energy balance beyond the instrumental period.

Table 6.2: Details of Global Energy Balance Archive (GEBA) stations used in Fig. 6.2

Station Name	Country	Latitude	Longitude	Altitude [m asl]	Time interval
Altay	China	47°43.8'N	88°04.0'E	735	1960 - 2000
Urumqi	China	43°46.8'N	87°37.2'E	918	1959 - 2007
Ulaangom	Mongolia	49°51.0'N	92°4.2'E	934	1964 - 2005

6.3.4 Geochemical record comparison

Comparing reconstructions of two Altai ice cores allows investigation of the spatial extent of the derived proxies. Here we use the geochemical records to distinguish local from regional components. First we performed a Principle Component Analysis (PCA) with the 10-year means of the 9 major ions and the $\delta^{18}\text{O}$ of the Tsambagarav ice core for the period AD 1200 to AD 1940. After AD 1940 anthropogenic emissions of SO_2 , NO_x and NH_3 changed the atmospheric mixing ratios in Siberia, impeding the attribution of the natural origin. The main pre-industrial sources of the chemical species are identified and related to previous findings from the Belukha ice core (Table 6.3 & 6.4). Second, concentrations of selected ions are compared to examine actual atmospheric concentrations north and south of the Altai.

Principal component analysis

Previous studies discuss in detail the PCA of the Belukha ice core data (Eichler et al., 2009b, 2011), variability and loadings are given in Table 6.3. Dust related species have the highest loadings in the PC1 and account for 50% variability. The PC2 shows high loadings in biogenic species and temperature explaining 23% of the data variance.

Biomass burning is associated with the PC3.

Table 6.3: Loadings of the Belukha PCA performed on the normalized 10-year means of the 9 major ions and $\delta^{18}\text{O}$ and the variance explained by each component for the time period AD 1250-1940 and attributed sources.

	PC1	PC2	PC3
Mg ²⁺	0.93	-0.15	-0.09
Ca ²⁺	0.90	0.11	-0.21
Cl ⁻	0.88	-0.22	-0.07
Na ⁺	0.86	-0.16	-0.35
SO ₄ ²⁻	0.83	0.13	-0.26
HCOO ⁻	0.41	0.84	-0.06
NH ₄ ⁺	0.28	0.82	0.29
$\delta^{18}\text{O}$	-0.01	0.82	0.13
K ⁺	0.56	-0.33	0.67
NO ₃ ⁻	0.73	-0.17	0.57
<i>Variance explained</i>	<i>50%</i>	<i>23%</i>	<i>11%</i>
	Mineral dust	Biogenic emissions	Biomass burning

Table 6.4: Loadings of the Tsambagarav PCA performed on the normalized 10-year means of the 9 major ions and $\delta^{18}\text{O}$ and the variance explained by each component for the time period AD 1250-1940 and attributed sources.

	PC1	PC2	PC3
Ca ²⁺	0.90	-0.15	-0.31
Na ⁺	0.89	-0.23	-0.25
Cl ⁻	0.88	-0.37	-0.10
SO ₄ ²⁻	0.86	0.06	0.10
Mg ²⁺	0.85	-0.16	-0.34
NH ₄ ⁺	0.60	0.76	0.01
HCOO ⁻	0.63	0.68	-0.20
NO ₃ ⁻	0.63	-0.05	0.64
K ⁺	0.62	-0.26	0.58
$\delta^{18}\text{O}$	0.30	0.20	0.51
<i>Variance explained</i>	<i>55%</i>	<i>14%</i>	<i>13%</i>
	Mineral dust	Biogenic emissions	Biomass burning

Applying PCA on the Tsambagarav data yields a similar picture (Table 6.4). In general the PCAs of Tsambagarav and Belukha result in very similar partitioning of the components, except for $\delta^{18}\text{O}$. The three leading modes of the Tsambagarav ice-core array cumulatively explain 82% data variance. Mineral dust related species (Ca²⁺, Na⁺, Cl⁻, SO₄²⁻, Mg²⁺) have significant loadings in the PC1 explaining 55% of the variance. In this

6 Comparison of two Altai ice cores

mode all components except $\delta^{18}\text{O}$ have loadings higher than 0.60. The PC2 shows high loadings in the concentration of the biogenic species in the ice core (NH_4^+ , HCOO^-) and explain 14% data variance. The third mode (PC3) explains 13% data variance, similar to the second mode. According to previous studies we relate PC3 to biomass burning due to the strong contribution of NO_3^- and K^+ . The role of $\delta^{18}\text{O}$ in this mode remains unclear.

The temporal evolution of the three leading PC modes of the two ice cores is illustrated in Fig. 6.3. The differences between the Russian and Mongolian Altai can be used to separate local and regional components. Differences in the PCs are discussed in the following.

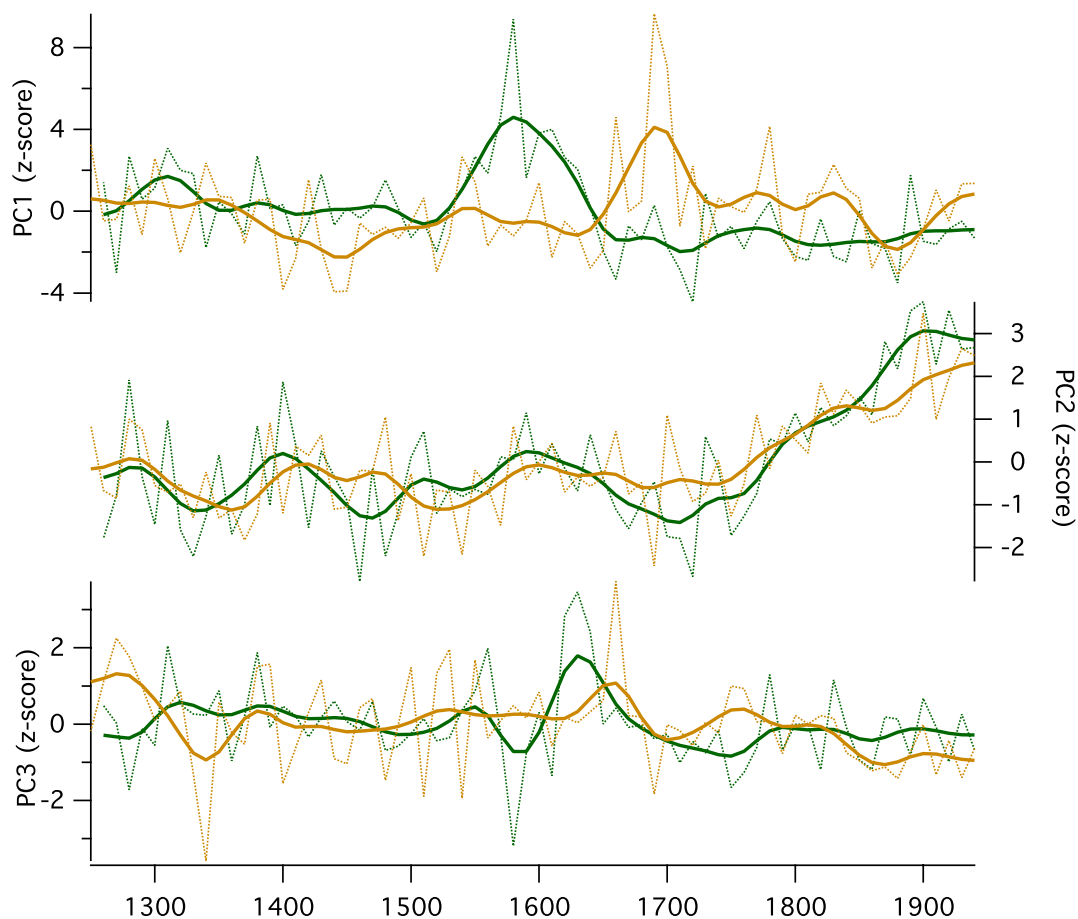


Figure 6.3: Tsambagarav (brown) and Belukha (green) PC1 (*top*), PC2 (*middle*) and PC3 (*bottom*). 10-year resolution values (thin line) smoothed with a 5-point binomial filter (bold curves).

For both sites the transport of dust to the glacier plays an important role, since the PC1 explains a major part of the data variance. The Tsambagarav massif surrounded by steppe-like vegetation is more subject to local dust transport than Belukha. All ions have loadings exceeding 0.6 and the explained data variance is 5% higher for the Mongolian site. The different contribution in the loadings between the two sites, suggests that mineral dust related species transported to the glacier have a strong local component. Temporal evolution of the two PC1s confirms this spatial difference between the two sites (Fig. 6.3). For the Belukha ice core the dominant source areas of mineral dust are likely the deserts of Central Asia like the Taklimakan desert, the Kazakh loess hills, and the Aral Sea Basin (Olivier et al., 2006). Dust storms in the Taklimakan desert transport particles to elevation of 5000 m from where they reach the Altai with the Westerlies (Sun et al., 2001). Backtrajectory analysis from Southern and Northern Altai show similar origins. Therefore long-range transport may be identical for both sites. However, the records do not follow the same trend and maximum values do not occur simultaneously, which points to a strong local mineral dust contribution. In contrast the records of PC2 have a similar trend, indicating spatially more uniform and extended source of biogenic emissions. The important contribution of $\delta^{18}\text{O}$ in the Belukha PC2, a good proxy of atmospheric temperature (Eichler et al., 2009a), suggests a strong connection between biogenic emissions and temperature in Siberia. The low loading of $\delta^{18}\text{O}$ in the PC2 of the Tsambagarav ice core points towards stable isotope composition not only controlled by temperature, but rather as source indicator for atmospheric moisture. This corroborates previous stable isotope studies (Schotterer et al., 1997), and confirms general expectation of the arid Mongolian Altai being more subject to internal moisture sources during summer months than the more humid Russian Altai (Aizen et al., 2006). While the $\delta^{18}\text{O}$ cannot be used for the same purposes north and south of the mountain range, both PC2s bear similar trends and patterns for the past 700 years (Fig. 6.3). Biogenic emissions stored in the glaciers by means of NH_4^+ and HCOO^- can be attributed to a regional signal. The interdependency between Siberian temperature and biogenic emissions recorded in the ice cores allow to present a new temperature proxy (Herren et al. in prep, see Chapter 5). Regarding PC3 both sites show high loadings of K^+ and NO_3^- . Through combination with pollen and charcoal data a new geochemically-based proxy for biomass burning was derived (Eichler et al., 2011). The trend of both PC3 records is similar, especially for the maximum value in the mid 17th century. While the PC1 related to the mineral dust reflects more local conditions, the remaining PC2 and PC3 seem to capture a more regional signal. Thus through comparison of the modes we are able to corroborate previous work (Eichler et al., 2011). Reconstructed

6 Comparison of two Altai ice cores

Siberian forest fire history for the last 750 years derived from the Belukha ice core is likewise stored in the Tsambagarav ice core. The period of exceptionally high forest-fire activity between AD 1600 and 1680 is also observed in the Tsambagarav mode. However, the identified extremely dry period preceding high intensity forest fires cannot be seen in the PC1 from the Mongolian Altai. The importance of the Taiga belt as major source of NH_4^+ and HCOO^- becomes evident by comparing the modes of biogenic ionic species found in both ice cores (Eichler et al., 2009b). Although 350 km apart, both PC2 display similar pattern, differences in the lower parts of the ice cores can be attributed to dating uncertainties of both ice cores.

Anthropogenically influenced ionic species

During recent decades anthropogenic emissions changed the atmospheric concentrations. This signal would dominate the PCA, thus it was conducted only for the preindustrial time. To test the spatial distribution, geochemical records are directly analyzed. For illustration we selected two ions (SO_4^{2-} and NO_3^-) influenced by anthropogenic emissions and formed in the atmosphere from the precursor gases SO_2 and NO_x . Here we present the Tsambagarav records on annual resolution for the period AD 1815 to 2009 and compare them with the Belukha values (Fig. 6.4).

In order to separate the anthropogenic sulfate contribution from mineral dust related sulfate we use the non-dust SO_4^{2-} record (Herren et al., 2013). The records of the two sites are correlated (NO_3^- : $r = 0.44$ $p < 0.001$, non-dust SO_4^{2-} : $r = 0.58$ $p > 0.001$). Long-term changes are almost identical for both sides of the Altai. A first increase in concentration is identifiable at beginning of the 20th century. Enhanced anthropogenic emissions of SO_2 and NO_x (precursors of SO_4^{2-} and NO_3^-) for the period 1940-2008 are reflected in concentration maxima of SO_4^{2-} and nitrate around 1975 and 1980, and severely affect the natural composition of diluted ionic species in the ice cores. Fossil fuel combustion is the main source for SO_2 , whereas for NO_x increased traffic and agricultural usage of fertilizer have been proposed (Eichler et al., 2009b). As suggested in previous studies the temporal evolution of the concentration of anthropogenically influenced species fits best with Eastern European emission estimates (Eichler et al. (2009b, 2012), Fig. 6.4). The Tsambagarav site being located downwind of the Westerlies reaching Belukha, results in slightly lower concentrations in contrast to other species and the pre-industrial period. This confirms larger distance to sources for the Tsambagarav site.

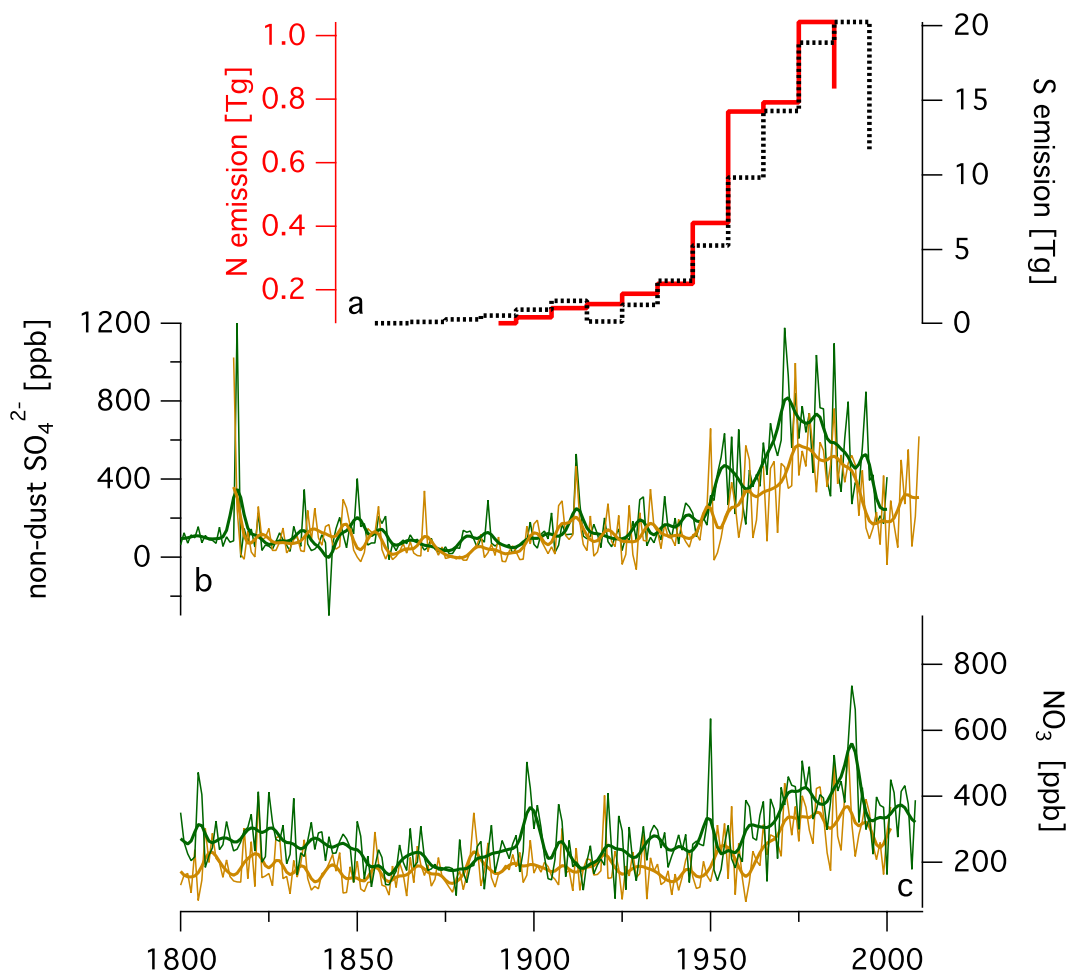


Figure 6.4: (a) Historical Eastern European emission estimates of NO_x (Tg N van Aardenne et al. (2001)), and SO_2 (TgS Stern (2005, 2006)). Tsambagarav (brown) and Belukha (green) non-dust SO_4^{2-} (b) and NO_3^- (c) concentrations. Annual values (thin line) smoothed with a 5-point binomial filter (bold curves).

The trends of anthropogenic pollutants correspond to the AMP record, especially for the non-dust SO_4^{2-} . The importance of SO_4^{2-} on the earth radiative balance has been studied regarding major volcanic eruptions (Robock and Jianping, 1995) and anthropogenic emissions (IPCC, 2007). The increase in SO_4^{2-} concentration corresponds to the transition from 'early brightening' to the 'dimming'. The 'brightening' occurs simultaneously with the decrease of non-dust SO_4^{2-} . Elevated concentrations for the beginning of the 21st century confirms suggested 'renewed dimming'. The agreement of two independent

reconstructions supports the hypothesis of radiation driven melting.

6.4 Conclusions

Paleoclimate reconstructions derived from two ice cores located in the Altai mountain range provide the unique opportunity to test their spatial representativeness. Geochemical records from the two sites were compared. Regarding melt rates, long-term trends are similar for the north and south side of the Altai. Increased melting in recent decades affected the glacier's mass balance independent of their geographical location in the mountain range. Differences on smaller timescale can partly be attributed to dating uncertainties, confined accumulation period to summer month in the Mongolian Altai and local geometric influences. The Tsambagarav massif consists of ice caps, thus the glaciers are constantly exposed to the incident radiation. The West and East Belukha summit (both top the drill site by 400 m) can shield the incident radiation and influence surface melt at the saddle. The Mongolian melt record reflects radiation changes attributed to 'dimming' and 'brightening' of the atmosphere. SO_4^{2-} and NO_3^- concentrations in the ice core follow anthropogenic Eastern European emission estimates of SO_2 and NO_x . This further points to radiation controlled surface melting in the Altai.

Biogenic emissions and forest fires reconstruction in both ice cores have identical trends, suggesting large-scale phenomena. The agreement of most proxies, particularly on decadal resolution, between two 350 km distant sites demonstrates the strength of ice-core based climate proxies. This motivates to investigate new sites to add the regional climate reconstruction.

Acknowledgements

This project was supported by the Swiss National Science Foundation (200021_119743) and the Russian Academy of Sciences (Integration project No. 92 of SB RAS and project 16.12 of Presidium RAS). We would like to thank Beat Rufibach, Michael Sigl, Manuel Schläppi, Horst Machguth and Heinz Gäggeler for their help in drilling the ice core, Sergey Mironov, the Federal Security Service of the Russian Federation, Dr Beket from the Social Economy Research Center in Bayan-Ulgii, Mongolia, Veronica Morozova from the IWEP for their help during the expedition and M. Wild for providing the radiation data and valued suggestions.

References

- Aizen, V. B., Aizen, E. M., Joswiak, D. R., Fujita, K., Takeuchi, N., Nikitin, S. A., 2006. Climatic and atmospheric circulation pattern variability from ice-core isotope/geochemistry records (Altai, Tien Shan and Tibet). *Annals of Glaciology* 43 (1), 49–60.
- Bezuglova, N. N., Zinchenko, G. S., Malygina, N. S., Papina, T. S., Barlyaeva, T. V., 2012. Response of high-mountain Altai thermal regime to climate global warming of recent decades. *Theoretical and Applied Climatology* 110 (4), 595–605.
- Bradley, R. S., Briffa, K. R., Cole, J., Hughes, M. K., Osborn, T. J., 2003. The Climate of the Last Millennium. In: Alverson, K., Pedersen, T., Bradley, R. (Eds.), *Global Change — The IGBP Series*. Springer Berlin Heidelberg, pp. 105–141.
- Charlson, R. J., Schwartz, S. e., Hales, J. M., Cess, R. D., Coakley, J. A., Hansen, J. E., Hofmann, D. J., 1992. Climate forcing by anthropogenic aerosols. *Science* 255 (5043), 423–430.
- Dyrgerov, M. B., Meier, M. F., 1999. Analysis of winter and summer glacier mass balances. *Geografiska Annaler Series A-Physical Geography* 81A (4), 541–554.
- Eichler, A., Olivier, S., Henderson, K., Laube, A., Beer, J., Papina, T., Gäggeler, H., Schwikowski, M., 2009a. Temperature response in the Altai region lags solar forcing. *Geophysical Research Letters* 36 (1), L01808.
- Eichler, A., Olivier, S., Papina, T., Brütsch, S., Schwikowski, M., 2009b. A 750 year ice core record of past biogenic emissions from Siberian boreal forests. *Geophysical Research Letters* 36 (18), L18813.
- Eichler, A., Tinner, W., Brütsch, S., Olivier, S., Papina, T., Schwikowski, M., 2011. An ice-core based history of Siberian forest fires since AD 1250. *Quaternary Science Reviews* 30 (9–10), 1027–1034.
- Eichler, A., Tobler, L., Eyrikh, S., Gramlich, G., Malygina, N., Papina, T., Schwikowski, M., 2012. Three centuries of Eastern European and Altai lead emissions recorded in a Belukha ice core. *Environmental Science & Technology* 46 (8), 4323–4330.
- Fisher, D., Zheng, J., Burgess, D., Zdanowicz, C., Kinnard, C., Sharp, M., Bourgeois, J., 2012. Recent melt rates of Canadian arctic ice caps are the highest in four millennia. *Global and Planetary Change* 84-85 (C), 3–7.

6 Comparison of two Altai ice cores

- Gäggeler, H., von Gunten, H., Rössler, E., Oeschger, H., 1983. ^{210}Pb -Dating of cold Alpine firn/ice cores from Colle Gnifetti, Switzerland. *Journal of Glaciology* 29 (101), 165–177.
- Haefeli, R., 1961. Contribution to the movement and the form of ice sheets in the Arctic and Antarctic. *Journal of Glaciology* 3, 1133–1151.
- Hansen, J., 2006. Global temperature change. *Proceedings of the National Academy of Sciences* 103 (39), 14288–14293.
- Hansen, J., Sato, M., Glascoe, J., Ruedy, R., 1998. A common-sense climate index: Is climate changing noticeably? *Proceedings of the National Academy of Sciences* 95 (8), 4113–4120.
- Henderson, K., Laube, A., Gäggeler, H., Olivier, S., 2006. Temporal variations of accumulation and temperature during the past two centuries from Belukha ice core, Siberian Altai. *Journal of Geophysical Research* 111 (D3), D03104.
- Herren, P.-A., Eichler, A., Machguth, H., Papina, T., Tobler, L., Zapf, A., Schwikowski, M., 2013. The onset of Neoglaciation 6000 years ago in western Mongolia revealed by an ice core from the Tsambagarav mountain range. *Quaternary Science Reviews* 69 (C), 59–68.
- IPCC, 2007. *Climate Change 2007 - The Physical Science Basis: Working Group I Contribution to the Fourth Assessment Report of the IPCC*. Cambridge University Press, Cambridge, UK and New York, NY, USA.
- Jenk, T. M., Szidat, S., Bolius, D., Sigl, M., Gäggeler, H., Wacker, L., Ruff, M., Barbante, C., Boutron, C. F., Schwikowski, M., 2009. A novel radiocarbon dating technique applied to an ice core from the Alps indicating late Pleistocene ages. *Journal of Geophysical Research* 114 (D14), D14305.
- Kaspari, S., Mayewski, P., Handley, M., 2009. Recent increases in atmospheric concentrations of Bi, U, Cs, S and Ca from a 350-year Mount Everest ice core record. *Journal of Geophysical Research* 114 (D4), D04302.
- Klinge, M., Böhner, J., Lehmkuhl, F., 2003. Climate pattern, snow- and timberlines in the Altai Mountains, Central Asia. *Erdkunde* 57 (4), 296–308.
- Koerner, R., 1990. A record of Holocene summer climate from a Canadian high-Arctic ice core. *Nature* 343 (5), 630–631.

- Koerner, R., Devon Island ice cap: core stratigraphy and paleoclimate. *Science* 196 (4285), 15–18.
- Kotlyakov, V. M., Arkhipov, S. M., Henderson, K. A., Nagornov, O. V., 2004. Deep drilling of glaciers in Eurasian Arctic as a source of paleoclimatic records. *Quaternary Science Reviews* 23 (11-13), 1371–1390.
- Lydolph, P. E., 1977. *Climates of the Soviet Union*. Vol. 7 of *World Survey of Climatology*. World Survey of Climatology, Amsterdam.
- Ohmura, A., 2001. Physical basis for the temperature-based melt-index method. *Journal of Applied Meteorology* 40, 753–761.
- Ohmura, A., 2007. Observed long-term variations of solar irradiance at the Earth's surface. In: Calisesi, Y., Bonnet, R. M., Gray, L., Langen, J., Lockwood, M. (Eds.), *Space Sciences Series of ISSI*. Springer New York, pp. 111–128.
- Okamoto, S., Fujita, K., Narita, H., Uetake, J., Takeuchi, N., Miyake, T., Nakazawa, F., Aizen, V. B., Nikitin, S. A., Nakawo, M., 2011. Reevaluation of the reconstruction of summer temperatures from melt features in Belukha ice cores, Siberian Altai. *Journal of Geophysical Research* 116 (D2), D02110.
- Olivier, S., Blaser, C., Brüttsch, S., Frolova, N., Gäggeler, H., Henderson, K. A., Palmer, A. S., Papina, T., Schwikowski, M., 2006. Temporal variations of mineral dust, biogenic tracers, and anthropogenic species during the past two centuries from Belukha ice core, Siberian Altai. *Journal of Geophysical Research* 111 (D5), D05309.
- Olivier, S., Schwikowski, M., Brüttsch, S., Eyrikh, S., 2003. Glaciochemical investigation of an ice core from Belukha glacier, Siberian Altai. *Geophysical Research Letters* 30 (19), 2019.
- PAGES2k-Consortium, 2013. Continental-scale temperature variability during the past two millennia. *Nature Geoscience* 6 (5), 339–346.
- Pattyn, F., De Smedt, P., De Brabander, S., Van Huele, W., Agatova, A., Mistrukov, A., Declerq, H., 2003. Ice dynamics and basal properties of Sofiyskiy glacier, Altai mountains, Russia, based on DGPS and radio-echo sounding surveys. *Annals of Glaciology* 37, 286–292.
- Reeh, N., Fisher, D. A., Koerner, R. M., Clausen, H. B., 2005. An empirical firn-densification model comprising ice lenses. *Annals of Glaciology* 42, 101–106.

6 Comparison of two Altai ice cores

- Robock, A., Jianping, M., 1995. The volcanic signal in surface temperature observations. *Journal of Climate* 8, 1086–1103.
- Ruff, M., Wacker, L., Gäggeler, H., Suter, M., Synal, H.-A., Szidat, S., 2007. A gas ion source for radiocarbon measurements at 200 kV. *Radiocarbon* 49 (2), 307–314.
- Sahsamanoglou, S. H., Makrogiannis, T. J., Kallimopoulos, P. P., 1991. Some aspects of the basic characteristics of the Siberian anticyclone. *International Journal of Climatology* 11 (8), 827–839.
- Schotterer, U., Fröhlich, K., Gäggeler, H. W., Sandjordj, S., Stichler, W., 1997. Isotope records from Mongolian and Alpine ice cores as climate indicators. *Climatic Change* 36 (3), 519–530.
- Schwikowski, M., Döscher, A., Gäggeler, H. W., Schotterer, U., 1999. Anthropogenic versus natural sources of atmospheric sulphate from an Alpine ice core. *Tellus* 51 (5), 1–14.
- Shahgedanova, M., Nosenko, G., Khromova, T., Muraveyev, A., 2010. Glacier shrinkage and climatic change in the Russian Altai from the mid-20th century: An assessment using remote sensing and PRECIS regional climate model. *Journal of Geophysical Research* 115 (D16), D16107.
- Sidorova, O. V., Saurer, M., Myglan, V. S., Eichler, A., Schwikowski, M., Kirdyanov, A. V., Bryukhanova, M. V., Gerasimova, O. V., Kalugin, I. A., Daryin, A. V., Siegwolf, R. T. W., 2011. A multi-proxy approach for revealing recent climatic changes in the Russian Altai. *Climate Dynamics* 38 (1-2), 175–188.
- Sigl, M., Jenk, T., Kellerhals, T., Szidat, S., 2009. Towards radiocarbon dating of ice cores. *Journal of Glaciology* 55 (194), 985–996.
- Stern, D. I., 2005. Global sulfur emissions from 1850 to 2000. *Chemosphere* 58 (2), 163–175.
- Stern, D. I., 2006. Reversal of the trend in global anthropogenic sulfur emissions. *Global Environmental Change-Human and Policy Dimensions* 16 (2), 207–220.
- Streets, D. G., Yan, F., Chin, M., Diehl, T., Mahowald, N., Schultz, M., Wild, M., Wu, Y., Yu, C., 2009. Anthropogenic and natural contributions to regional trends in aerosol optical depth, 1980-2006. *Journal of Geophysical Research* 114.

- Sun, J., Zhang, M., Liu, T., 2001. Spatial and temporal characteristics of dust storms in China and its surrounding regions, 1960–1999: Relations to source area and climate. *Journal of Geophysical Research* 106 (D10), 10325–10333.
- Synal, H.-A., Stocker, M., Suter, M., 2007. MICADAS: A new compact radiocarbon AMS system. *Nuclear Instruments and Methods in Physics Research Section B: Beam Interactions with Materials and Atoms* 259 (1), 7–13.
- Szidat, S., Jenk, T. M., Gäggeler, H. W., Synal, H.-A., Hajdas, I., Bonani, G., Saurer, M., 2004. THEODORE, a two-step heating system for the EC/OC determination of radiocarbon (^{14}C) in the environment. *Nuclear Instruments and Methods in Physics Research Section B: Beam Interactions with Materials and Atoms* 223–224, 829–836.
- Tarussov, A., 1992. The Arctic from Svalbard to Severnaya Zemlya: Climatic reconstructions from ice cores. In: Bradley, R. S., Jones, P. D. (Eds.), *Climate Since 1500 A.D.* Routledge, pp. 505–516.
- Thompson, L. G., Mosley-Thompson, E., Davis, M., Bolzan, J. F., Dai, J., Klein, L., Gundestrup, N., Yao, T., Wu, X., Xie, Z., 1990. Glacial stage ice core records from the subtropical Dunde ice cap, China. *Annals of Glaciology* 14, 288–297.
- Tsutomu, K., Davaa, G., 2007. Recent glacier variations in Mongolia. *Annals of Glaciology* 46 (1), 185–188.
- van Aardenne, J. A., Dentener, F. J., Olivier, J. G. J., Goldewijk, C. G. M. K., Lelieveld, J., 2001. A $1^\circ \times 1^\circ$ resolution data set of historical anthropogenic trace gas emissions for the period 1890–1990. *Global biogeochemical cycles* 15 (4), 909–928.
- Wild, M., 2009. Global dimming and brightening: A review. *Journal of Geophysical Research* 114 (D10), D00D16.
- Wild, M., Gilgen, H., Roesch, A., Ohmura, A., Long, C. N., Dutton, E. G., Forgan, B., Kallis, A., Russak, V., Tsvetkov, A., 2005. From dimming to brightening: decadal changes in solar radiation at Earth's surface. *Science* 308 (5723), 847–850.

7 ^{10}Be -Beryllium

The role of the sun for the earth's energy budget is of major importance (Kiehl and Trenberth, 1997). Understanding the mutual interactions between the sun's energy input and the earth climate is necessary to identify forces controlling climate change. In recent debates about the reasons of global warming the importance of solar variability has been frequently addressed (Bard and Frank, 2006). However, the disentanglement between the effects of anthropogenic greenhouse gas emissions, internal climate feedbacks and external climate forcing such as solar variability, is challenging (Ruddiman, 2007). Long-term reconstructed solar variability can help to decipher the role of the sun on earth climate.

Since 1978 total solar irradiance (TSI) from space is available (Fröhlich, 2006). Extending solar variability data into the pre-satellite era is necessary to identify centennial trends. Reconstructions prior to AD 1610 are based on ^{14}C measurements in tree-rings or ^{10}Be from ice cores drilled in Greenland and Antarctica (Steinilber et al. 2012, Fig. 7.1). Although the different records agree well in their shape, the amplitude of the changes remains unclear (e.g., Krivova et al., 2011; Lean et al., 2011). Further efforts are necessary to improve our understanding in the terrestrial-solar relationship. Here we present the first non-polar ^{10}Be ice core measurements.

Cosmogenic nuclides (^{10}Be and ^{14}C) are produced in the atmosphere by interaction of galactic cosmic rays with gases (Masarik and Beer, 2009). The produced ^{10}Be attaches to aerosols and reaches the earth surface within 1-2 years (Steinilber et al., 2012). The ^{10}Be production rate and solar irradiance are anticorrelated, due to magnetic shielding by solar wind and the geomagnetic dipole field (Masarik and Beer, 2009). This relationship allows using ^{10}Be concentration as a proxy for solar activity. The ice core based ^{10}Be reconstructions all originate from polar regions where the stratosphere-troposphere exchange is reduced compared to mid latitudes (Field et al. (2006), Fig. 7.2). Thus, an additional ^{10}Be record from non-polar regions is an important contribution to improve our understanding of global production rates of cosmogenic nuclides. The location of Tsambagarav combined with the period covered by the ice core, provides a unique opportunity to reconstruct ^{10}Be production rates.

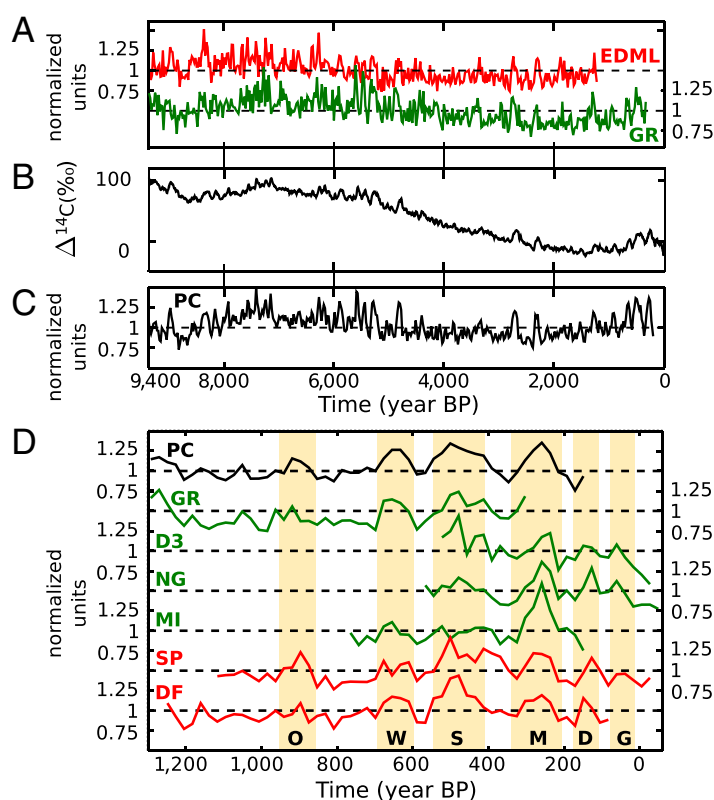


Figure 7.1: Examples of radionuclide records. (A) ^{10}Be record from the EDML in Antarctica (red) & GRIP in Greenland (GR) ice core (green). (B) $\Delta^{14}\text{C}$ measured in tree rings. (C) ^{14}C production rate. (D) ^{14}C production rate and ^{10}Be concentrations for several available ice cores (modified from Steinhilber et al. 2012).

The method to analyze ^{10}Be in an ice core is described in Section 3.7. At this time a total of 134 samples have been processed for ^{10}Be analysis, covering the period AD 2009 to 1717. Strong thinning of annual layers combined with relative large sample volumes of 200 to 250 g impeded annual resolution. With increasing depth the resolution decreases but never exceeds 5 years, for possible identification of the 11-year solar cycle (Steinhilber et al., 2009). For the period AD 2009-1970 AMS measurements of the first 26 samples are presented in Fig. 7.3, together with neutron counting rates (NCRs) of McMurdo station and Sun spot numbers (SSN). The ^{10}Be concentration and the ^{10}Be flux allow speculating on the occurrence of the 11-year cycle. A significant peak around 1991 disagrees with the expected trend of low ^{10}Be concentration and flux. Input of sulfate aerosols through stratospheric volcanic eruptions enhance the scavenging of ^{10}Be (Baroni et al., 2011) and thus increase the ^{10}Be concentration and flux artificially. For the industrial period

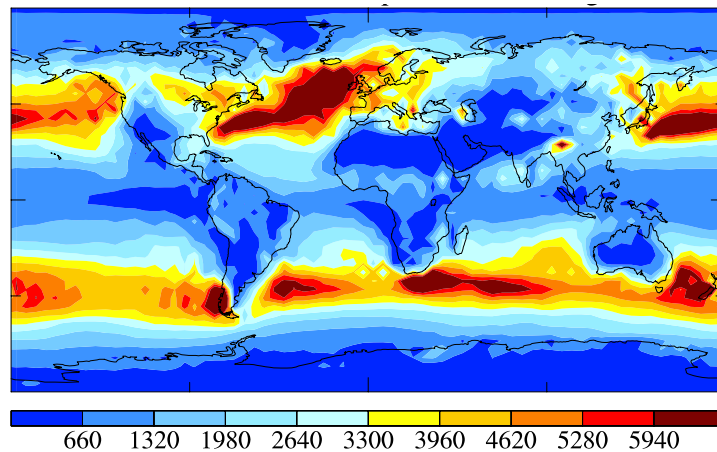


Figure 7.2: Annual mean wet deposition of ^{10}Be [$\text{kg} \cdot \text{m}^{-2} \cdot \text{s}^{-2}$]

identification of volcanic eruptions is hampered through anthropogenic emissions, which prevent an unambiguous identification of volcanic eruption (Section 4.4, Fig. 4.4). The Vostock, Antarctica sulphate concentration can be used to circumvent the predominating anthropogenic signal, and reconstruct ^{10}Be production rates (Baroni et al., 2011). Before AD 1940 the anthropogenic emissions have not altered the Tsamabagarav sulfate record, enabling direct correction of volcanic eruptions without requiring the Vostock data.

A reconstruction back to AD 1250 is intended, depending on the remaining ice. Such a record would be beneficial in two points: First, new insights in the global ^{10}Be production help to better understand past solar variability. Second, periods with significant low solar activity, such as Maunder (AD 1645-1715), Dalton (AD 1790-1830) or Spörer (AD 1415-1535) Minimum can be used as additional dating parameter of the ice core. A ^{10}Be record from the Altai offers the unique opportunity to directly investigate the correlation between solar forcing and temperature reconstruction from the Belukha ice core (Eichler et al., 2009).

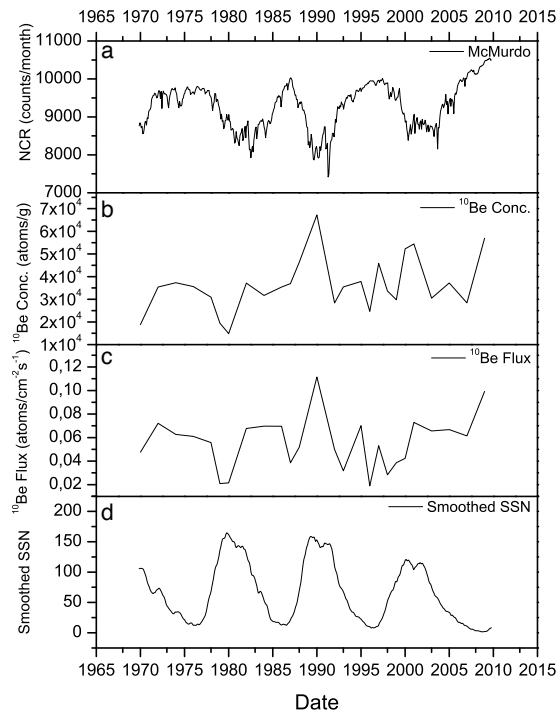


Figure 7.3: NCR (a) & SSN (d) of McMurdo station, ^{10}Be concentration (b) & flux (c) for the period AD 1970–2009 (courtesy of F. Inceoglu).

References

- Bard, E., Frank, M., 2006. Climate change and solar variability: What's new under the sun? *Earth and Planetary Science Letters* 248 (1–2), 1–14.
- Baroni, M., Bard, E., Petit, J. R., Magand, O., Bourlès, D., 2011. Volcanic and solar activity, and atmospheric circulation influences on cosmogenic ^{10}Be fallout at Vostok and Concordia (Antarctica) over the last 60 years. *Geochimica et Cosmochimica Acta* 75 (22), 7132–7145.
- Eichler, A., Olivier, S., Henderson, K., Laube, A., Beer, J., Papina, T., Gäggeler, H., Schwikowski, M., 2009. Temperature response in the Altai region lags solar forcing. *Geophysical Research Letters* 36 (1), L01808.
- Field, C. V., Schmidt, G. A., Koch, D., Salyk, C., 2006. Modeling production and climate-related impacts on ^{10}Be concentration in ice cores. *Journal of Geophysical Research* 111 (D15), D15107.

- Fröhlich, C., 2006. Solar irradiance variability since 1978. *Space Science Reviews* 125 (1-4), 53–65.
- Kiehl, J. T., Trenberth, K. E., 1997. Earth's annual global mean energy budget. *Bulletin of the American Meteorological Society* 78 (2), 197–208.
- Krivova, N. A., Solanki, S. K., Unruh, Y. C., 2011. Towards a long-term record of solar total and spectral irradiance. *Journal of Atmospheric and Solar-Terrestrial Physics* 73 (2-3), 223–234.
- Lean, J. L., Woods, T. N., Eparvier, F. G., Meier, R. R., Strickland, D. J., Correia, J. T., Evans, J. S., 2011. Solar extreme ultraviolet irradiance: Present, past, and future. *Journal of Geophysical Research* 116 (A1), A01102.
- Masarik, J., Beer, J., 2009. An updated simulation of particle fluxes and cosmogenic nuclide production in the Earth's atmosphere. *Journal of Geophysical Research* 104 (D10), 12099–12111.
- Ruddiman, W. F., 2007. *Earth's Climate. Past and Future.* W. H. Freeman.
- Steinhilber, F., Abreu, J. A., Beer, J., Brunner, I., Christl, M., Fischer, H., Heikkila, U., Kubik, P. W., Mann, M., McCracken, K. G., Miller, H., Miyahara, H., Oerter, H., Wilhelmsf, F., 2012. 9,400 years of cosmic radiation and solar activity from ice cores and tree rings. *Proceedings of the National Academy of Sciences* 109 (16), 5967–5971.
- Steinhilber, F., Beer, J., Fröhlich, C., 2009. Total solar irradiance during the Holocene. *Geophysical Research Letters* 36 (19), L19704.

8 Outlook

A number of challenges related to alpine ice cores and regionally resolved climate reconstructions have been addressed in this thesis. The successful collection of an ice core in such a remote area as the Mongolian Altai enables a variety of possible paleoclimate investigations, especially in combination with the Belukha ice core. In the following ideas of potential future work that sprout while processing the ice, analyzing data or discussing results are enumerated.

- The physical meaning of the water stable isotope record ($\delta^{18}\text{O}$) remains unclear. There are strong indications that its composition is controlled by both temperature and atmospheric moisture source. Although significant correlation with Khovd temperature data for the past 60 years was observed, the long-term trend showed unexpected values. Since the LIA signal was absent in the record, $\delta^{18}\text{O}$ was not considered as temperature proxy. Additional work is required to disentangle the temperature signal from the atmospheric moisture origin. Deuterium (δD) measurements and d-excess combined with high-resolution model studies may provide valuable insights.
- The unique location of the Altai between the Siberian forest and the desert of Central Asia makes it an interesting site for paleoclimate archives. To the north the precipitation is mostly related to cyclones controlled by westerly winds, whereas to the south the Monsoon is the major moisture contributor. Relating Altai records from Belukha and Tsambagarav with Tibetan and Tien Shan records can help to reconstruct regional atmospheric circulation, such as temporally varying northward intrusion of the Monsoon. Major changes in atmospheric circulation can affect the origin of the moisture source and thus explain unexpected pattern of the water stable isotope record.
- The outcome of PCA with the Tsambagarav ice core records depends on the period considered (see Table 5.1 & 6.4). Changes in the attribution of the loadings within the different PCs suggest a nonsteady proxy-climate parameter relation. Additional

8 Outlook

analysis and data processing could help to investigate this relation beyond the calibration period.

- The collapse of the U.S.S.R resulted in strongly reduced economic and mining activities leading to a decrease in emission of pollutants. However, subsequently the economic boom of China and its demand in natural resources especially of rare-earth elements required in the production of the micro-electronic industry, initiated enhanced mining in Mongolia. Lung diseases and other mining-sector health risks pose major difficulties for the country. A solution considering both economic growth and health issues will be a crucial challenge for the upcoming decade. The Tsambagarav ice core could help to put the current air pollution from mining into a longer perspective, through analysis of trace elements with the CIM ICP-SFMS.
- A Black Carbon (BC) concentration record could be used to (i) investigate radiation effects potentially related to glacier retreat analogous to former studies from the Himalayas and (ii) to derive a forest fire history in the Altai similar to the work on the Belukha ice core where geochemical records, pollen analysis and charcoal measurements were combined. Comparison of geochemical records between Belukha and Tsambagarav provided encouraging results regarding the geographical extent of forest fire proxies (see Section 6.3.4).
- The Mongolian Altai is an arid region. Changes in precipitation affect the nomadic population and their cattle living in the steppe. A humidity record with higher resolution than presented in Section 4.6 could be useful to reconstruct the natural variability of precipitation and drought occurrence in this region. Combined with reconstructed atmospheric circulation pattern, strategies could be designed to avoid water shortage in future. Which record to use as proxy for reconstructing humidity remains unclear, especially since the mineral dust related species could not be linked to general humidity trends.
- The arid part of the Altai together with northwestern China is a major contributor in atmospheric dust supply to the Northern Hemisphere. However, mineral dust storm evolution and dust emission processes in the past remain unclear due to the scarcity of geological archives in this region. Although related to local sources the mineral dust related geochemical records could provide a long-term perspective of dust storms and atmospheric dust input.

- The Siberian High is controlling winter climate in the Altai and Siberia. Connections between varying intense anticyclonic conditions and the regional climate have been identified. The Tsambagarav ice core is located within the area of influence. Consequently geochemical records might provide adequate proxies for reconstructing anticyclonic intensity and extent, similar to the non-sea-salt potassium (nssK) record from GISP2 used to derive a Siberian High index. However, one should keep in mind that the majority of precipitation occurs during summer month, complicating the reconstruction of a winter phenomena.
- Ongoing projects like ^{10}Be and pollen analysis need to be further conducted. Results from these records can help for a more in depth interpretation of the already performed measurements.
- With two ice cores from the Altai we dispose of optimal prerequisites to provide profound climate reconstruction for this region of Central Asia. In this regard an additional ice core from e.g. the Sutai Uul (see Section 2.1) or from the Belukha saddle this time reaching bedrock might be very beneficial. These extra records would be especially valuable for the aforesaid analysis and interpretations.

9 Appendix

9.1 Supplementary information: *Late-Holocene temperature reconstruction from Siberia*

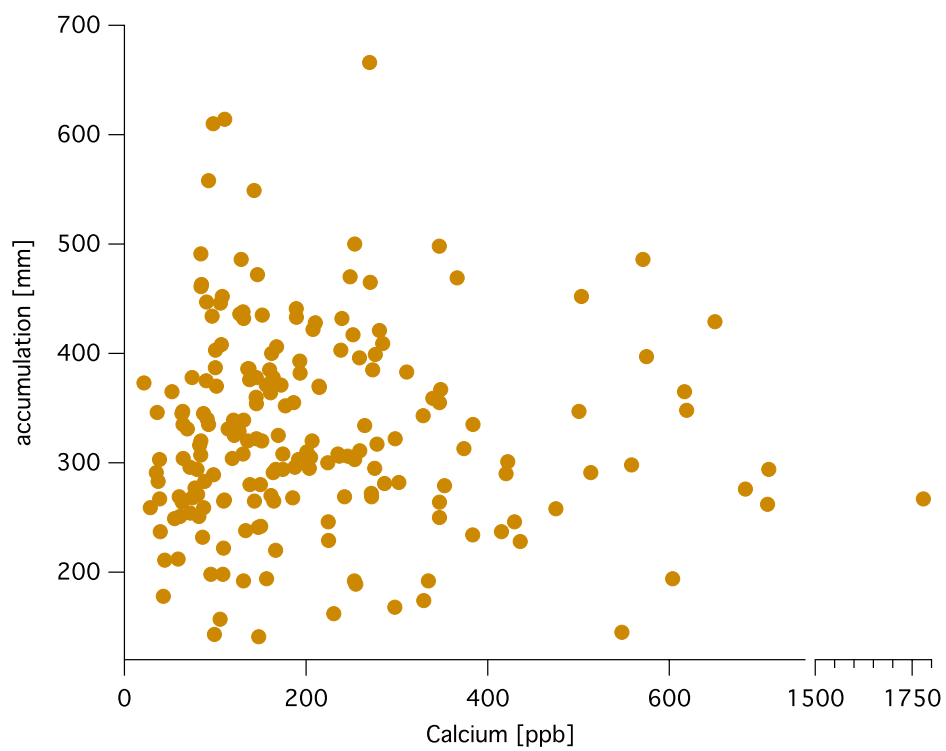


Figure 9.1: Accumulation rates (mm/year) at the Tsambagarav ice core site against Ca²⁺ concentration in ppb for the period AD 1815 to 2008.

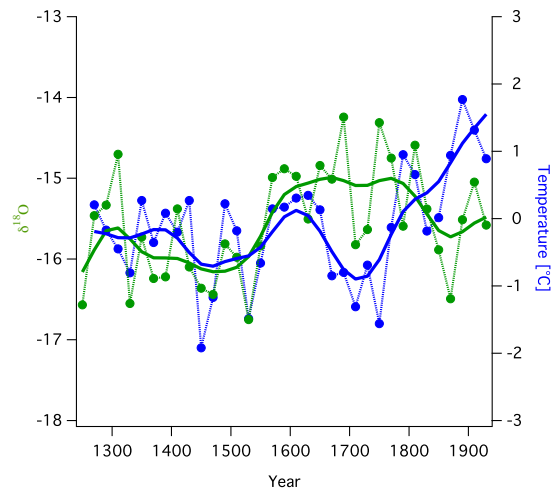


Figure 9.2: . Stable isotope record ($\delta^{18}\text{O}$) for Tsambagarav (green) and Belukha (blue). 20-year resolution values (thin line) smoothed with a 5-point binomial filter (bold curves).

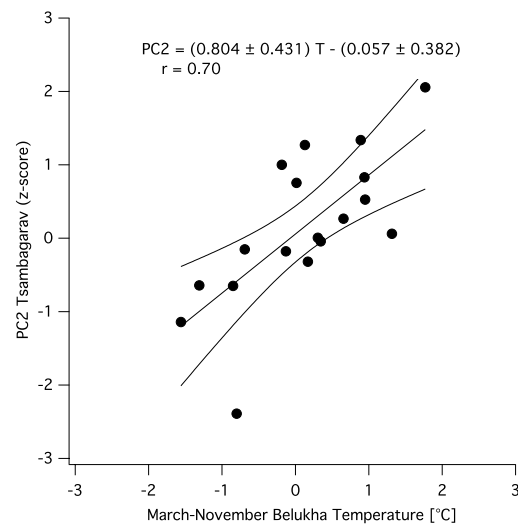


Figure 9.3: Correlation between 20-year PC2 means from Tsambagarav and March-November temperature means from the Belukha $\delta^{18}\text{O}$ in the period 1580-1980. Given are the 95% confidence bands and 2σ uncertainties of the slope and intercept values.

9.2 Totality of conducted ^{14}C measurements

Table 9.1: Overview of all the ^{14}C samples of the Tsamagarav 2009 ice core, analyzed at ETH Zürich. The fraction of modern (fM) is given with the corresponding 1σ -range. For the calibrated age, ranges are given with 68% probability. All the values correspond to the particulate organic carbon (POC) fraction of the sample. (†) samples with high carbon concentration separated in two glass tubes but only one measured. (††) bottom sample, partly degassed and twice measured.

Core segment #	Depth [m weq]	Ice Sample mass [kg]	Absolute carbon amount [μg]	AMS Lab Nr.	Radiocarbon fM	Calibrated age years BP = 1950
66	32.98	0.171	13	ETH43432.1.1	0.966±0.020	130-460
72	36.45	0.182	21	ETH43434.1.1	0.955±0.018	210-530
75	38.19	0.166	33	ETH43436.1.1	0.983±0.012	280-10
81	41.64	0.181	19	ETH43438.1.1	0.996±0.017	270-10
87	44.43	0.166	12	ETH43440.1.1	1.046±0.027	50-250
92	47.55	0.219	33	ETH42822.1.1	0.891±0.010	930-770
97	49.65	0.183	32	ETH42824.1.1	0.800±0.010	1860-1570
102	52.21	0.186	22	ETH42826.1.1	0.666±0.014	3720-3270
105.1	53.59	0.278	58	ETH42156	0.605±0.007	4800-4420
105.2	53.73	0.229	29	ETH42166	0.597±0.010	4850-4240
107.1	55.05	0.143	23	ETH42828.1.1	0.578±0.015	5440-4710
107.2†	55.08	0.038	117	ETH42830.1.1	0.570±0.009	5170-5350
109	55.8	0.194	32	ETH42157	0.548±0.009	5710-5330
111.1†	57.38	0.147	167	ETH42833.1.1	0.521±0.008	6020-6170
111.2	57.45	0.161	55	ETH42836.1.1	0.532±0.008	5920-5660
111.3†	57.53	0.136	143	ETH42838.1.1	0.521±0.009	6020-6180
112††	57.95	0.247	341-101	ETH42158 / ETH42256	0.535±0.007 / 0.535±0.008	5660-5890 / 5650-5910

9.3 Snowpit samples during fieldwork 2009 and 2011

Table 9.2: Concentration of cations and anions in the snow pit and the snowfall samples, collected during the Tsambagarav deep drilling campaign 2009 in ppb.

Depth [cm]	F ⁻	CH ₃ COO ⁻	HCOO ⁻	CH ₃ SO ₃ ⁻	Cl ⁻	NO ₃ ⁻	SO ₄ ²⁻	C ₂ O ₄ ²⁻	Na ⁺	NH ₄ ⁺	K ⁺	Mg ²⁺	Ca ²⁺
0-8	2.79	56.33	331.69	NaN	69.13	387.09	466.67	29.95	34.01	314.03	34.85	18.71	181.09
8-16	3.90	21.99	456.77	NaN	120.62	443.32	724.85	41.88	72.06	346.10	23.07	34.86	367.87
16-23	3.25	22.72	270.16	NaN	59.78	343.02	541.74	18.62	31.46	268.53	14.79	19.25	184.71
23-31	3.10	30.29	235.61	6.47	30.51	358.08	602.70	20.39	13.69	278.82	14.76	14.79	110.60
31-39	3.04	51.00	161.47	7.79	31.05	544.81	891.74	26.59	11.65	346.79	15.98	13.48	105.12
39-48	3.89	53.70	312.93	8.25	38.44	620.98	823.33	36.14	14.31	420.27	16.55	13.55	119.55
48-56	6.47	67.77	457.51	NaN	54.25	695.22	696.53	47.89	30.55	446.21	27.79	23.12	210.36
56-64	9.68	106.63	760.15	NaN	1128.10	1126.30	2421.50	237.45	584.18	693.40	72.32	204.62	2790.10
64-72	6.61	87.66	538.25	NaN	565.55	772.97	1709.90	131.85	317.78	447.53	48.94	127.65	1564.60
72-80	4.24	67.01	289.06	NaN	115.06	507.79	1070.00	30.35	83.98	296.79	28.81	52.18	484.84
80-88	4.15	82.75	161.63	NaN	140.11	512.17	1109.60	30.94	98.49	297.05	22.63	55.66	508.00
88-95	5.77	64.62	281.71	NaN	148.99	564.53	1149.70	100.62	120.47	308.65	39.89	75.88	772.69
Snowfall 9.7.2009	2.027	77.178	235.04	NaN	21.827	293.09	598.36	30.023	7.589	323.05	10.725	8.205	48.564
Snowfall 9.7.2009	4.029	61.016	278.55	NaN	48.472	615.24	782.66	52.605	19.681	464.2	18.441	19.477	163.98

Table 9.3: Concentration of cations and anions in the snow pit collected on summit of Sutai Uul in summer 2011 in ppb.

Snow pit	Depth [cm]	F ⁻	CH ₃ COO ⁻	HCOO ⁻	CH ₃ SO ₃ ⁻	Cl ⁻	NO ₃ ⁻	SO ₄ ²⁻	C ₂ O ₄ ²⁻	Na ⁺	NH ₄ ⁺	K ⁺	Mg ²⁺	Ca ²⁺	δ ¹⁸ O
	0-12	3	4	4	4	35	121	216	2	8	140	6	6	25	-15.4
	12-24	3	5	5	2	77	582	558	2	44	439	15	11	92	-16.6
	24-36	11	6	5	2	266	1753	723	NaN	630	305	60	181	1419	-15.4
	36-48	7	6	4	3	301	1658	515	NaN	192	310	46	158	1294	-13.8
	48-60	7	5	6	3	320	1195	622	NaN	200	390	55	123	1132	-12.7

9.4 Raw geochemistry & stable isotope records

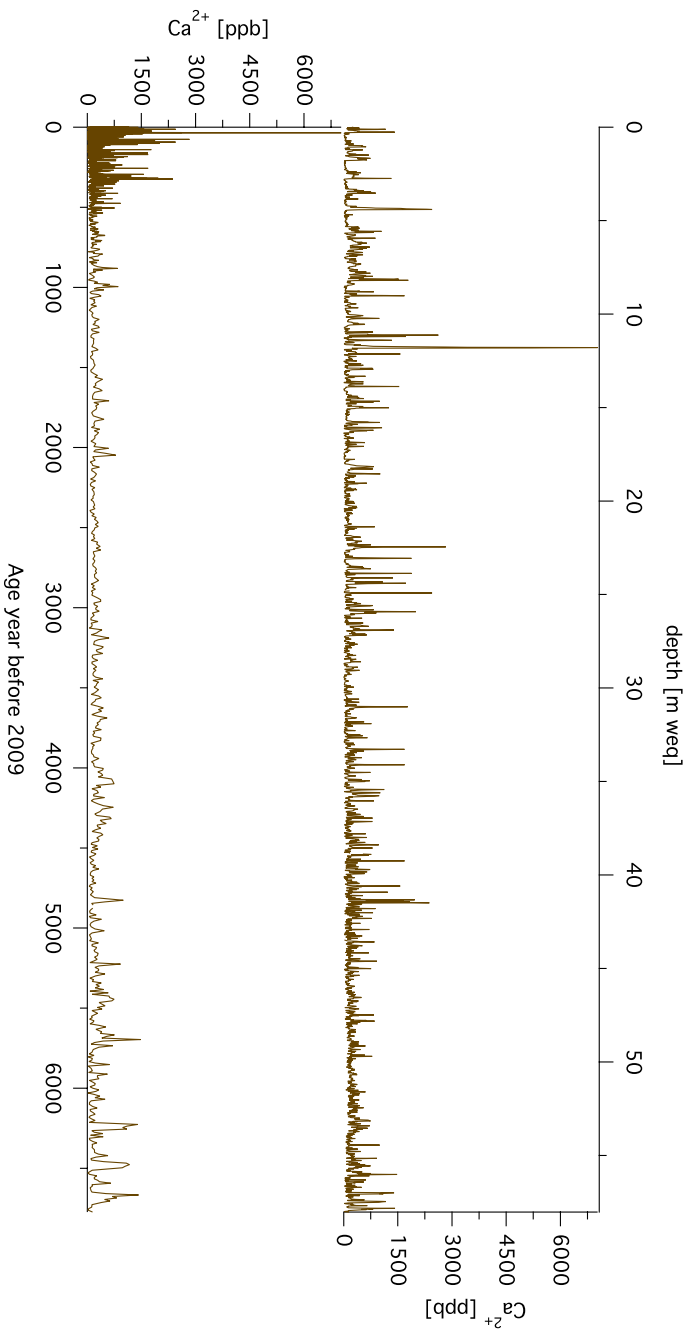


Figure 9.4: Raw data of the Tsambagarav Ca^{2+} record against depth (*top*) and time (*bottom*).

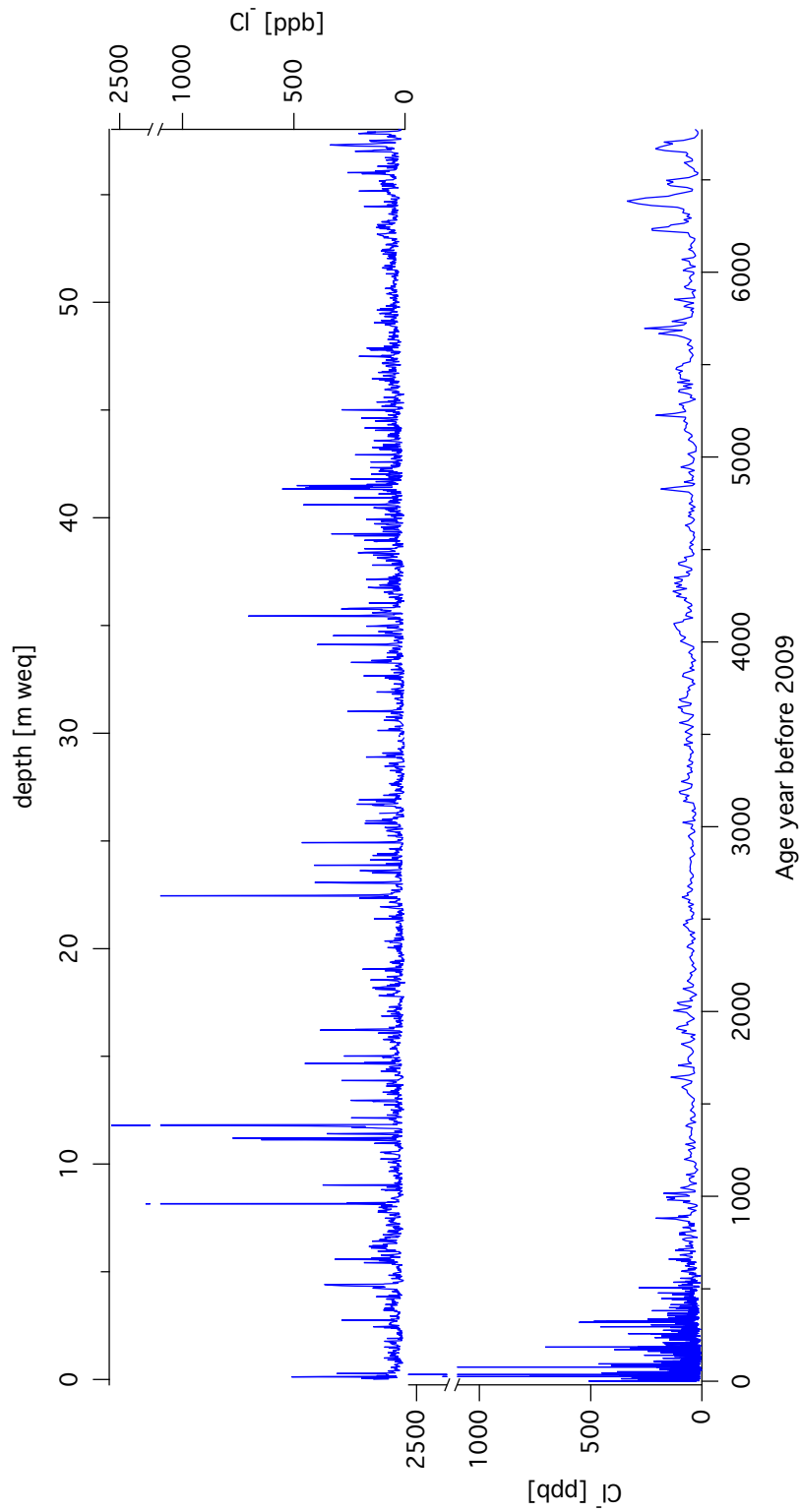


Figure 9.5: Raw data of the Tsambagarav Cl^- record against depth (*top*) and time (*bottom*).

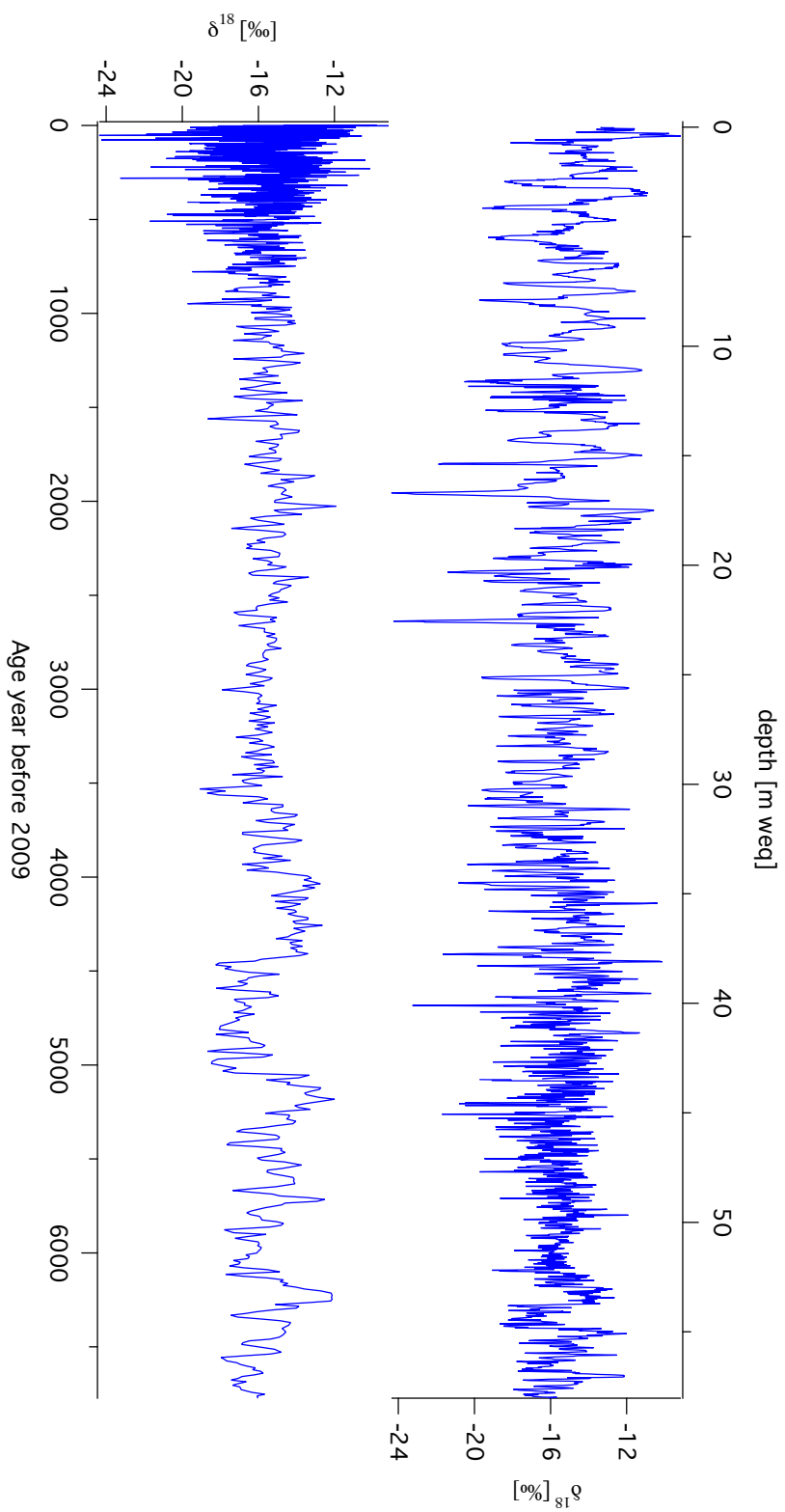


Figure 9.6: Raw data of the Tsanbagarav $\delta^{18}\text{O}$ record against depth (*top*) and time (*bottom*).

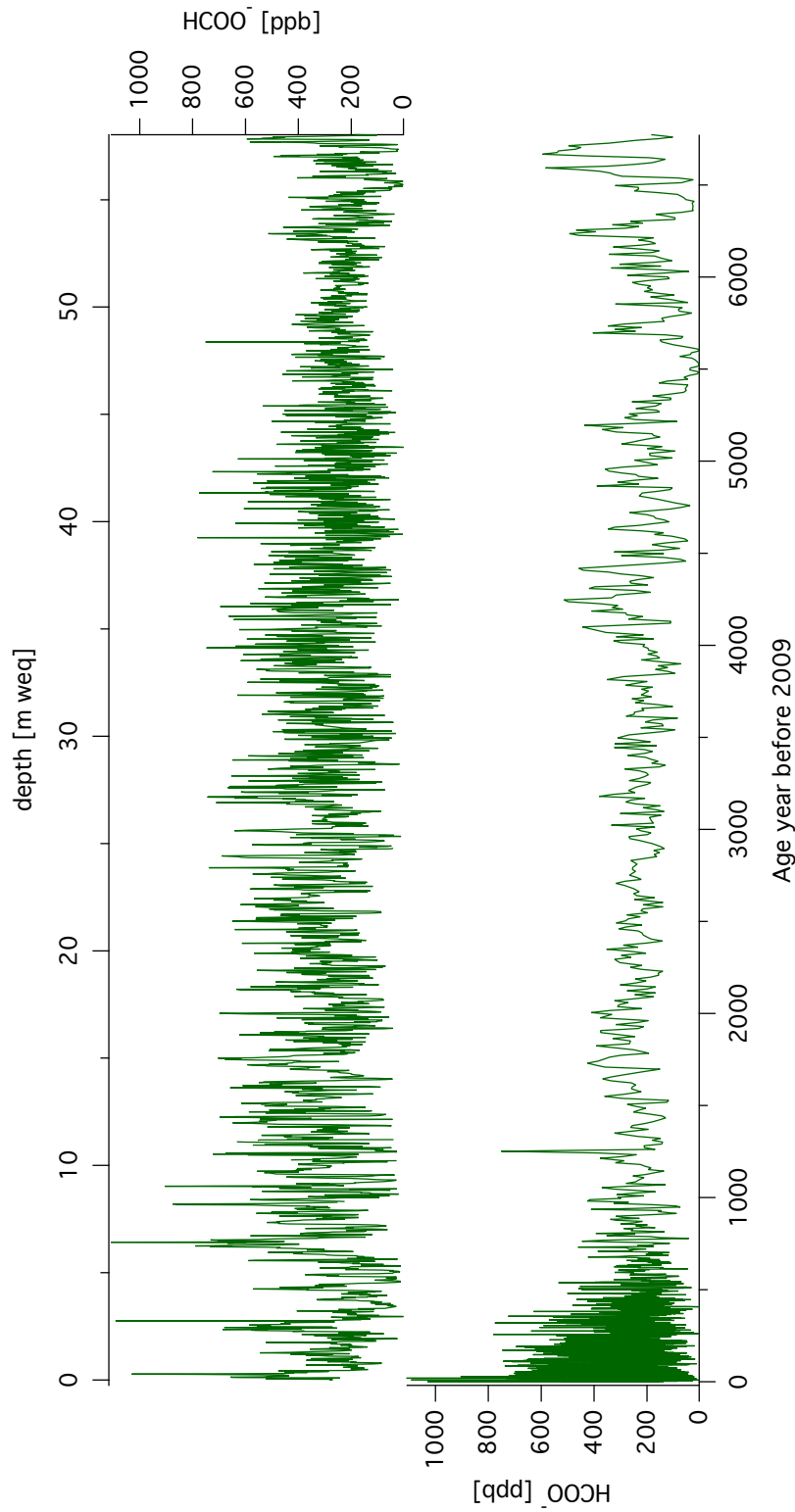


Figure 9.7: Raw data of the Tsambagarav HCOO^- record against depth (*top*) and time (*bottom*).

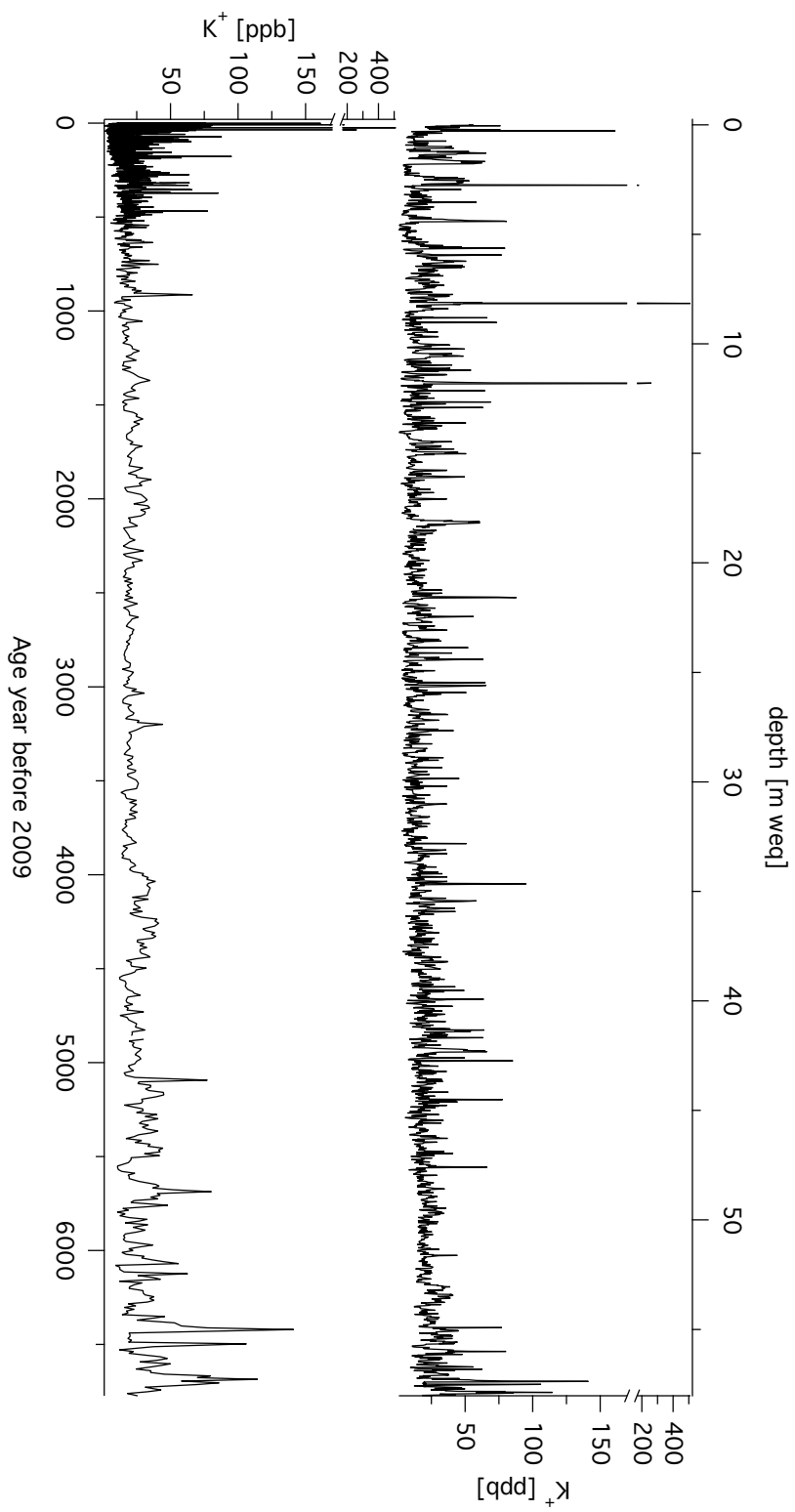


Figure 9.8: Raw data of the Tsambagarav K^+ record against depth (*top*) and time (*bottom*).

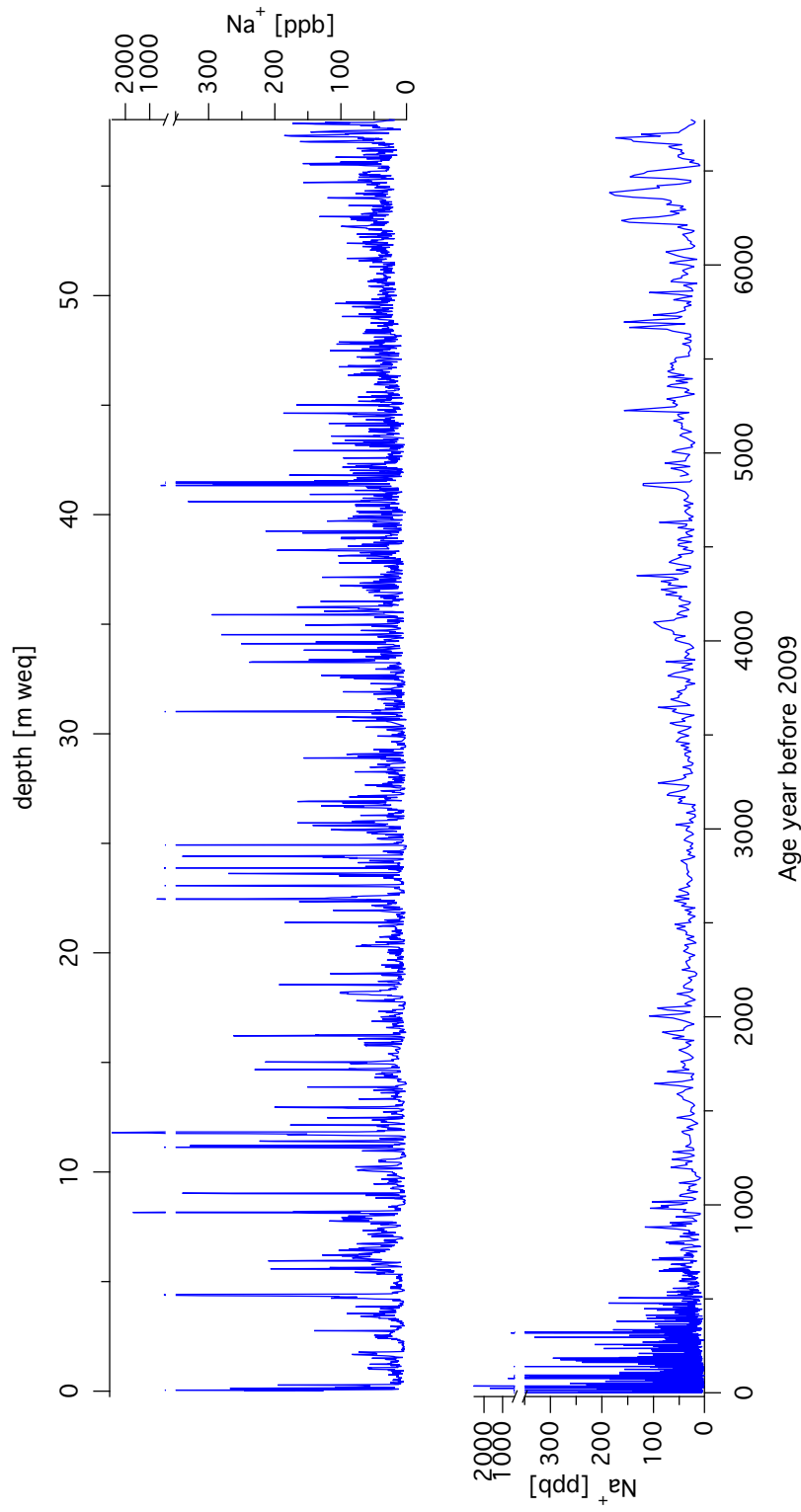


Figure 9.9: Raw data of the Tsambagarav Na^+ record against depth (*top*) and time (*bottom*).

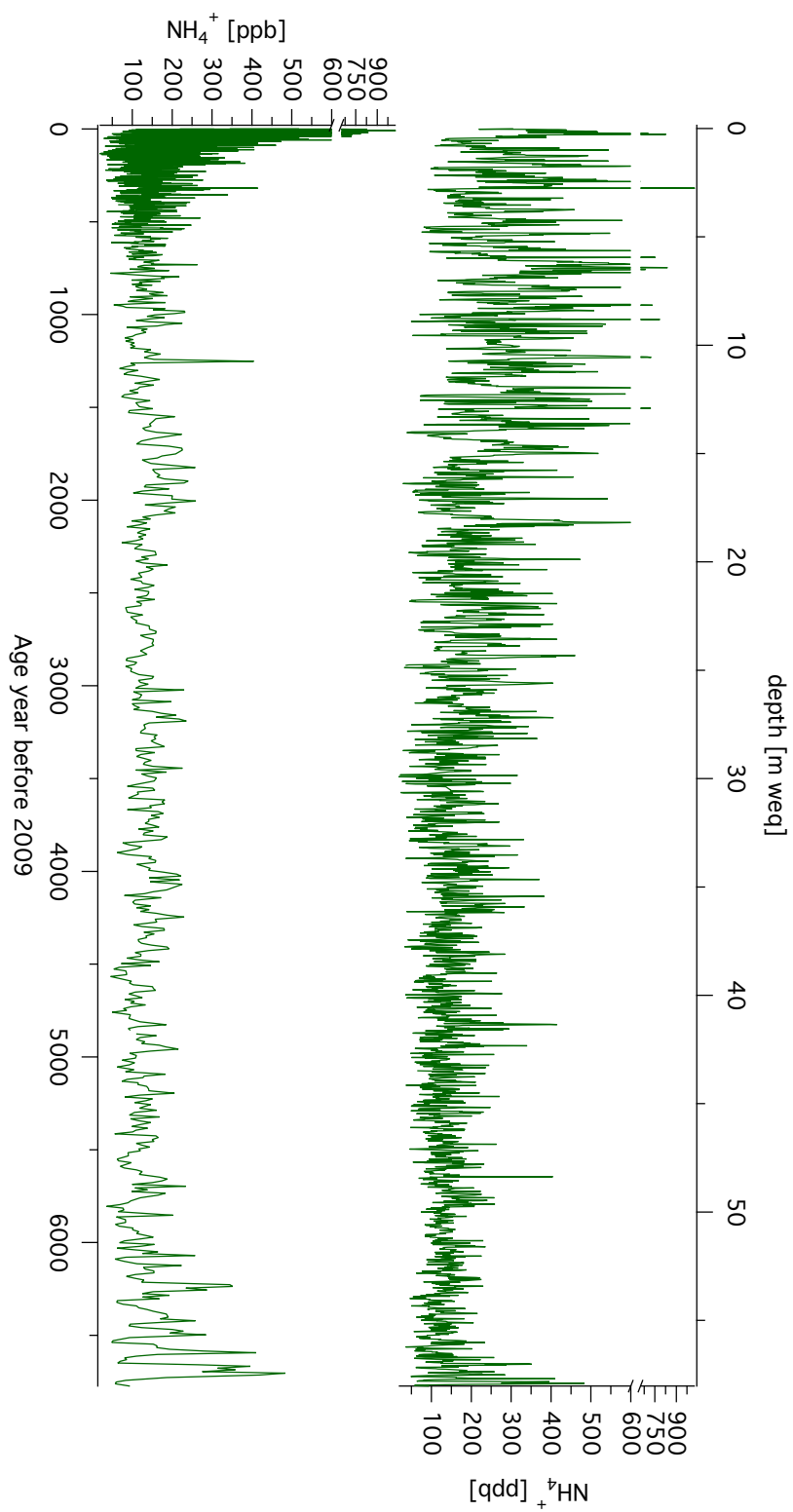


Figure 9.10: Raw data of the Tsanbagarav NH_4^+ record against depth (*top*) and time (*bottom*).

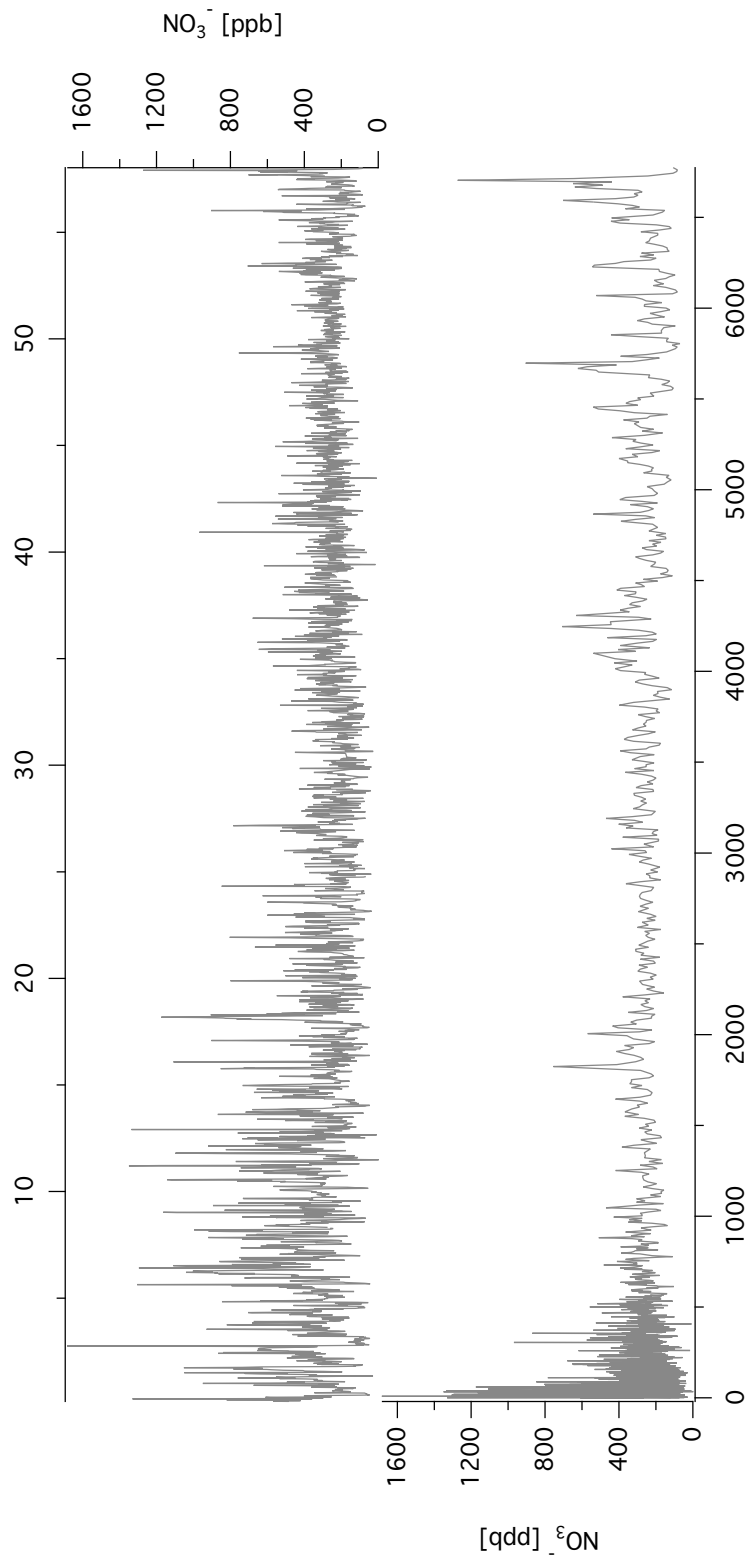


Figure 9.11: Raw data of the Tsambagarav NO_3^- record against depth (*top*) and time (*bottom*).

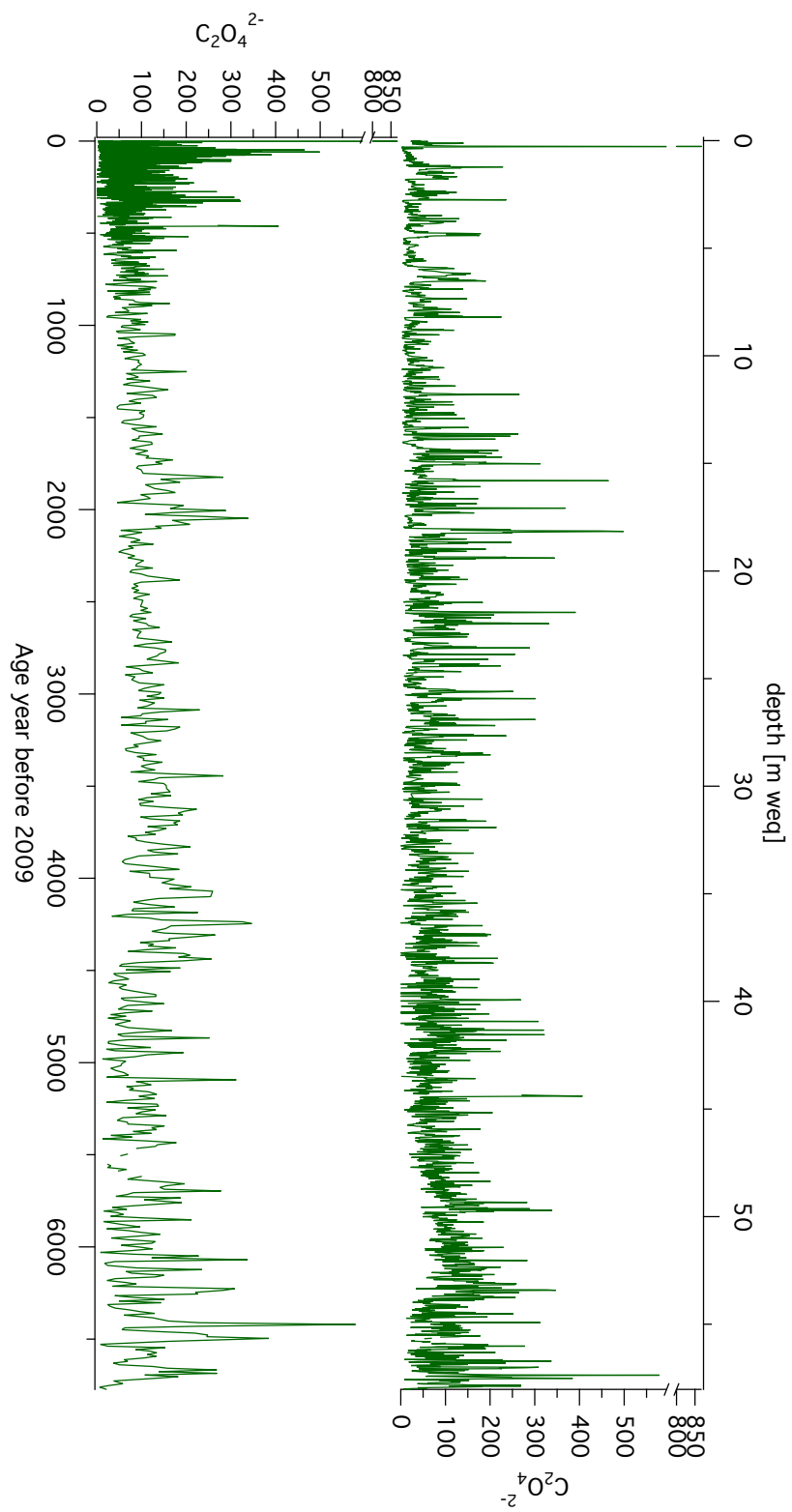


Figure 9.12: Raw data of the Tsambagarav $C_2O_4^{2-}$ record against depth (*top*) and time (*bottom*).

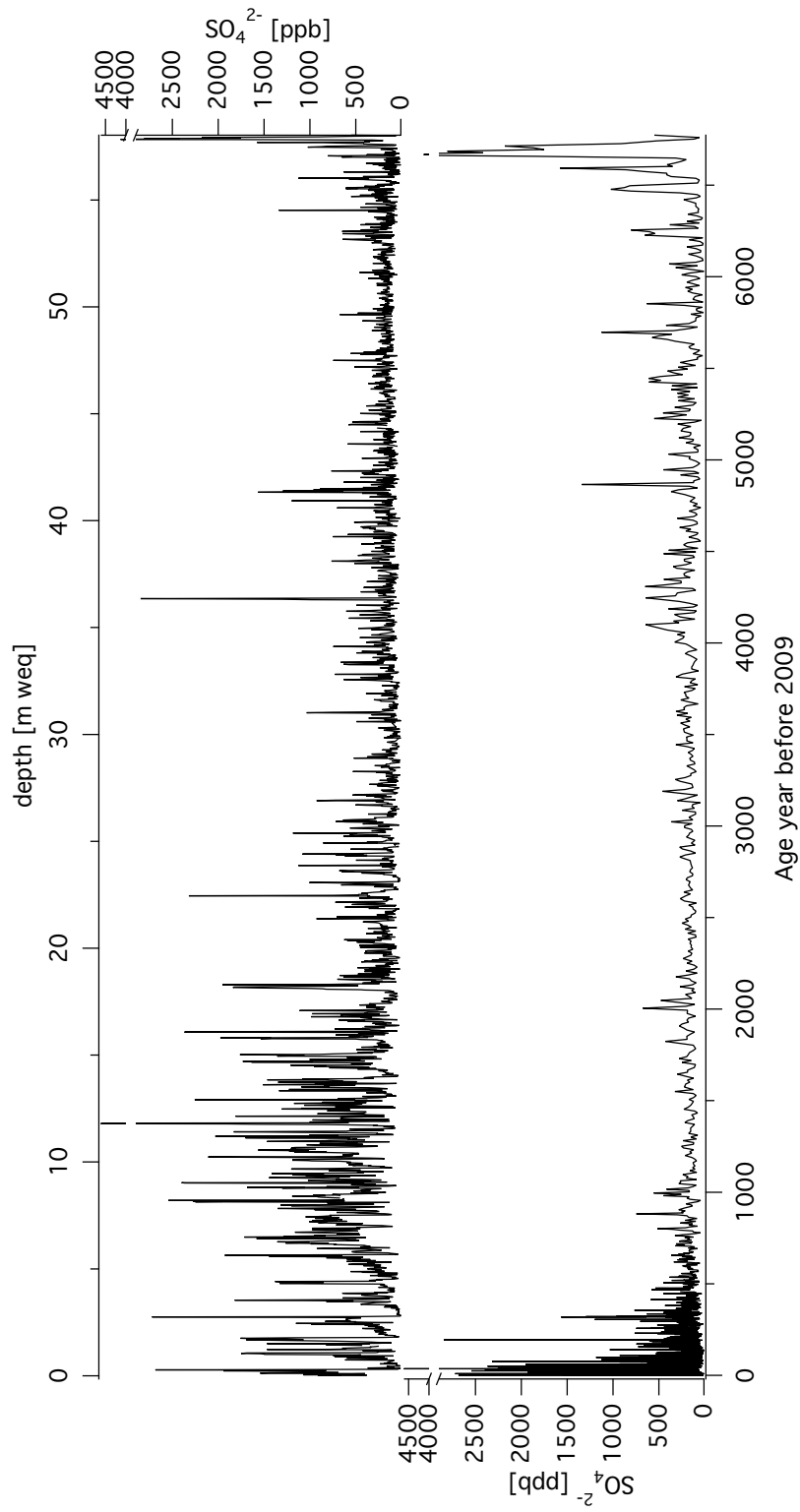


Figure 9.13: Raw data of the Tsambagarav SO_4^{2-} record against depth (*top*) and time (*bottom*).

Acknowledgments

Many persons contributed to the successful completing of this thesis. Through scientific input, support in instrumental set up or as friend and colleague.

- A substantial merit goes to Margit Schwikowski for initiating this work. I highly appreciated your confidence while taking me along for field work in Mongolia during summer 2009 although we barely knew each other. All the field work expeditions allowed me to discover incredible places on earth and made the last four years unforgettable. Thank you for your patience and time to answer my questions and for suggesting ideas how to interpret our results.
- Anja Eichler for the endless discussions how to interpret the records and always reminding me the limits of our work. The debates between your previous work and our new results led to a better work.
- Tatyana Papina for all the administrative work enabling a successful deep drilling campaign in 2009. Thank you for all the help and suggestions to understand the Siberian climate.
- Horst Machguth for speaking Russian during our field work. Thank you for bringing me safe down from the summit of Sutai Uul in the densest fog I ever experienced.
- The group of analytical chemistry for the discussions and providing a good working atmosphere.
- Leo Tobler for sharing countless hours with me in the cold room. Your calm even in the biggest hurry was always very inspiring.
- The drilling team of the Tsambagarav 2009 campaign for retrieving a high quality core, Heinz Gäggeler, Manuel Schläppi, Michael Sigl and Beat Rufibach.
- Sabina Brütsch for introducing me to the ion chromatography and for assisting me in the laboratory.

- Jost Eikenberg and Max Rüthi for their help in the ^3H analysis. Rolf Siegwolf and Matthias Saurer for their assistance in the $\delta^{18}\text{O}$ analysis.
- Martin Pidoux, Matthias Ryffel & Philippe Blanc for ensuring my outdoor activities next to my PhD.
- All the colleagues from the Laboratory of Radio- and environmental Chemistry at PSI and University of Bern.
- Je voudrais aussi remercier mes parents Nelly et Erwin pour m'avoir toujours soutenu et remis sur les bons rails le moment venu. Chacune de mes sœurs chéries pour me faire revenir sur terre.
- Mes remerciements vont finalement à Sophie pour tout ce que tu sais déjà.

Zum Schluss möchte ich noch Alex und Beat danken. Ohne sie wäre diese Arbeit nie möglich gewesen. Beat für seine Fähigkeit auf dem Feld jede noch so prekäre Situation zu entschärfen und Alex für sein kritisches Denken und seine aufmunternden Worte sobald ich diese brauchte. Leider haben uns beide zu früh verlassen und hinterlassen am Ende dieser Arbeit eine sehr grosse Leere.

Erklärung

gemäss Art. 28 Abs. 2 RSL 05

Name/Vorname: Herren, Pierre-Alain

Matrikelnummer: 02-916-740

Studiengang: Climate Sciences

Bachelor Master Dissertation

Titel der Arbeit: Ice core based climate reconstruction
from the Mongolian Altai

LeiterIn der Arbeit: Prof. Dr. Margit Schwikowski

Ich erkläre hiermit, dass ich diese Arbeit selbständig verfasst und keine anderen als die angegebenen Quellen benutzt habe. Alle Stellen, die wörtlich oder sinngemäss aus Quellen entnommen wurden, habe ich als solche gekennzeichnet. Mir ist bekannt, dass andernfalls der Senat gemäss Artikel 36 Absatz 1 Buchstabe r des Gesetzes vom 5. September 1996 über die Universität zum Entzug des auf Grund dieser Arbeit verliehenen Titels berechtigt ist.

Bern, 27. August 2013

Ort/Datum

.....
Unterschrift

Curriculum vitae

Pierre-Alain Herren

Born on the 6th of November 1982 in Zürich, Switzerland

Swiss citizen

Education

- | | |
|-----------|---|
| 2009-2013 | Preparation of a doctoral thesis at the Paul Scherrer Institut and the University of Bern, Switzerland

<u>Dissertation Title:</u> <i>Ice core based climate reconstruction from the Mongolian Altai</i>
<u>Advisor:</u> Prof. Dr. Margit Schwikowski |
| 2003-2009 | ‘Master of Science in Umweltnaturwissenschaften’ from the ‘Eidgenössische Technische Hochschule Zürich’ (ETHZ).

<u>Title of the Master thesis:</u> <i>Analysis of soil moisture evolution using a deterministic model based on Richards’ equation</i>
<u>Advisor:</u> Prof. Dr. Sonja Seneviratne, Dr. Ryan Teuling |
| 1998-2002 | ‘Maturität (College graduation)’, Collège Ste-Croix, Fribourg, with focus on applied mathematics und physics. |
-

Contribution to conferences and workshops

- 2010 *(Participation)*
9th NCCR Young Researchers Meeting, Löwenberg, Switzerland, 10-11 July
- 2010 *Reconstruction of past climate from an ice core of the Mongolian Altai (Poster)*
9th International NCCR Climate Summer School, 'Adaptation and Mitigation: Responses to Climate Change', Grindelwald, Switzerland, 29 August-3 September
- 2011 *(Participation)*
GAW-CH Conference, Zürich, Switzerland, 18-19 January
- 2011 *An ice-core based history of Siberian forest fires since AD 1250 (Presentation)*
XVIII INQUA Congress, Bern, Switzerland, 21-27 July
- 2011 *(Participation)*
IASC Workshop, Pontresina, Switzerland, 23-26 March
- 2011 *Ice core based climate reconstruction of the Mongolian Altai (Presentation)*
9th Swiss Geoscience Meeting, ETH Zürich, Switzerland, 11-13 November

- 2012 *Ice core based climate reconstruction of the Mongolian Altai (Presentation)*
International Partnerships in Ice Core Sciences, First Open Science Conference, Presqu'île de Giens, France, 1-5 October
- 2012 *Complex age-depth relation in a mid-latitude glacier (Poster)*
10th Swiss Geoscience Meeting, Bern, Switzerland, 16-17 November
- 2013 *Holocene climate in Western Mongolia from an Altai ice core (Presentation)*
PAGES 2nd Young Scientists Meeting, Goa, India, 11-12 February
- 2013 *Holocene climate in Western Mongolia from an Altai ice core (Poster)*
PAGES 4th Open Science Meeting, Goa, India, 13-16 February
- 2013 *Holocene climate in Western Mongolia from an Altai ice core (Presentation)*
Davos Atmosphere and Cryosphere Assembly, Air, Ice & Process Interactions, Davos, Switzerland, July 8-12
-

Contribution to scientific field work

2009	Khukh Nuru Uul in the Tsambagarav massif (Mongolian Altai, 4300 m asl), ice core deep drilling
2010	La Mesa (Argentinian Andes, 5800 m asl), shallow core drilling
2011	Sutai Uul (Mongolian Altai, 4210 m asl), reconnaissance study for deep drilling
2011	Kilimanjaro (Kilimanjaro massif, Tanzania, 5800 m asl), sampling the vertical ice cliffs
2011	Silvretta glacier (Swiss Alps, 2927 m asl), ice core deep drilling
2012	Plaine Morte glacier (Swiss Alps, 2700 m asl), ice core deep drilling
2009-2012	several 1 to 2 day field campaigns in the Swiss Alps
